FLOW AND SEDIMENT PROPERTIES INFLUENCING EROSION OF FINE-GRAINED MARINE SEDIMENTS: SEA FLOOR AND LABORATORY EXPERIMENTS

by

ROBERT ALEXANDER YOUNG

B.S., Brooklyn College
(1969)

M.S., Massachusetts Institute of Technology
(1972)

SUBMITTED IN PARTIAL FULFILLMENT OF THE
REQUIREMENTS FOR THE DEGREE OF
DOCTOR OF PHILOSOPHY

at the

MASSACHUSETTS INSTITUTE OF TECHNOLOGY

and the

WOODS HOLE OCEANOGRAPHIC INSTITUTION

September, 1975

Signature of Author.....
Joint Program in Oceanography, Massachusetts Institute of Technology-Woods Hole Oceanographic Institition, and Department of Earth and Planetary Sciences, and Department of Meteorology, Massachusetts Institute of Technology, September, 1975

Certified by.....
Thesis Supervisor

Accepted by.....
Chairman, Joint Oceanography Committee in the Earth Sciences, Massachusetts Institute of Technology-Woods Hole Oceanographic Institution

FLOW AND SEDIMENT PROPERTIES INFLUENCING EROSION OF FINE-GRAINED MARINE SEDIMENTS: SEA FLOOR AND LABORATORY EXPERIMENTS

Robert Alexander Young

Submitted to the Massachusetts Institute of Technology-Woods Hole Oceanographic Institution Joint Program in Oceanography on August 11, 1975, in partial fulfillment of the requirements for the degree of Doctor of Philosophy

ABSTRACT

Erosion processes involving fine-grained marine sediments were studied by using an in situ flume to erode undisturbed bottom sediments on the sea floor in Buzzards Bay, a shallow marine embayment off the Massachusetts coast. The muddy sea floor in that area is characterized by a deposit-feeding infauna that reworks the sediments.

Observations made with the in situ flume suggest that erosion resistance of compacted bottom sediments is up to twice as great as the erosion resistance of biogenically reworked sediments. Estimates of erosional bed shear stress from the in situ flume experiments are similar to estimates made during this study of bed shear stress developed in near-bottom tidal currents. It is inferred that erosion by the in situ flume produces reasonable estimates of bed shear stress necessary to erode undisturbed bottom sediments on the sea floor.

Buzzards Bay muds were redeposited in a laboratory flume and eroded after various periods of reworking by the deposit-feeding organisms contained in them. Other Buzzards Bay mud samples were treated to remove organic matter, and the erosion resistance of flat beds of these sediments was also investigated in a laboratory flume.

The surface of a biogenically reworked bed after two months was covered with mounds, burrows, trails, and

aggregates composed of sediments and organic material. This bed was similar in appearance to many of the beds eroded by the in situ flume. The two month bed eroded at an erosional shear stress similar to the erosional shear stress necessary to erode the in situ Buzzards Bay muds (0.8 dynes/cm^2). Beds biogenically reworked for shorter periods had high values of erosional shear stress, up to twice that of the two month bed.

The bed shear stress necessary to erode flat beds of Buzzards Bay sediments increased as the concentration of organic matter in the sediments increased. Deposit-feeders were absent in these beds, and the mode of deposition was kept uniform, so the increase of erosion resistance with increase in organic content is considered a reliable indication of sediment behavior, and not an artifact of experimental conditions.

During the in situ experiments, lee drifts were created behind resistant roughness elements on the sea floor. A brief study of lee drift formation in the laboratory suggests that the formation of lee drifts from fine-grained sediments can be predicted to take place when the body Reynolds number of the resistant roughness elements is below a critical value.

Thesis Supervisor: Dr. J. B. Southard

ACKNOWLEDGMENTS

The assistance of many people made this study possible. In particular, I thank Drs. J.B. Southard and D.A. Ross for their help during this study. Their continuous support, advice and encouragement are deeply appreciated. The encouragement and support given by Dr. C.D. Hollister is also acknowledged.

Assistance in the construction of equipment was given by Mr. W. Gardner and Mr. S. Briggs. Dr. G. Rowe, Mr. C.H. Clifford and Mr. T. Stetson assisted during diving operations. Mr. M. McCamus and Mr. R. Nowak rendered engineering assistance. Ms. H. Quinby performed the ATP analyses. The expert seamanship of Mr. R. Coburn, Mate of the R.V. ASTERIAS, contributed to the success of the field experiments. Mr. R. Edwards provided time on his own vessel for some field testing of research gear. R. Flood assisted in a current velocity survey in Buzzards Bay.

An Ocean Industries Program grant to Dr. David A. Ross of W.H.O.I. funded a pilot project from

which this study grew. The Education Program at the Woods Hole Oceanographic Institution provided salary support through part of the study; the Office of Naval Research also supported this research and provided salary support through grants to the Woods Hole Oceanographic Institution and the Massachusetts Institute of Technology.

Drs. J.B. Southard and D.A. Ross read the manuscript and gave valuable suggestions for its improvement.

TABLE OF CONTENTS

Table of contents continued Page

Table of Contents continued Page

LIST OF FIGURES

LIST OF TABLES

GLOSSARY OF SYMBOLS

Symbol	Meaning
C	Cohesion
h	channel height
K	roughness element size
l	characteristic length
u	flow velocity
u_c	critical erosion velocity
u_{100}	velocity at one meter above the bed
u_0	characteristic velocity
u_*	shear velocity
τ	bed shear stress
τ_y	Bingham yield stress
ρ	fluid density
μ	dynamic molecular viscosity
ν	kinematic viscosity
R	Reynolds number
R_K	body Reynolds number
σ'	effective stress
ϕ	friction angle of sediment particles
$\gamma_{(W \text{ or } M)}$	specific weight of water and manometer, respectively

CHAPTER I

INTRODUCTION

The purpose of this thesis is to characterize some of the important flow and sediment parameters influencing the erosion of fine-grained marine sediments. Many workers have focused their attention on erosion in fresh water; much less effort has been expended on marine erosion.

Attempts have been made during some recent laboratory experiments to estimate the resistance of estuarine and deep sea sediments to erosion. It will be shown that the results of these experiments are difficult to compare to erosion on the sea floor, because the effect of sampling and laboratory preparation on erosional resistance has not been adequately determined.

Direct observations of the effects of near-bottom currents on the underlying sediments have been made during a number of long term experiments in several marine environments (e.g. Sternberg, 1969; Rowe et al, 1974). However, in most environments erosional events are usually infrequent and aperiodic; long periods of observation and high sampling rates are thus required.

THESIS OBJECTIVES

An empirical approach was used in this thesis to study the behavior of fine marine sediments during erosion. Specifically, field and laboratory experiments were conducted to:

1) determine the critical flow conditions (erosion velocity and bed shear stress) necessary to initiate *in situ* erosion of undisturbed beds of predominantly fine-grained marine sediments;

2) compare the *in situ* results with erosion of the same sediments in the laboratory, redeposited under conditions both similar and dissimilar to those in the natural sedimentary environment;

3) determine the relationship between biological activity, concentration of organic material, and erosion of fine marine sediments.

To accomplish the first objective of this study an *in situ* flume has been developed. Estimates were made with this device of the critical shear stress necessary to initiate erosion of undisturbed marine sediments. The *in situ* flume was also used to study development of bedforms during erosion.

To accomplish the second and third objectives, beds made

from sediments collected at the site of the sea floor experiments were eroded in a laboratory flume after being deposited under a variety of conditions. In one type of laboratory erosion experiment, bed surfaces having properties comparable to bed surfaces of the natural deposits were produced by allowing the organisms found in the sediments to rework the bed for various periods of time after deposition. The effect of organic bonding on erosion resistance of flat beds was studied by preparing beds from sediments of varying organic concentration. The generation of certain bed forms characteristic of the fine-grained sediments was also studied in the laboratory flume.

In the following section a brief review is presented of previous work. This is followed by chapters describing results of the field and laboratory work. In the final chapter the observations made during the study of the behavior of fine sediment during erosion are discussed and compared with natural processes in various sedimentary environments.

PREVIOUS WORK

Physical properties such as cohesion, floc fabric, thixotropy, composition and size distribution seem to be important in determining the erosional resistance of a fine

sediment. Composition and concentration of organic material, both living and dead, as well as bioturbation and habitat building also affect the erosional resistance of fine sediments to some degree. The significance of the above physical properties is discussed in detail in Appendix A, and biological aspects are discussed throughout the text, where applicable.

While some theoretical and empirical relationships among these properties are known, they are exceedingly complex, and it has not been possible to use them as a basis for developing a predictive model for erosion of fine sediments.

Most progress in this field has come from empirical studies. Sundborg's (1956) modification of Hjulstrom's (1939) curve is a typical example (Figure 1) of the several empirical and theoretical curves expressing the current velocity or bed shear stress necessary to erode, transport, and deposit sediments as a function of grain size. Other investigators whose work has produced similar curves include Shields (1936), Inman(1963), Heezen and Hollister (1964), Postma (1967), and Sternberg (1972). An important but generally overlooked point is that the data on which these curves are based apply mainly to flows over noncohesive

Figure 1. Sundborg's (1956) curve expressing the current velocity (measured at various heights above the bed) necessary to erode, transport, and deposit sediments of various grain sizes. All data used by Sundborg to create this curve are from fresh water flows over essentially noncohesive sediments. The uppermost and lowermost curves encompass the velocities and grain sizes at which erosion should occur. See text for further explanation.

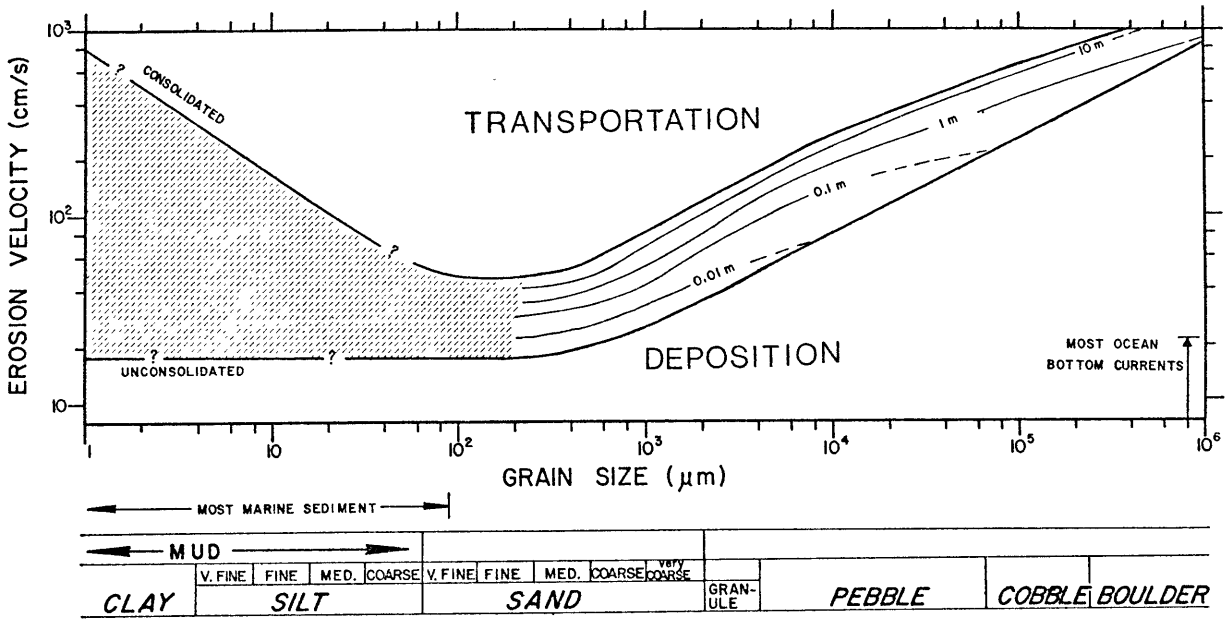
EROSION VELOCITY (cm/s)
10^3
10^2
10
CONSOLIDATED
?
TRANSPORTATION
10 m
1 m
0.1 m
0.01 m
UNCONSOLIDATED
DEPOSITION
MOST OCEAN BOTTOM CURRENTS
1
10
10^2
10^3
10^4
10^5
10^6
GRAIN SIZE (μm)
MOST MARINE SEDIMENT
MUD
V. FINE
FINE
MED.
COARSE
V. FINE
FINE
MED.
COARSE
very COARSE
CLAY
SILT
SAND
GRAN-ULE
PEBBLE
COBBLE
BOULDER

sediments of coarse silt size or larger. The broadly defined portion of the curve of grain size versus erosion velocity below about 62 μ (silt) shown in Figure 1 (and in the other curves cited above) is sometimes drawn to give the impression that its boundaries have been determined by extensive field or laboratory measurements. Actually, this part of the curve is a region of uncertainty based on one semi-quantitative laboratory experiment, intuition of the workers, and extrapolation of trends from coarser grain sizes. Therefore, the curves cited above cannot be used to infer erosion velocities of fine sediments.

An important point stressed by some previous workers is that average flow velocity is not the best flow property to use in describing erosion of sediments. This is because the relationship between average flow velocity (total discharge divided by flow cross-section) and bed shear stress τ (frictional force exerted by the flow per unit area of the bed) is not unique. That is, two flows of the same average velocity may have widely differing τ. It has therefore been suggested that the critical condition for erosion should be expressed as a function of τ, a flow parameter which

(theoretically at least) can be uniquely defined.

This concept was used by Partheniades (1962, 1965), Einstein and Krone (1961), and Krone (1962), who were among the first to rigorously explore the sediment and flow properties controlling the initiation and rate of fine sediment erosion. A single type of sediment was used by the above workers: San Francisco Bay mud; an estuarine mud composed of equal parts silt and clay with 2-3% organic material. Two types of beds were used by Partheniades for erosion in a laboratory flume. The first type was formed by remolding the mud at its original water content, spreading it in the flume by hand, and smoothing to form a compact bed 5-10 cm thick. The second type of bed was deposited presumably by flocculation, from slowly flowing, highly concentrated suspensions. Bulk shear strength varied by 100 to 1 between the two bed types.

Partheniades (1962, 1965) showed that erosion of both types of beds was initiated at the same critical value of bed shear stress; this suggests that bulk shear strength is not a good estimator of erosional resistance. It was also observed that erosion rates for a given value

of τ were up to three times higher for the flocculated beds than for the remolded beds. The preceding observations also suggest that the physical properties of the sediments which govern initiation of erosion are similar in the surface layers of both the flocculated and remolded beds, although properties governing erosion of subsurface layers may be dissimilar.

The relationship between suspended sediment concentration in eroding flows and erosion rate of the bed was also explored. When τ was the same it was observed that, although the erosion mechanisms may have differed, erosion rates were independent of supension concentrations in the eroding flow. Both Partheniades and Krone noted that bed shear stress at the initiation of deposition from dilute suspensions was less than the critical erosional shear stress.

Partheniades (1965) proposed the following model for erosion of fine cohesive sediments. Fine sediment particles exist as open networks of flocs at the bed surface. Large floc groups are bonded to only a few adjacent flocs, so that their total bond strength is weak compared to the strength of bonds between smaller flocs or between individual particles within the flocs. Erosion is initiated when the

instantaneous τ exceeds the bond strength between the more weakly bonded flocs. As the surficial floc layer is removed, groups of flocs which have successively larger numbers of bonds with their neighbors are exposed to the flow. Higher average and instantaneous τ is required to remove these flocs, because of their higher total bond strength. Erosion finally ceases when the maximum instantaneous τ is smaller than the smallest bond strength between the flocs.

Experimental conditions during Partheniades' and Krone's studies were unlike natural environmental conditions in several ways. Concentrations of suspended sediments far in excess of those occurring in nature were used to prepare beds for erosion, and this probably produced unnatural bed fabrics (see discussion of microfabric in Appendix A). The artificial sea water used had high concentrations of iron which coated and partially cemented the sediments during some extended experiments, thus increasing erosional resistance. During deposition experiments, the fabric of suspended-sediment flocs was altered in an unknown way by each passage they made through the intensely turbulent pump and return-flow piping system in the flume. Finally, the importance of

organic binding or biogenic reworking in the estuarine sediments was not investigated.

Postma (1962, 1967) and Kuenen (1965) both used circular flumes to explore the relationship between water content and erosion velocity in an estuarine mud. Both series of Postma's experiments showed that critical erosion velocity varied inversely with water content and directly with compaction time, while Kuenen found an opposite relationship between erosion velocity and water content. Neither author comments on the disagreement found in their results, and descriptions given of their experimental techniques are too brief to allow post facto interpretation. One important result of Postma's was that small variations of water content correspond to large variations in erosion velocity. Except for extreme cases, water content of sediment does not by itself indicate the state of aggregation or strength of a sediment (see Appendix A); it is therefore not surprising that water content is not a sensitive predictor of erodibility.

Migniot (1968) examined the erodibility and some physical properties of 15 estuarine muds of various compositions. Migniot found that, to a first approximation, the critical value of shear velocity u_* (square root of bed shear stress

divided by fluid density) necessary to initiate erosion can be given by the equation $u_* = 0.5\,\tau_y^{1/2}$ where τ_y is the "initial rigidity" or Bingham yield strength of the sediment. Migniot's results apply only to those sediments having τ_y more than 10 dynes/cm^2. By comparison, Krone (1963) measured τ_y values of 1 to 14 dynes/cm^2 for eight different estuarine muds, but over 70% of his measurements were well below 10 dynes/cm^2.

Terwindt et al (1968) studied erosion of sand-clay laminations deposited on a tidal flat by digging rectangular channels into the sediments, leveling the channel floors by hand, and pumping water through at various velocities. Their results, which must be viewed with caution because of the initial disturbances to the sediments, showed that τ was about 11 dynes/cm^2. Average erosion rates varied between 1 to 3 mm/hr for stresses of 11 to 40 dynes/cm^2. Erosion rates at a constant stress decreased toward very low values with time. No other estimates of τ for sand-clay beds are known to the writer, but for comparison, τ for a quartz-sand bed with median diameter 100 μm is 1 to 2 dynes /cm^2 (Sternberg, 1971).

Pierce et al (1970) obtained a crude estimate of the erosional resistance of the muddy sediments exposed on a

tidal flat by eroding them with a bottomless circular flume. A critical erosion velocity was defined when a rapid and large increase in the concentration of suspended sediment took place. Muds collected in the same area were reconstituted and eroded in a similar circular flume in the laboratory; the same criteria for erosion were used. Erosion velocities and rates of erosion (increase in the concentration of suspended sediment with time) were similar in both the field and laboratory experiments. However, the manner in which the water in the circular flume was circulated makes comparison with natural erosion processes difficult. Water was stirred in the circular flume by four paddles which extended vertically almost to the sediment surface. As the paddles were accelerated, the water in the area between paddles moved faster than the water in the area between the bottom of the paddles and the sediments. Internal shearing of the water would then cause the formation of non-stationary eddies and nonuniform secondary circulations in the flow. If so, then the distribution of bed shear stress probably also would be nonuniform and no quantitative inferences can be drawn from this study.

Southard et al (1971) eroded a slightly cohesive,

calcareous deep-sea ooze with sea water in a recirculating laboratory flume. Beds were formed by deposition from dense, still suspensions. As in some other studies, critical erosion velocities varied inversely with water content and directly with compaction time. The data of Southard et al also suggest that the effect of compaction and dewatering on erodibility asymptotically approaches a maximum within the first 10-20 hours after initial deposition. One of the main distinctions of these experiments was that they were the first erosion experiments on deep-sea sediments using sea water in a laboratory flume.

MacIlvaine (1973) obtained a small box-cored sample of clayey silt from the New England continental slope using a research submersible and performed two erosion experiments in a straight laboratory flume. Erosion of the "undisturbed" box-cored sediments commenced at a velocity in the flume which was approximately equivalent to a velocity (u_{100}) of 65 cm/sec at one meter above the sea floor. After mixing and redepositing u_{100} was somewhat lower, about 35-45 cm/sec. Fibrous, organic-looking material which collected in low spots on the bed was very similar to "organic" aggregates

observed at the surface of the continental slope sediments during the submersible dive. This material was easily transported as bed load and was deposited when u_{100} was less than about 23 cm/sec. Although it is not possible to evaluate the effect of sampling disturbance and sampling preparation techniques on sediment erodibility, MacIlvaine's estimates of critical u_{100} are probably the best available for this type of sediment.

Lonsdale and Southard (1974) studied the erodibility of a red clay from the central Pacific Ocean in a laboratory flume. Beds were prepared from still suspensions of various concentrations and allowed to compact for 24 hours. Measurements which were made during these experiments showed that resistance to erosion depended on compaction time and original water content of the suspensions from which beds were deposited. Lonsdale and Southard estimated that a u_{100} of 30 to 70 cm/sec would be required to erode red clay sediments having water content of 70 to 85%. Small changes in water content in the red clay beds corresponded to large changes in erosion velocity. No bed properties other than water content, grain size, and mineralogy were measured during the above study.

The reservations applied to the results of previous investigators relative to bed-preparation techniques apply also to the results of Lonsdale and Southard.

SUMMARY

The physical properties of muds formed from suspensions depend, among other things, on concentration of suspended matter during deposition (see Appendix A). Beds used in most previous experimental studies of erosion processes were deposited from relatively dense suspensions, so comparisons with beds formed from natural, dilute suspensions should be made with caution. Slow deposition from very dilute (1-5 mg/liter of suspended solids) flowing suspensions has been done in one previous experiment to form beds for erosion in a flume (Einsele et al, 1975). However, flocculation processes in fresh water are much different than those which occur in marine waters (see Appendix A), so extrapolation of the results of Einsele et al to the marine environment is difficult.

Size and shape of flocs formed in flowing suspensions also depend on hydrodynamic conditions such as shearing rate. The experimental beds formed from dense still-water suspensions do not take into account this important effect.

Except for Partheniades (1962, 1965), investigators have given little attention to the mechanisms involved in erosion of marine muds. This is primarily because of the complexities of theoretical analysis and difficulties in direct observation of the erosional process at the bed surface. Recent advances in electron microscopy have led to a better understanding of the fabric of mud floccules (Bowles, 1968; Pusch, 1970; Collins and McGown, 1974; Appendix A) which may result in a better understanding of the relationship between floc fabric and erodibility.

An important observation made during earlier experiments was that erosion velocity or bed shear stress is a function of sediment water content and compaction time. This also points out the importance of thixotropic strength increases on erodibility.

A second important observation was that bulk shear strength apparently is not directly related to initiation of erosion. In some experiments it has been possible to infer that properties of the surface layers which control initial resistance to erosion may be the same for beds having different values of bulk shear strength.

Finally, and perhaps most importantly, there is no

doubt that properties influencing erosion resistance of fine marine sediments are altered in some way during sampling and laboratory preparation procedures. Neither the sense nor the magnitude of these changes was determined in previous work. Hence, no matter how much care is taken in sediment sampling, there is no direct link between field and laboratory estimates of critical erosional velocity or bed shear stress for fine marine sediments.

CHAPTER II

IN SITU FLUME EXPERIMENTS

INTRODUCTION

The in situ flume lowerings were done from R.V. ASTERIAS. Dates and locations of the in situ experiments are summarized in Table 1 in the following section.

Location of The In Situ Experiments

Table 1 summarizes the locations and dates of the field experiments. The site of the first experiment (AST 74-16) was in Tarpaulin Cove in Vineyard Sound (Figure 2; symbol TC). The station was located approximately 100 m offshore in the northeastern extremity of the Cove.

The remaining experiments were all conducted at Station K in Buzzards Bay (Figure 2, symbol K). Station K was located at a range of 0.75 nm and a bearing of 260° on the permanent navigational buoy (BW "WI" gong) shown at approximately 41°32'10" N, 70°44'55" W on C.&G.S. map 249. DECCA radar was used to locate Station K during the first three experiments, and a maximum error-circle radius of 100 m was estimated for reoccupying the station. A bottom-moored surface buoy was left at the station to locate it for the remaining four experiments. The depth at Station K is about 16 m.

TABLE 1

Listing of stations, dates, and activities

Experiment No.	Date	Station	Activity
BBPS 1	11/6/72	Station K, Buzzards Bay	coring
BBPS 2	1/12/73	Station K, Buzzards Bay	coring
AST 74-4	3/1/74	Station K, Buzzards Bay	coring
AST 74-16	8/13/74	Tarpaulin Cove, Vineyard Sound	flume
AST 74-17	8/15/74	Station K, Buzzards Bay	flume
AST 74-18	8/20/74	Station K, Buzzards Bay	flume
AST 74-19	8/30/74	Station K, Buzzards Bay	flume
AST 74-21	9/19/74	Station K, Buzzards Bay	flume
AST 74-23	10/30/74	Station K, Buzzards Bay	flume
AST 74-24	10/30/74	Station K, Buzzards Bay	flume
AST 75-1	2/4/75	Station K, Buzzards Bay	flume

Figure 2. Map showing stations occupied during field experiments with the *in situ* flume and the approximate distribution of the mud facies in Buzzards Bay.

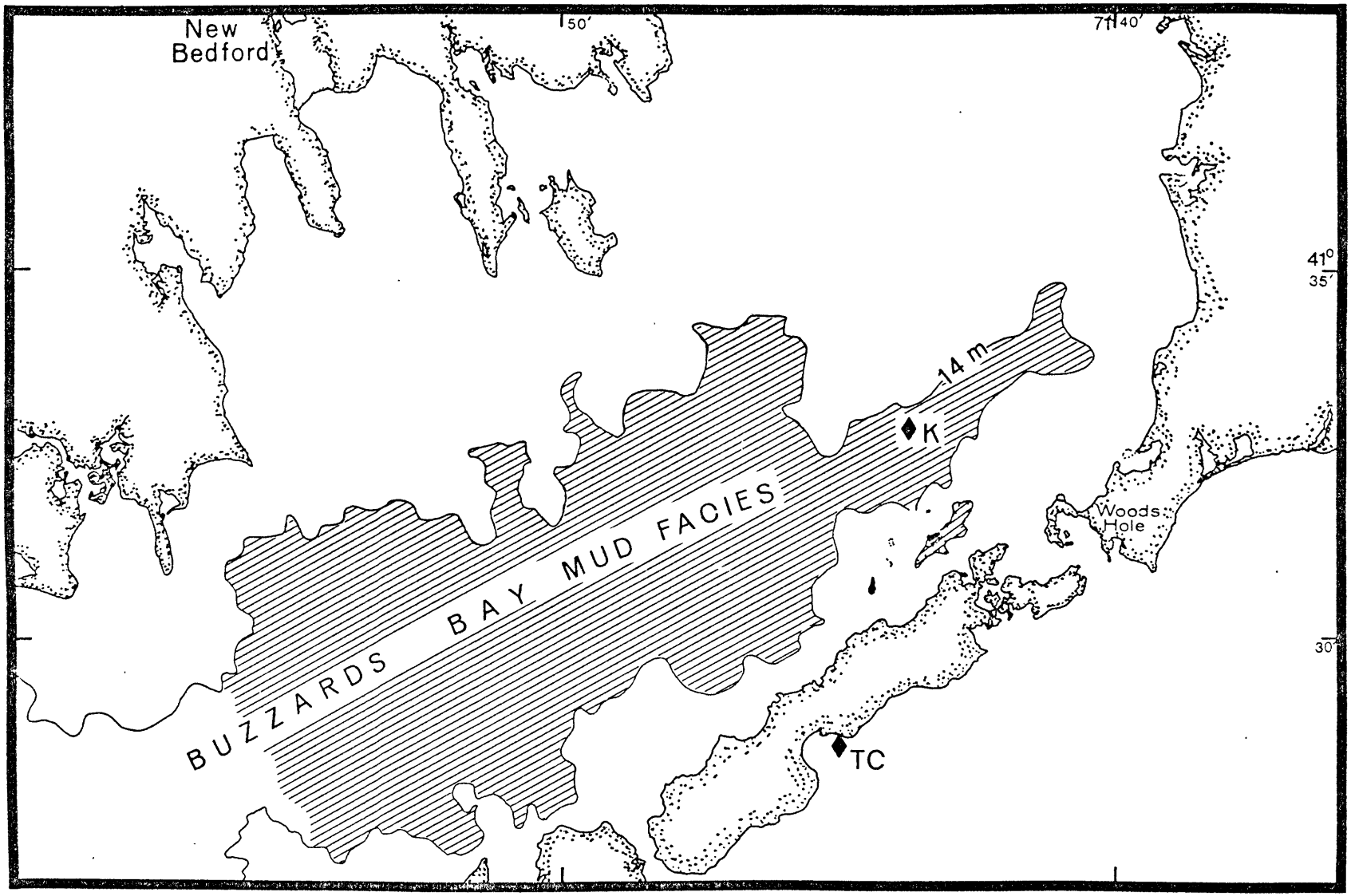
New Bedford
50'
71°40'
41°
35'
30'
14 m
K
TC
Woods Hole
BUZZARDS BAY MUD FACIES

PHYSICAL AND BIOLOGICAL PROPERTIES OF FINE SEDIMENTS IN BUZZARDS BAY

In this section the results of a survey of the physical and biological properties at Station K is presented. The general character and extent of the mud facies in Buzzards Bay was previously established by Hough (1940), Moore (1963), and Sanders (1958, 1960); it is found in the deeper central portions of the Bay below a depth of about 14 m (Figure 2). The above workers have shown that about 80% or more of the primary particles in the mud facies are finer than silt-size (< 62 μ), with clay-size (< 2 μ) particles averaging 30-50%. X-ray diffraction analyses of the sediments collected for this study showed that illite and kaolinite dominated the layer silicate fraction.

The site of the in situ experiments in Buzzards Bay is Station K of Sanders (1958; see Figure 2). It was chosen because the sediments there are typical of the mud facies and because interpretation of my results could be enhanced by previous and ongoing studies of the infauna and sediments in the mud facies (Sanders, 1958, 1960; Rhoads and Young, 1970; Young, 1971; Rhoads, 1973; Rhoads et al, 1974; Gilbert Rowe, personal communication; Nichols-Driscoll et al, in preparation;

Gschwend and Bowen, in preparation; Mason Brown, personal communication).

Physical Properties of the Sediment

Thirty-two cores (15 cm in length and 3.4 cm in diameter) taken at Station K were studied to establish the range of variation that could be expected in grain size, water content, and organic content of sediments eroded by the in situ flume. Cores were taken by SCUBA divers from randomly selected points within three sampling grids. The first two sample groups (BBPS1, BBPS2; Table 2) were taken from 1 m^2 and 10 m^2 grids, respectively, while AST 74-4 samples were taken along a 100 m linear strip at 5 m intervals.

Cores were quickly frozen and slices (1.0 cm to 1.5 cm thick) were taken from the near-surface layer and from a layer 5.0 cm to 5.5 cm below the surface. Water content was determined by weight loss after drying and is expressed as the weight of water divided by the wet weight of the sediment. No correction was made for the weight of salt in the water. Size fractionation was done either by standard pipette technique or by centrifugation after the dried water-content samples were dispersed in Calgon solution. Organic carbon and nitrogen in BBPS1 and BBPS2 samples was measured using a LECO C/N Analyzer. Estimates of total organic content in AST 74-4 muds

were made by determining weight lost after treatment with H_2O_2.

Water content was 55% or more in all samples (Table 2). Rhoads (1970) measured water contents of 60% to nearly 80% in the upper 0.5 cm of some Buzzards Bay muds. Water content of the surface sediments can be related to the burrowing and feeding activities of benthic invertebrates, discussed in the following section. The higher water content of AST 74-4 samples may reflect reported seasonal changes in surface productivity and infaunal activity (Rhoads et al, 1974).

Grain-size distributions of near-surface samples are similar to those determined for samples from lower in the cores (Table 1). Differences in grain-size distribution between either BBPS1 or BBPS2 samples and AST 74-4 samples may be related to environmental causes, but may also be related to the different analytical techniques used (centrifugation for BBPS1 and BBPS2 samples versus pipetting for AST 74-4 samples). It appears that, in the 17-year interval since Sanders' (1958) study, the size distribution of sediments has remained relatively constant at Station K. The results of Hough (1940) and Moore (1963) also showed no differences, either in average grain size at other stations in the Bay, or in

TABLE 2

Physical properties of sediments at Station K, Buzzards Bay.
Mean values and standard deviations are shown.

	Depth Interval (cm)	Water Content (weight %)	Grain size in % by weight			
			62μ	62-16	16-2	2μ
BBPS 1 11/6/72 7 cores 1 m^2	0.5-2.0	56±3	14±3		77±5	9±4
	5.5-7.5	55±1	11±9		76±10	13±8
BBPS 2 1/12/73 5 cores 10 m^2	0.5-1.5	55±1	13±3		71±2	16±2
	5.0-6.0	55±2	6±2		74±0	19±2
AST 74-4 3/1/74 20 cores 1 x 100 m	0.0-1.0	62±2	7±2	27±6	20±2	46±5
Sanders (1958) Surface anchor dredge	——		7	28	48	17

lateral distribution of the mud facies.

Biological Properties

The muddy bottom sediments of Buzzards Bay are reworked extensively during some parts of the year by deposit-feeding benthic invertebrates, and it has been estimated from laboratory experiments (Rhoads, 1970) that surface sediments maybe turned over on the average of at least twice per year. Thus, no discussion of sediment properties in Buzzards Bay can be complete without inclusion of biogenic effects.

Many types of invertebrates are present, including burrowing anemones, gastropods, and worms, but the fauna is generally dominated numerically by the polychaete Nepthys incisa and the small protobranch bivalve Nucula proxima (Sanders, 1958, 1960). Surface sediments have a significant fraction which is biogenically modified, either by fecal pelletization or by burrowing, excavating, tube-building, or crawling activities of the benthos. Up to 20% by volume of the surface deposits in the mud facies may be fecal pellets (Rhoads, 1973).

One major effect of biogenic reworking should be mixing of organic detritus in the reworked zone. The values of %C, %N, and total organic material presented in Table 2 illustrate

TABLE 3

Organic content of sediments at Station K, Buzzards Bay.
Mean values and standard deviations are shown.
C is total organic carbon, and N is total organic nitrogen.

	Depth Interval (cm)	Organic Content (weight %)		
		%C	%N	Total Organic Material
BBPS 1 11/6/72 7 cores 1 m^2	0.5-2.0	2.33±.18	.32±.03	
	5.5-7.5	2.38±.15	.31±.04	
BBPS 2 1/12/73 5 cores 10 m^2	0.5-1.5	2.31±.14	.32±.03	
	5.0-6.0	2.31±.17	.30±.03	
AST 74-4 3/1/74 20 cores 1 x 100 m	0.0-1.0	___	___	5.7±2.3

this point. Mean values of %C and %N are nearly uniform in the upper and lower samples of each core group. A conversion factor of 1.8 is commonly used to multiply organic carbon values to obtain approximate values of total organic matter (by weight). The values of 4.2% total organic matter obtained for the BBPS1 and BBPS2 samples is considered to be in reasonable agreement with the value of 5.7% total organic matter obtained for the AST 74-4 samples in view of the approximate method used.

The present study thus shows that organic content of the mud facies is relatively homogeneous, even between samples 100 m apart. Although concentration is relatively homogeneous, composition of the living or particulate organic material may vary laterally or with greater depth (Sanders, 1958, 1960; Gilbert Rowe, personal communication, Nichols-Driscol et al, in preparation). The effect of varying organic concentration on erosional resistance of the mud facies was investigated in the laboratory flume experiments described in Chapter III.

THE IN SITU FLUME

An *in situ* flume was used to study erosion of fine-grained marine sediments for the following reasons. First, the fixed flow geometry of the *in situ* flume channel is similar to the flow geometry of the laboratory flume used in the study, a situation which eases comparisons between flow conditions in the laboratory and field experiments. Second, each sea floor experiment has essentially the same boundary conditions (i.e. the flume channel), except for the variable being studied which is the erosion resistance of the sediments. Third, since flow in the channel is created by a self-contained pump, it is possible to do the experiments in a relatively short period of time and to control the flow conditions. Finally, emplacement of the flume creates little disturbance to the sea floor (see discussion in following section), so that experiments on undisturbed sediments are possible.

Proper design of the *in situ* flume was crucial to the success of the experiments, so considerable effort was given to designing, testing, and modifying the flume. A brief description of the flume is given here; a more complete description of the flume design, operating procedures,

current-meter calibration, and model testing, is given in Appendix B.

The flume is essentially an open-bottomed rectangular channel constructed of acrylic plastic joined together with aluminum angles (Figure 3). The channel consists of two sections: a 1.8 m long sloping entrance section where flow velocity is kept below the erosional threshold; and a 2.4 m long rectangular observation section where most of the erosion occurs. The channel is 0.6 m wide; it slopes from a height of 0.31 m at the upstream opening to a height of 0.15 m where it joins the rectangular observation section.

Flow inside the channel is created by a self-contained 12 volt DC pump-motor system. Flow speeds of up to 50 cm/sec are regulated by a sliding panel-valve arrangement between the pump and channel. A 35 mm E.G. & G. camera system capable of taking up to 450 frames (one frame every 6 to 7 seconds) is focused on an area of about 15 cm by 15 cm of the sea floor enclosed by the flume (Appendix B, Figure B-1). Apparent relief in the photographs is enhanced by low-angle lighting from the 100 watt-sec strobe light source (Figure 3, lower). Current speed was measured by a sphere-

Figure 3. The *in situ* flume. Certain minor structural and electrical details are omitted for clarity: the pump-motor case is enclose by a protective cage, and the battery box is fastened to the flume with several supports. The surrounding sea water is pulled into and accelerated through the sloping entrance section on the left, brought through the rectangular observation section, and discharged through the space between the motor and pump. Discharge is regulated by the sliding panel-valve beneath the pump. *Section A* shows schematically the relative positioning of the camera and strobe and the arrangement by which low-angle lighting is brought inside the channel.

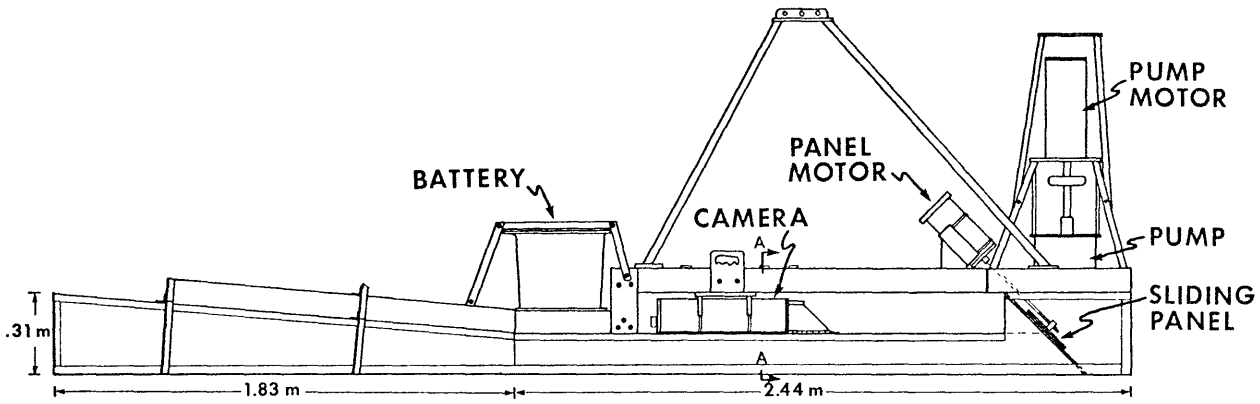

IN SITU FLUME

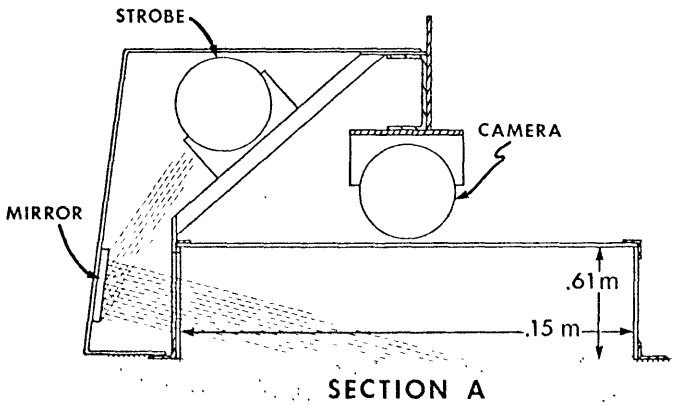

SECTION A

on-a-string which hangs from the top of the channel within the field of view of the camera. Details of current-meter calibration are given in Appendix B.

A bottom-contact switch turns on the pump and sliding panel motors and connects the camera with the strobe light. The frequency of photographs and amount of film limits the experiment to about 45 min. The time from emplacement of the flume to maximum flow inside the channel is about 32 minutes, but the flume is left on the bottom until all film is used.

Photographic Resolution

The smallest bed features resolved by the camera system were about 500 μ. The effects of erosion thus became apparent on film at some time beyond the actual initiation of erosion. The values of flow parameters cited in this study as the critical values for erosion therefore refer to the values of those parameters at the lower limit of photographic resolution.

This subjective definition of the incipient condition for erosion should not seriously affect the results of the experiments for the following reason. The size distribution of naturally occurring aggregates eroded from the sea floor at the site of the field experiments is thought to range

from perhaps 10 μ to 500 μ, with an average grain size 30-50 μ (Young, 1971; Rhoads, 1970; Gschwind and Bowen, in preparation; Mason Brown, personal communication). Thus, erosion of an average of about ten layers of bed material should be resolvable with the camera system.

Methods

The first three flume experiments (see Table 1) were carried out in the following way. After anchoring, time was allowed for the motion of the ship to reach equilibrium with the prevailing winds and currents. The flume was then slowly lowered to the sea floor until bottom contact was made. Winch and power lines to the flume were tended by hand during the experiments and slacked as necessary. Beginning with the fourth experiment it was not necessary to supply power to the flume from the ship; the flume was lowered with a nylon rope to the sea floor, and the bitter end tied to a surface float and then cast off. Observations by SCUBA divers indicate that once emplaced the flume was effectively decoupled from surface motions regardless of which lowering method was used. The presence of distinctive and persistant patterns of bed-surface features recognizable in virtually all photographs taken during each experiment also tends to

verify that the flume was not affected by either ship or buoy motion.

Sea Floor Disturbances

Possible disturbances to the sediment water interface during flume emplacement were investigated by having divers ride the flume from the surface to the sea floor. Divers' observations indicate that visibility inside the flume decreased initially due to suspension of parts of the upper 0.5 to 1.5 mm of the sediment surface. This bed layer consisted of a very porous network of flocculated bed material. Visibility returned to normal (ambient) after one to two minutes.

Since all flume experiments except one were conducted in the vicinity of one area in Buzzards Bay, there is a question of whether more than one erosion experiment took place on the same patch of sea floor. No evidence that this occurred was observed by divers during the first four experiments, and photographic data taken during the remaining experiments likewise gives no evidence of any superposition of one lowering site on a previous site.

The flat bearing surfaces along the walls and under the

pump section of the flume were observed to settle about 1 cm to 2 cm into the sediments. Observable effects of the apparent bed failure were limited to about 1 cm from the walls, and did not appear to affect the rest of the bed. A positive feature of this slight sinking-in is the good seal it ensures for the flow through the channel.

Based on the direct observations that I and other divers have made during testing and field experiments, it appears reasonable to assume that the sediment-water interface was not significantly disturbed by emplacement of the flume. What is learned from erosion experiments using the in situ flume can therefore be applied to erosion of the mud facies by bottom currents in Buzzards Bay. The results may also be applicable to the general behavior of fine-grained marine bottom sediments during erosion.

RESULTS OF THE IN SITU FLUME EXPERIMENTS

The symbol AST in the following descriptions refers to the R.V. ASTERIAS, the vessel from which the in situ experiments were done. The numbers separated by a hyphen following AST (i.e. AST 74-16,) refer to the year (1974) and cruise number (-16), respectively.

AST 74-16

This experiment took place in Tarpaulin Cove, a small inlet on Naushon Island opening into Vineyard Sound (Figure 2 symbol TC). Although it was thought that some muddy patches would be found in the Cove, only silty fine sands were found. Mechanical problems on the ship required premature ending of the experiment after about 10 min, but the data obtained showed that some erosion had already taken place.

Initially, several open bivalve shells and other unidentified coarse detritus was seen lying on the bed surface (Figure 4A). Just after flow was initiated two biogenic trails were apparently created by small benthic invertebrates (upper right of Figure 4B), one in the upper right and one under the velocity sphere. When flow velocity u reached about 5 cm/sec (Figure 4C) the trail in the upper

Figure 4. Erosion of a silty fine sand during AST 74-16, Tarpaulin Cove, Naushon Island. Flow is from top to bottom in this and following photographs. The sphere current meter is seen at the top of each photograph. An area of about 15 cm by 15 cm is encompassed in each photograph. The vertical line with short cross-tics in the center of the photographs is a reference scale, either on the 45° mirror in front of the camera, or on the flume top. Because of the angle of the mirror, distance between the scale lines varies from top to bottom of the mirror. Details of calibration of the sphere current meter and interpretation of flow velocities from flume photographs is given in Appendix B.

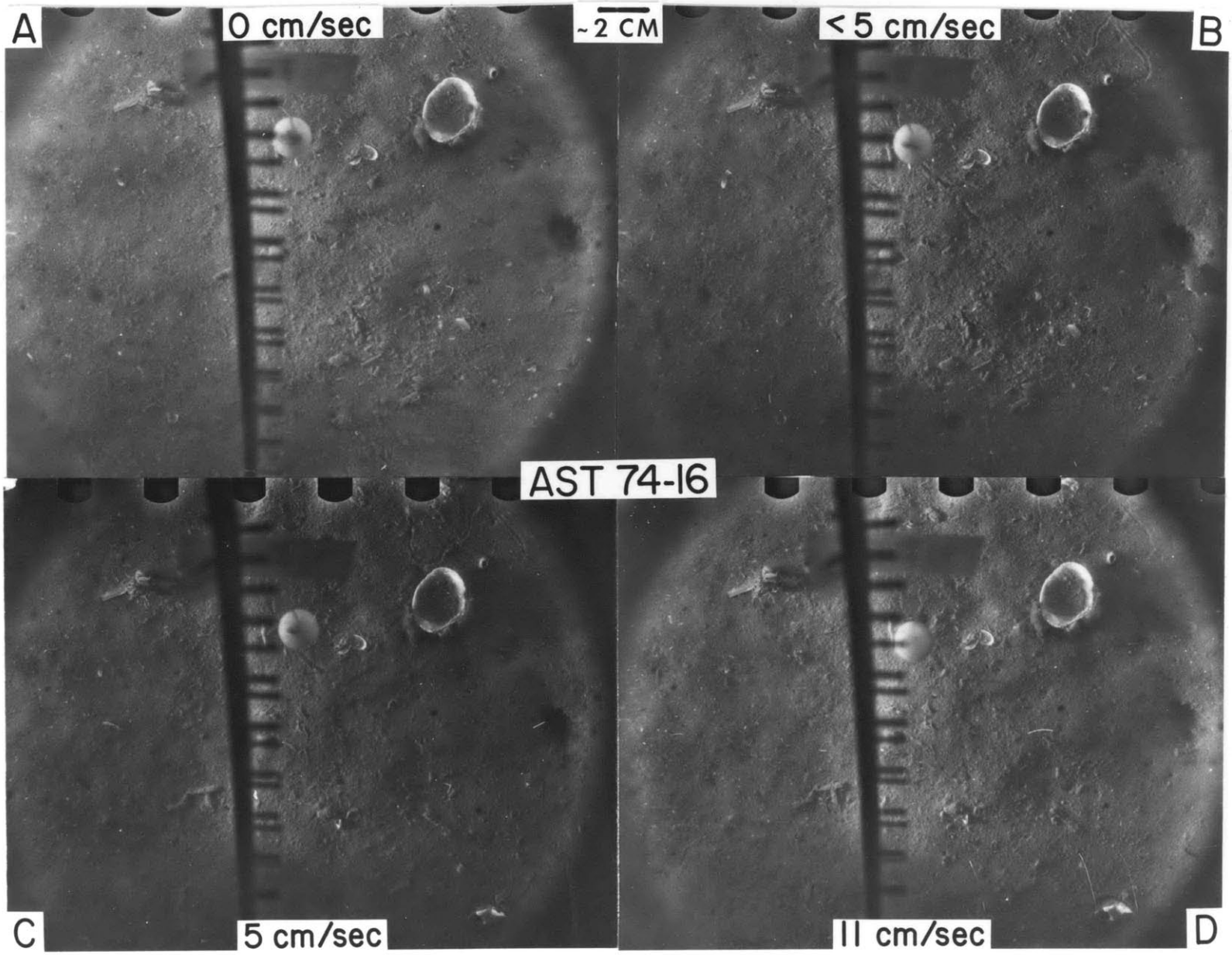
A
0 cm/sec
~2 CM
< 5 cm/sec
B
AST 74-16
C
5 cm/sec
11 cm/sec
D

right had lengthened and some of the loose surface detritus in the lower right of the bed had been removed. Near the end of this experiment, when u had reached 11 cm/sec (Figure 4D), the trails were noticeably eroded. There is also a suggestion in Figure 4D that surface features in the lower right of the bed were also being eroded.

A critical velocity u_c of about 9.5 cm/sec is inferred for erosion of the biologically disturbed portion of the bed. The surface detritus first moved by the flow at $u \doteq 5$ cm/sec may have been large particles of organic or shell material. Since the effectiveness of a flow in initiating movement of noncohesive sediment depends mainly on particle density and size, the observed low erosion velocity for large particles of surface detritus composed of low-density organic material seems reasonable.

AST 74-17

This experiment and the experiments described in the following sections took place on the mud facies at Station K, Buzzards Bay (Table 1, Figure 2). Biogenic trails were already present on the bed surface at the beginning of this experiment (Figure 5A). At low velocities (< 5 cm/sec; Figure 5B)

Figure 5. Erosion of a silty clay during AST 74-17, Station K, Buzzards Bay. Discussion of flow velocities and corresponding erosion processes is given in the text. See caption of Figure 4 for further explanation of photographs.

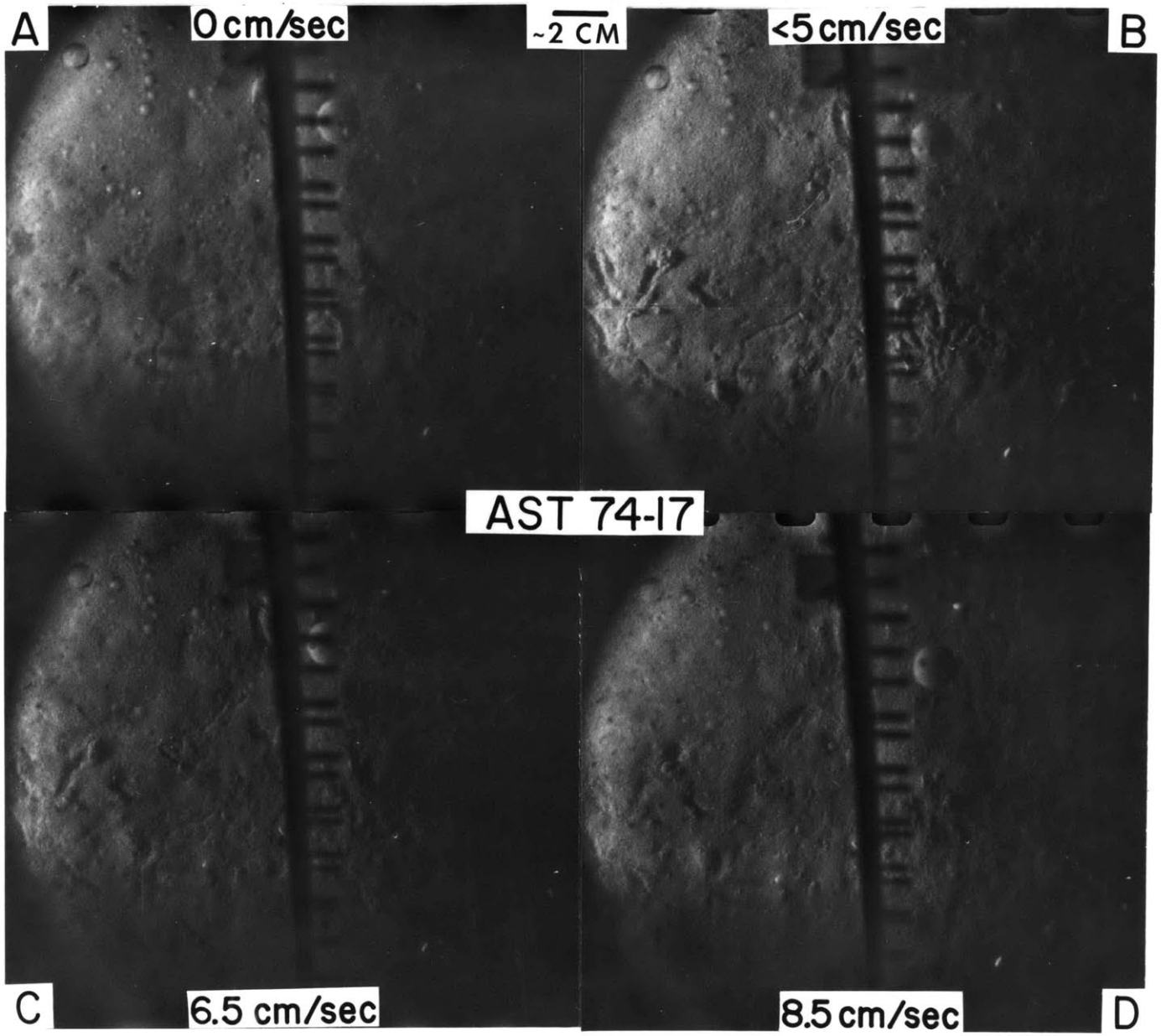
A
0 cm/sec
~2 CM
<5 cm/sec
B
AST 74-17
C
6.5 cm/sec
8.5 cm/sec
D

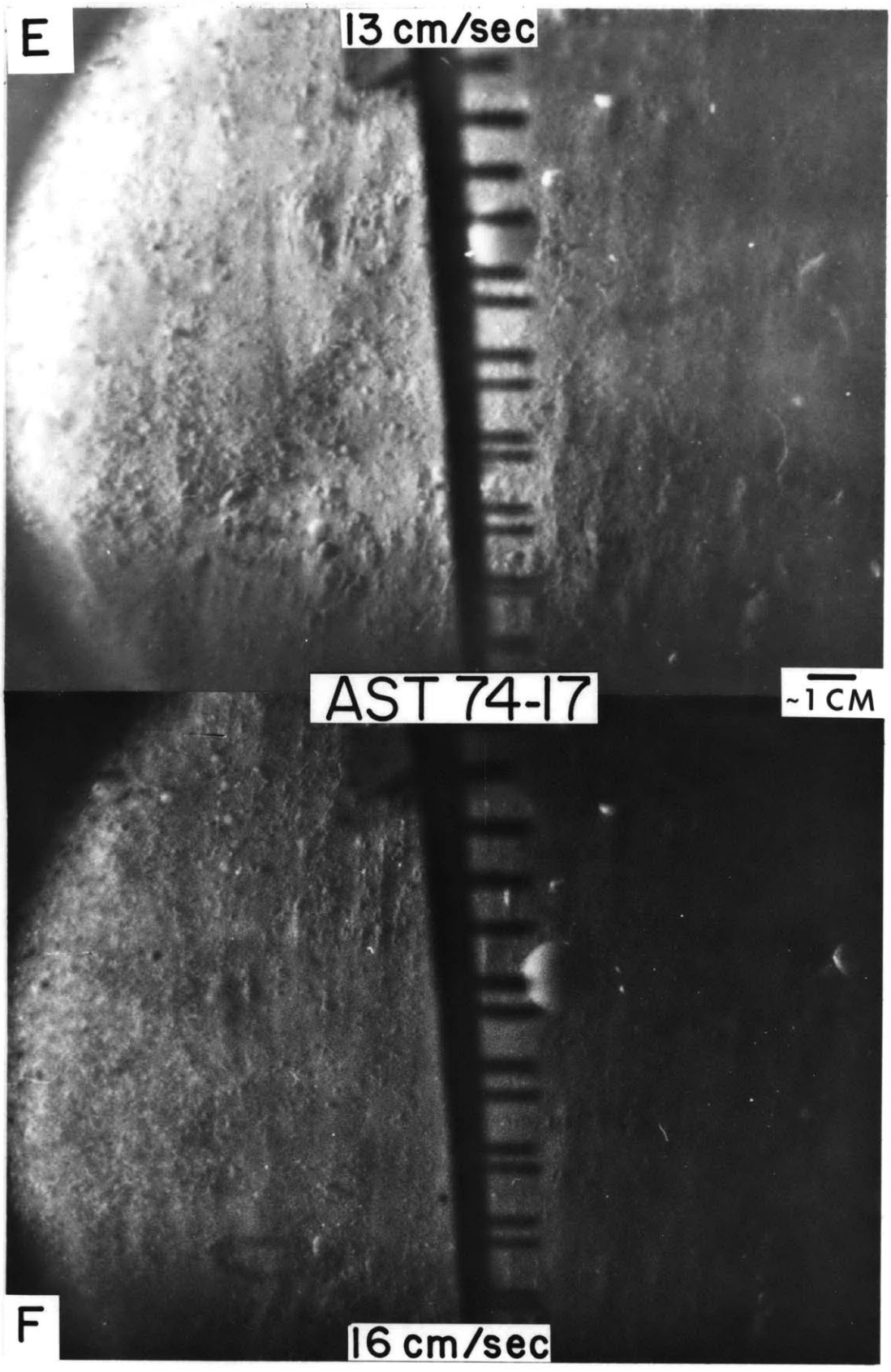
E
13 cm/sec
AST 74-17
~1 CM
F
16 cm/sec

the organisms continued to move about and create trails. At a velocity of about 6.5 cm/sec (Figure 5C) erosion of these freshly created trails was evident. As u reached about 8.5 cm/sec (Figure 5D) erosion of the deeply incised trails and smaller, presumably nonbiogenic, bed irregularities was clearly visible. When u reach 13 to 16 cm/sec (Figures 5E,F), nearly all surface features initially present had been eroded from the bed. Numerous lee drifts and longitudinal erosional features also were created behind more resistant portions of the bed. Depth of these longitudinal erosional features is estimated to be between 2 to 5 mm.

The value of u_c is estimated to be 6-7 cm/sec for the disturbed sediments around the biogenic trails. Erosion of the flatter portions of the bed was probably initiated at about 8.5 cm/sec.

AST 74-18

A large burrow opening (?) and a snail (?) were visible on the bed at the beginning of this experiment (Figure 6A). Several minutes later, but before flow velocity had reached 5 cm/sec, two biogenic trails were made parallel to the channel axis, one extending across the photograph to the left of center, and one from the bottom to the middle of the

Figure 6. Erosion of a silty clay by the in situ flume during AST 74-18, Buzzards Bay. Discussion of flow velocities and corresponding erosion processes are given in the text. See caption of Figure 4 for further explanation of photographs.

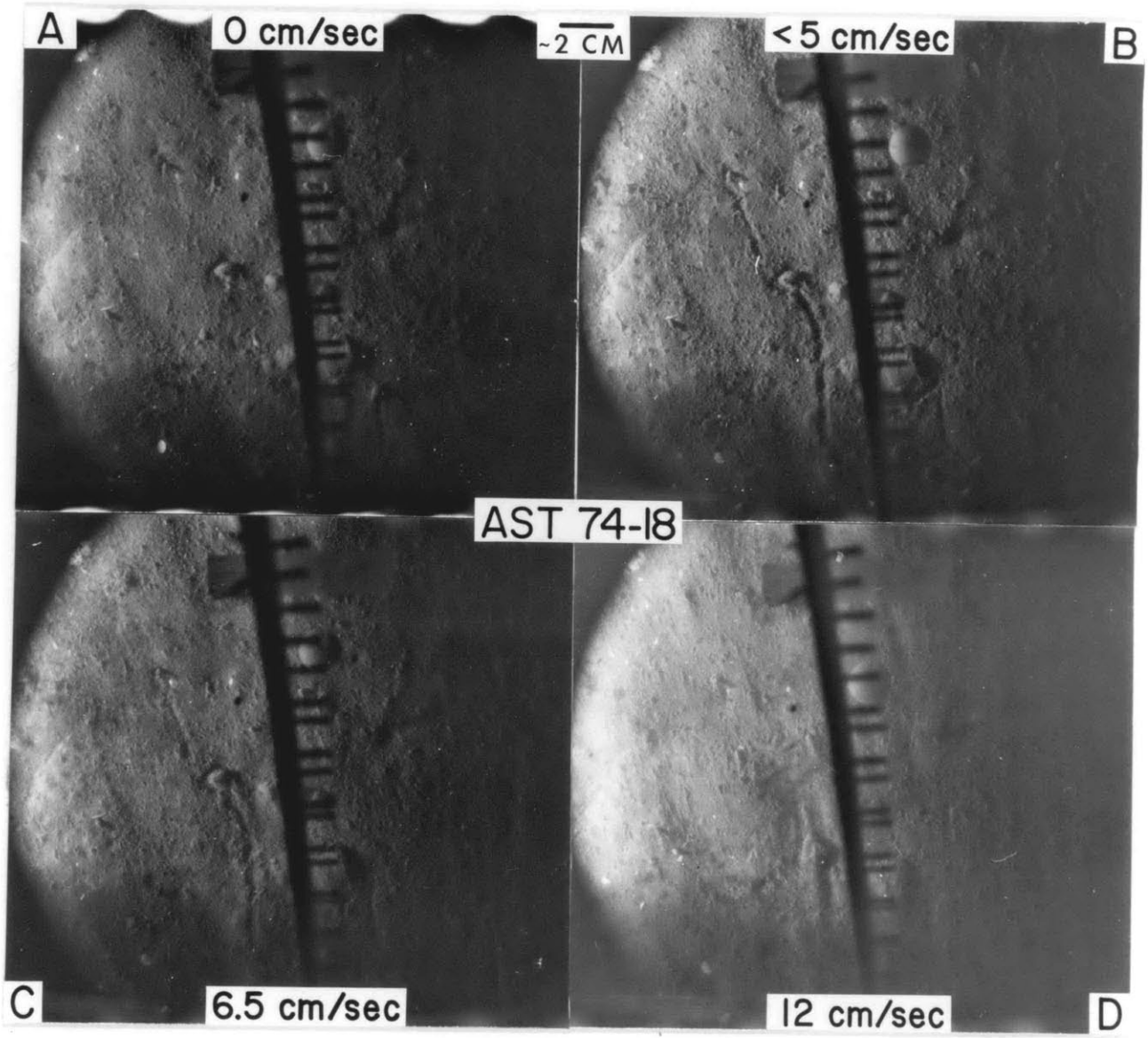
A
0 cm/sec
~2 CM
< 5 cm/sec
B
AST 74-18
C
6.5 cm/sec
12 cm/sec
D

photograph to right of center (Figure 6B). At about 6.5 cm/sec some smoothing of the bed was evident (Figure 6C). By the time velocity reached 12 cm/sec most of the bed features initially present were eroded or smoothed and reduced in size (Figure 6D). Lee drifts and longitudinal lineations were produced after erosion was initiated. For the biogenic trails u_c was about 6.5 cm/sec; the smoother, undisturbed portions of the bed began to erode at about 9.5 cm/sec.

AST 74-19

The portion of the sea floor enclosed by the flume was smooth initially except for one small (about 1.5 cm) mound transverse to the channel axis (Figure 7A). Shortly after emplacement of the flume and before flow reached 5 cm/sec a gastropod (?) crawled downstream on the bed, creating a fresh trail (Figure 7B).

Flow in the channel started between the time Figures 7B and 7C were taken, and a suggestion of smoothing of bed features is seen in Figure 7D when velocity had reached 7 to 8 cm/sec. A camera malfunction occurred shortly thereafter and no further photographs were taken. Comparison of my first-hand observations made while diving during this lowering with photographic data from the flume indicates that erosion

Figure 7. Erosion of a silty clay by the in situ flume during AST 74-19, Buzzards Bay. Discussion of flow velocities and corresponding erosion processes is given in the text. See Figure 4 for further explanation of photographs.

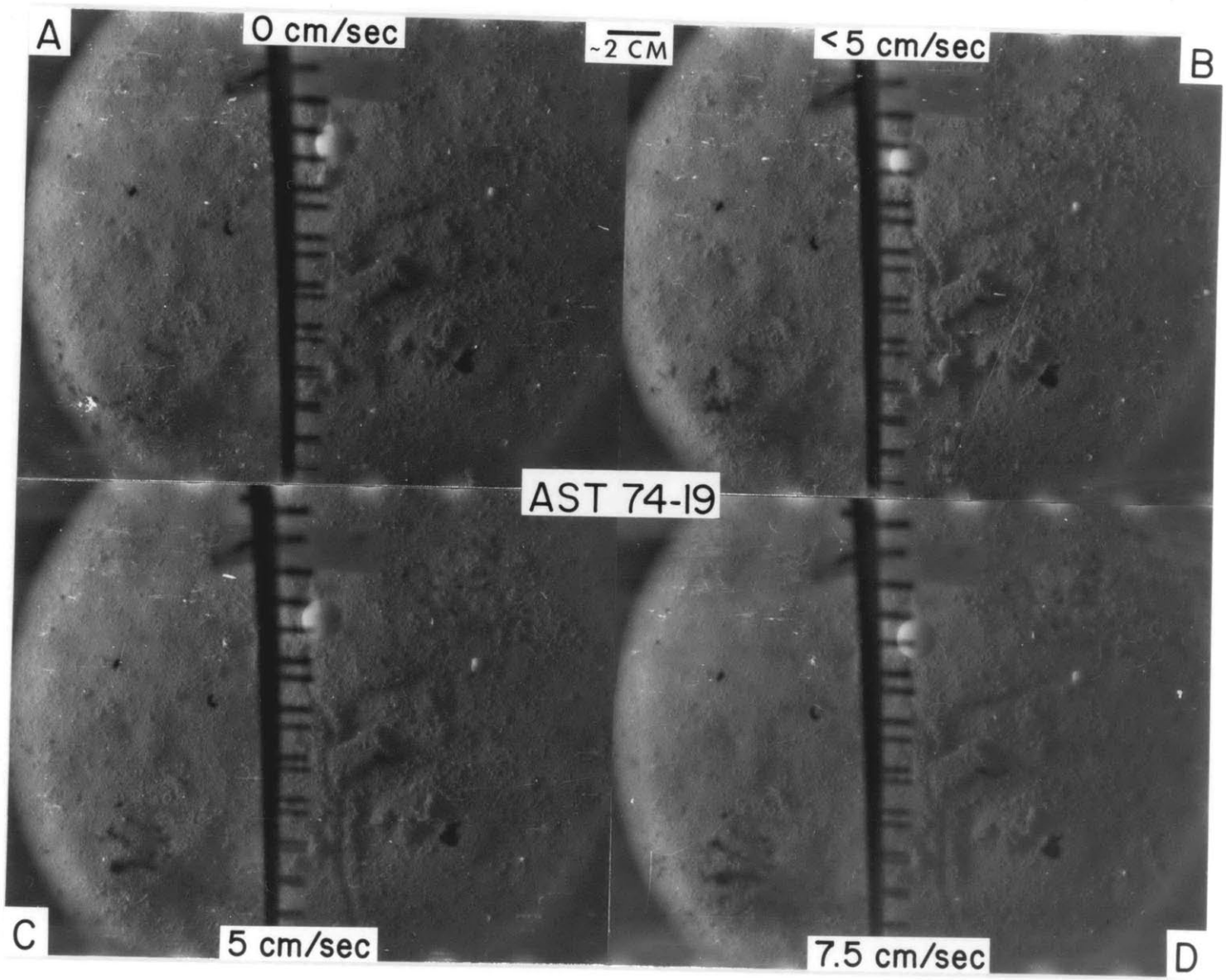
A
0 cm/sec
~2 CM
< 5 cm/sec
B
AST 74-19
C
5 cm/sec
7.5 cm/sec
D

probably commenced at about the time Figure 7D was taken; u_c is therefore inferred to be about 7.5 cm/sec. Erosional processes similar to those previously described followed, first smoothing the prominant mound seen in Figure 7D, and then gradually producing an eroded bed having numerous lee drift deposits.

AST 74-21

Concentration of suspended matter in the near-bottom waters at Station K was very high during this experiment; diver visibility was limited to about 30 cm. The turbidity was apparently a natural phenomenon not related to emplacement of the flume, since the turbid layer extended well away from the flume site.

Most of the photographs were not clear enough to resolve bed features. The few clear photographs obtained were taken after flow was well developed, so initial bed conditions were not recorded. Nevertheless, some interpretations of erosion processes are possible. Figure 8A shows the bed surface when the velocity was about 9 cm/sec. At this time several small (1-5 mm) biogenic and sedimentary mounds were present on the bed surface. A possible worm tube is seen at the upper left of the figure. The rest of the bed surface

Figure 8. Erosion of a silty clay by the in situ flume during AST 74-21, Station K, Buzzards Bay. Discussion of flow velocities and corresponding erosion processes is given in the text. See Figure 4 for further explanation of photographs.

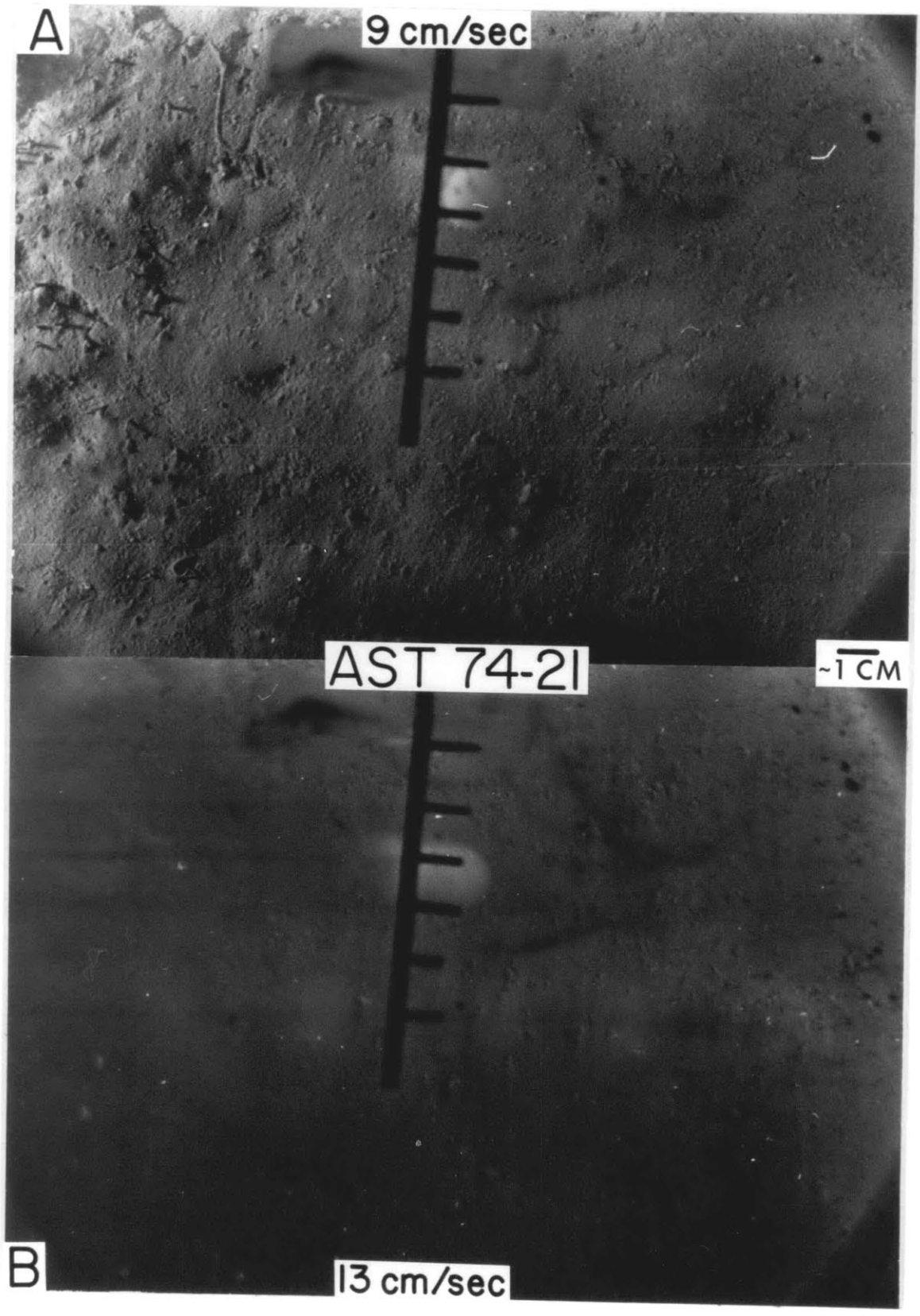
A
9 cm/sec
AST 74-21
~1 CM
B
13 cm/sec

appears smooth and flat but does not appear to have been eroded. By the time the photograph in Figure 8B was taken velocity had reached about 13 cm/sec. Resolution remained poor, but in this section of the film some lee drifts and other current lineations can be seen, implying that erosion had occurred. Critical conditions for erosion probably occurred in the interval between Figures 8A and 8B, so u_c is estimated to be about 11 cm/sec.

AST 74-23

Two sphere meters were used during this experiment, one more sensitive to velocities less than 10 cm/sec and one for the entire range of velocities. It is obvious from the photographs that the low-velocity meter did not behave in the expected way during this experiment. It was later determined that the metal ballast used to weight the nylon sphere had dropped out during the experiment, causing the sphere to become positively buoyant. Another method was therefore developed to approximate flow velocity. Values of flow velocity estimated by the sphere current meter during previous experiments were plotted against time after initiation of flow in the flume channel, and the resulting scatter plot (Figure 9) was approximated by a first order linear regression

Figure 9. Plot of velocity measured by the sphere current meter versus time after initiation of flow in the flume. A first-order linear regression curve fitted to this plot (straight line in plot) was used to estimate flow velocity during flume experiments when the sphere current meter malfunctioned.

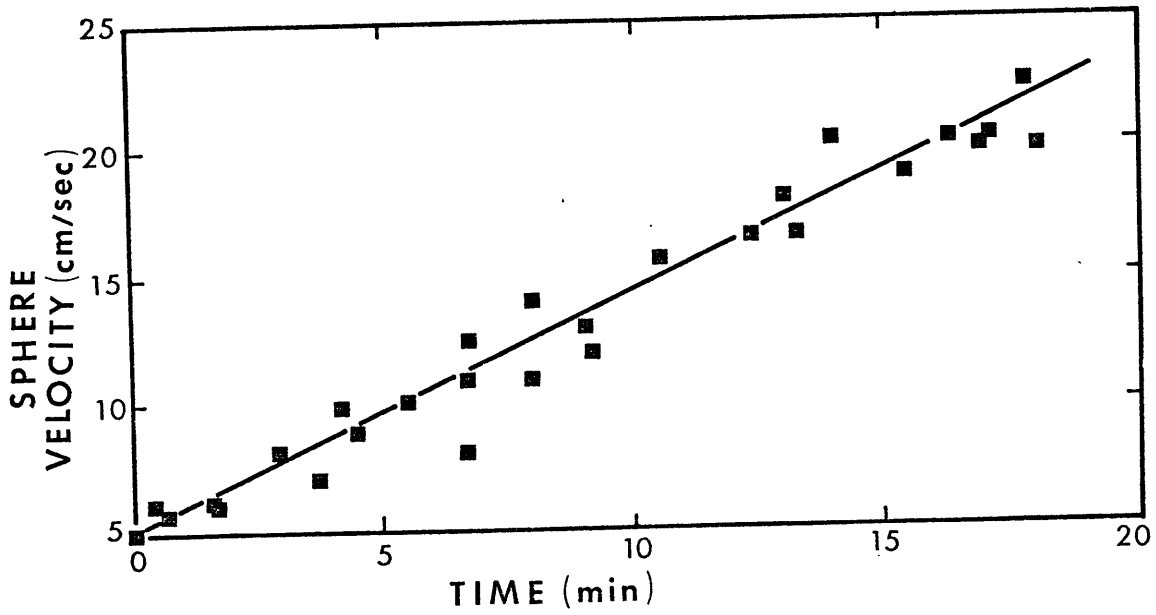
SPHERE VELOCITY (cm/sec)
25
20
15
10
5
0
5
10
15
20
TIME (min)

curve. Scatter was reasonably small (regression coefficient of 0.81; significant at the 95% confidence interval), so this curve was used to estimate flow velocity for experiments AST 74-23 and AST 75-1, when the ballast again dropped out of the sphere.

The bed surface was covered initially with numerous small (about 1 mm) mounds and several small depressions or burrow openings. One very small animal trail and several ropey fecal mounds also were seen on the bed, and a large anemone was visible at the top of the photographs under the sphere current meter. Another anemone and its shadow were just visible at the upper left margin of the photograph (Figure 10A).

Erosion of the bed probably started at a velocity of about 6 cm/sec (Figure 10B), and current lineations and lee drifts were clearly created by the time velocity reached about 9 cm/sec (Figure 10C).

Judging by the clarity of the first photographs, turbidity in the near-bottom water was very low. Photographs taken later in the experiment (Figure 10D), when u = 13 cm/sec, had much poorer resolution, and it is suspected that a rapid

Figure 10. Erosion of a silty clay by the in situ flume during AST 74-23, Station K, Buzzards Bay. Discussion of flow velocities and corresponding erosion processes is given in the text. See Figure 4 for further explanation of the photographs.

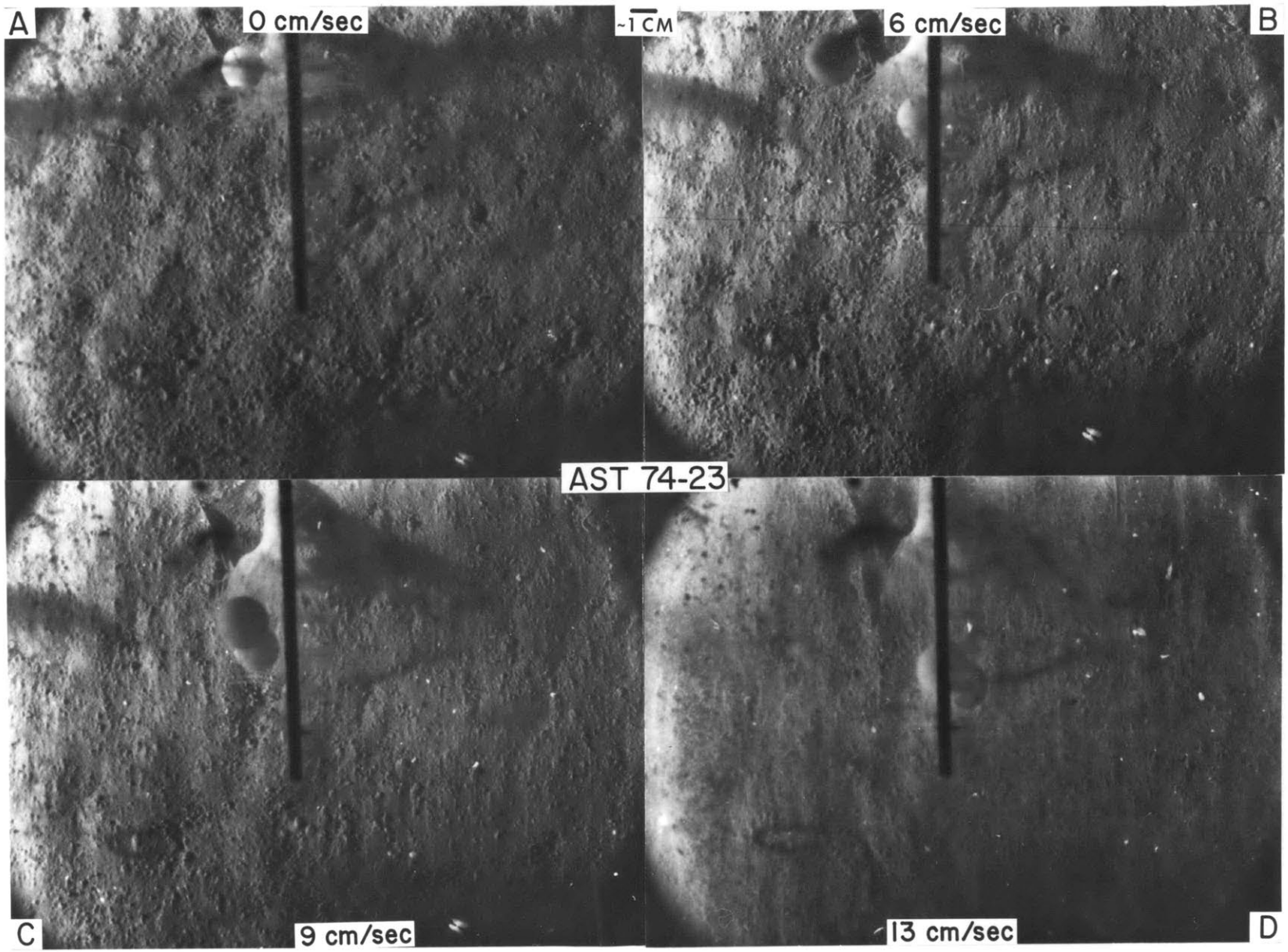
A
0 cm/sec
~1 CM
6 cm/sec
B
AST 74-23
C
9 cm/sec
13 cm/sec
D

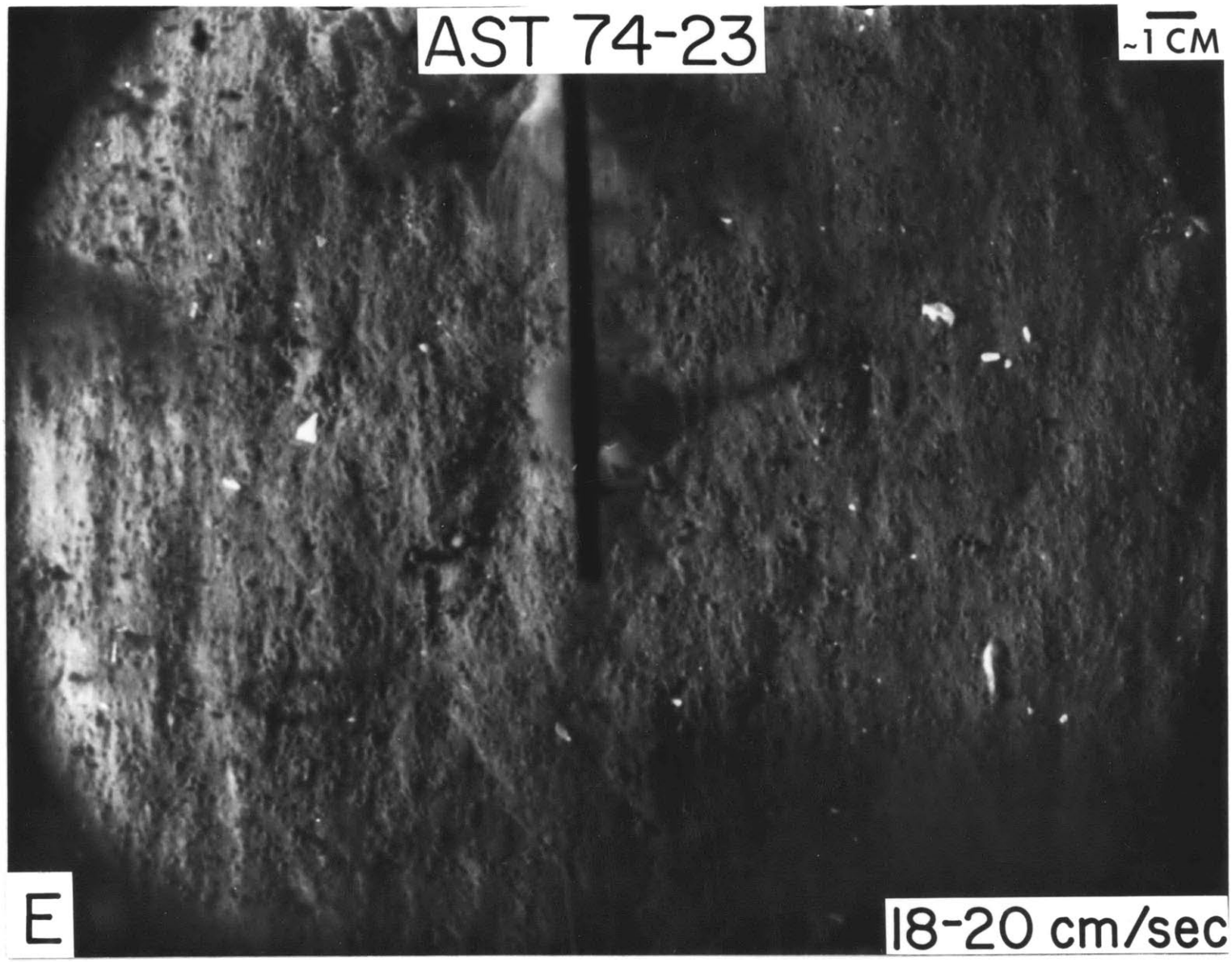
AST 74-23
~1 CM
E
18-20 cm/sec

rate of erosion may have caused the increased turbidity. In Figure 10E (u = 18-20 cm/sec) photographic resolution had again improved, and erosion had exposed numerous shell fragments and created current lineations and lee-drift deposits.

AST 74-24

The bed surface encountered during this lowering was flat and smooth, and can probably be regarded as hydrodynamically smooth because roughness elements on the bed at the beginning of the experiment were small (< 1 mm diameter mounds) and were dispersed evenly over the bed (Figure 11A). Large fecal mounds and biogenic trails were absent.

No erosion was seen as velocity increased to 11 cm/sec (Figures 11A,B). Erosion of the bed surface was not seen until flow reached about 17 cm/sec where small lee-drift deposits and some lineations were observed (Figure 11C). As erosion continued the bed was smoothed still further, removing the small conical mounds (Figure 11D; u = 24 cm/sec). After about 35 min (Figure 11E; u = 40 cm/sec) several small shell fragments were uncovered, and the bed was roughened by small lee drifts and other longitudinal lineations. As erosion continued under high velocities (Figures 11F) the

Figure 11. Erosion of a silty clay by the in situ flume, Buzzards Bay. Discussion of current velocities and corresponding erosion processes given in the text. See Figure 4 for further explanation of the photographs.

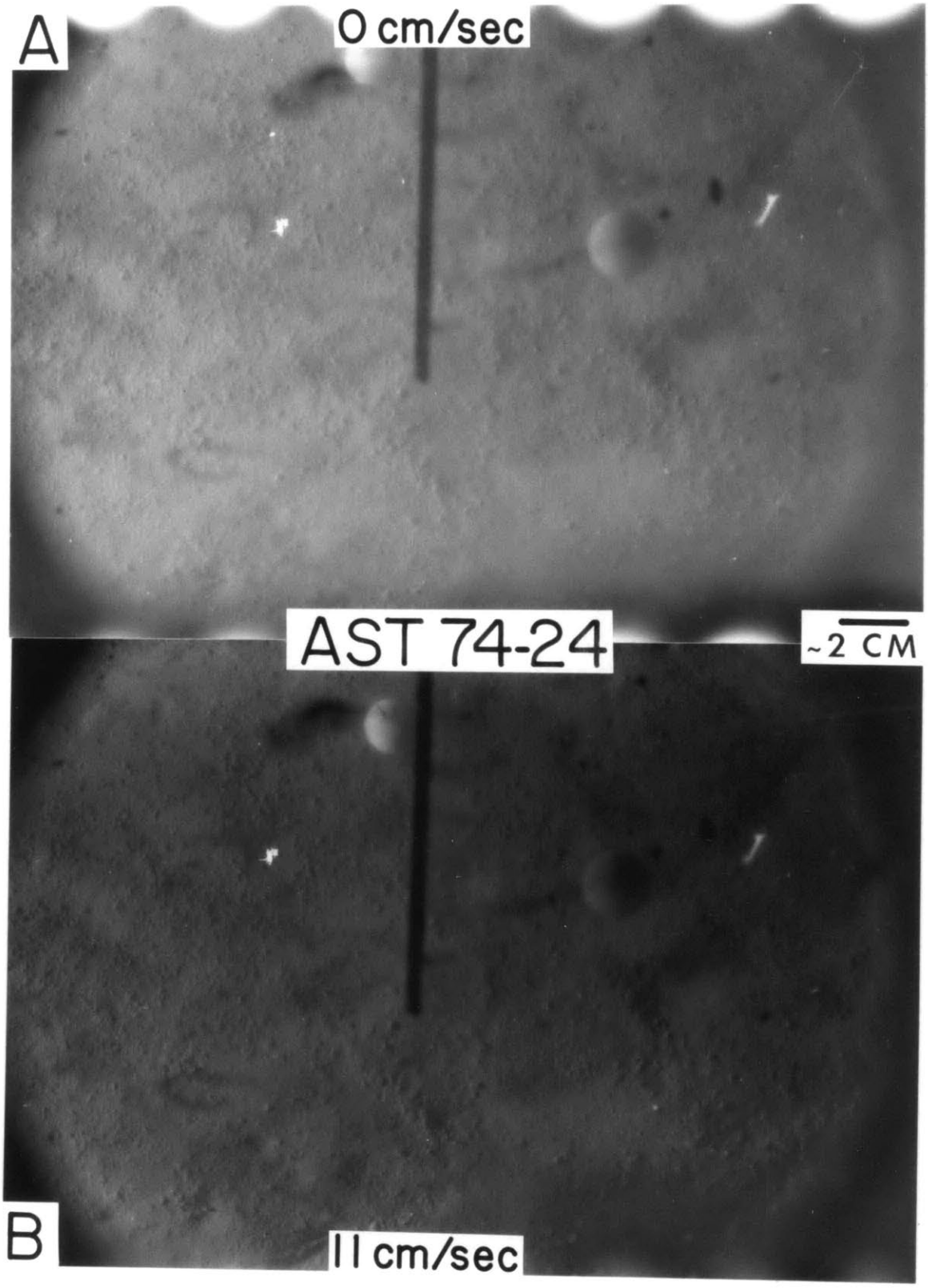
A
0 cm/sec
AST 74-24
~2 CM
B
11 cm/sec

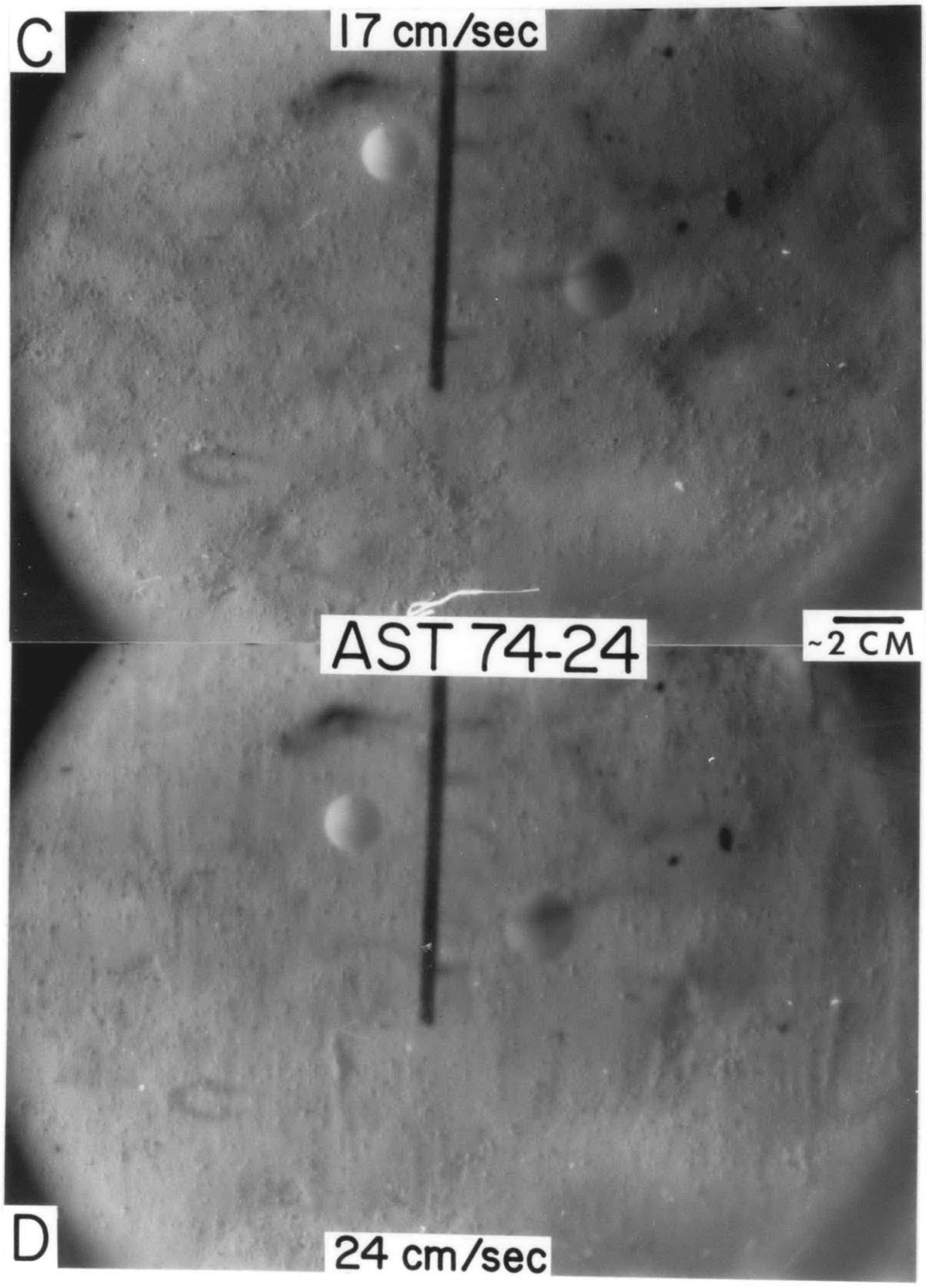
C
17 cm/sec
AST 74-24
~2 CM
D
24 cm/sec

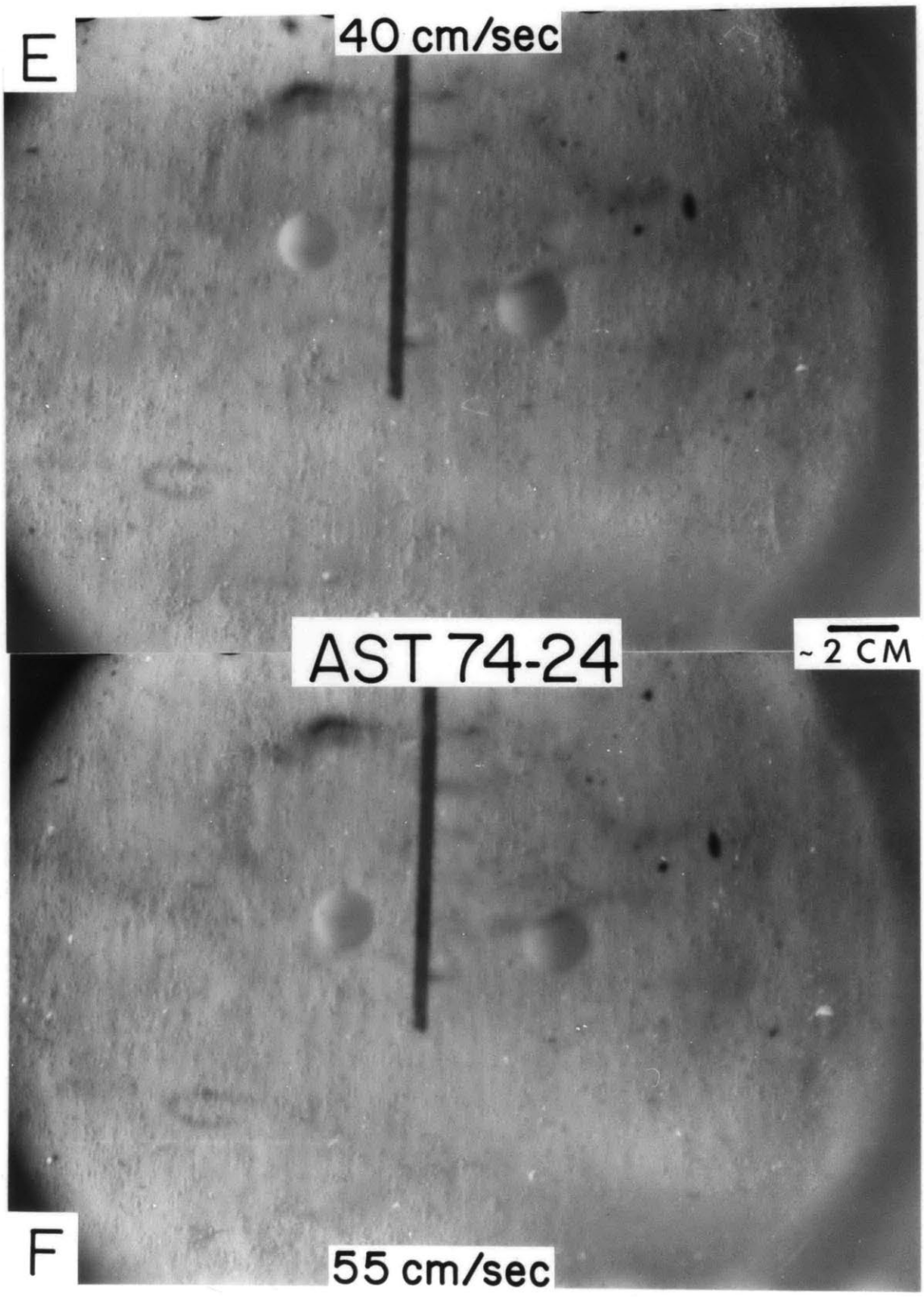
E
40 cm/sec
AST 74-24
~ 2 CM
F
55 cm/sec

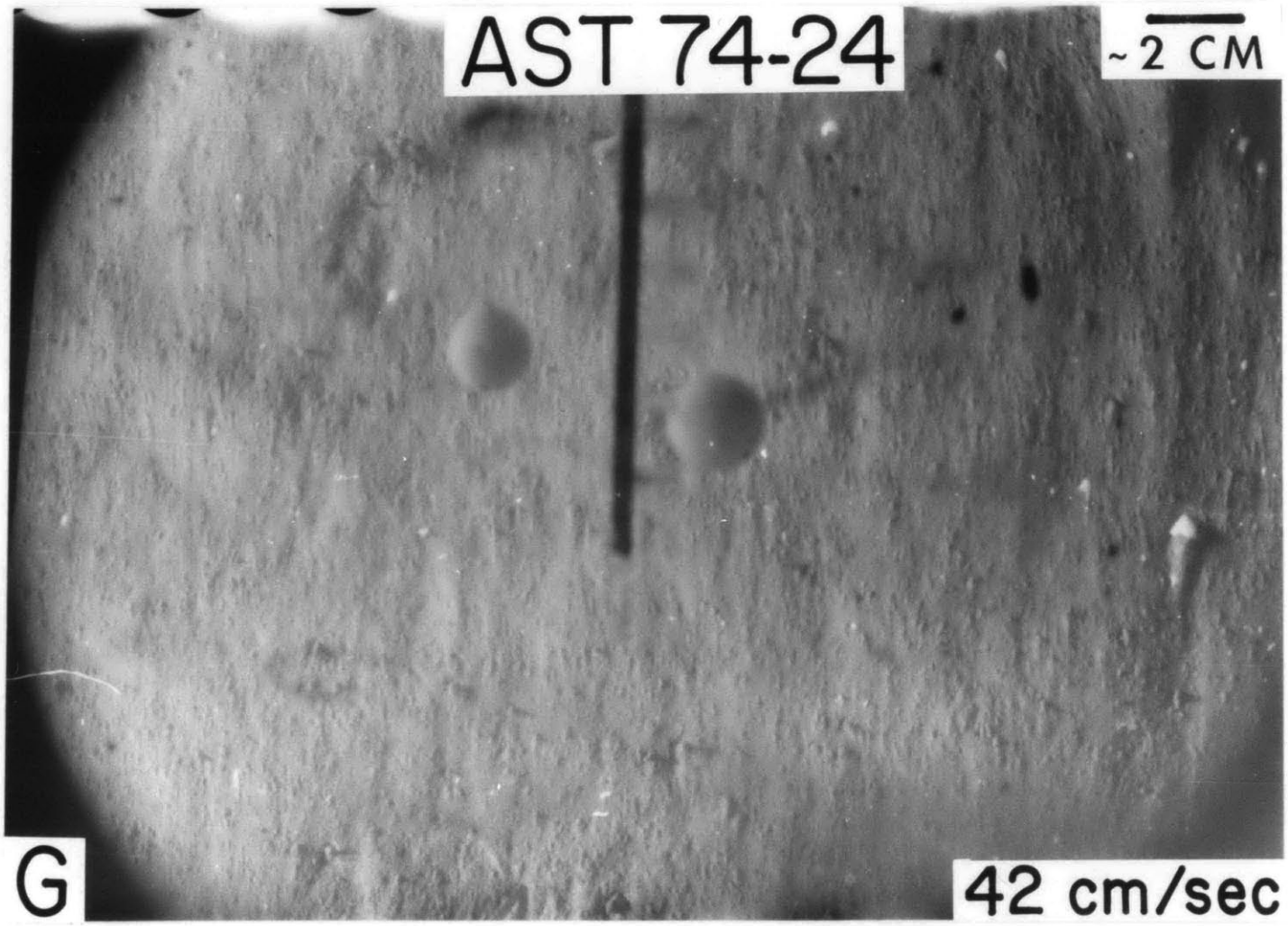
AST 74-24
~2 CM
G
42 cm/sec

bed surface remained nearly flat, as if a thin layer of material was being removed at similar rates from all parts of the bed. Near the end of the experiment, at a velocity of about 42 cm/sec (Figure 11G), the bed surface was very rough and was covered by longitudinal furrows and shell fragments.

AST 75-1

Only a few small biogenic and sediment mounds were (Figure 12A) observed on the bed at the beginning of this experiment. No organisms or biogenic trails were present. As in experiment AST 74-23, the sphere current meter again lost its metal ballast, so that flow velocities had to be estimated from the graphical relationship given in Figure 9.

Erosion of this bed apparently began at about 6 cm/sec, with lee drifts being created behind the biogenic and sedimentary mounds (Figure 12 B). As flow velocity increased to about 14 cm/sec some 25 min. after the beginning of the experiment (Figure 12C), numerous shell fragments were uncovered, longitudinal furrows were created, and the mounds initially present were eroded. Erosion rate appeared to decrease when velocity reached about 20 cm/sec, as evidenced by the similarity in appearance of the beds in Figure 12D (u = 20 cm/sec) and Figure 12E (u = 40 cm/sec).

Figure 12. Erosion of a silty clay by the *in situ* flume, AST 75-1, Station K, Buzzards Bay. Discussion of current velocities and corresponding erosion processes is given in text. See Figure 4 for explanation of photographic interpretation.

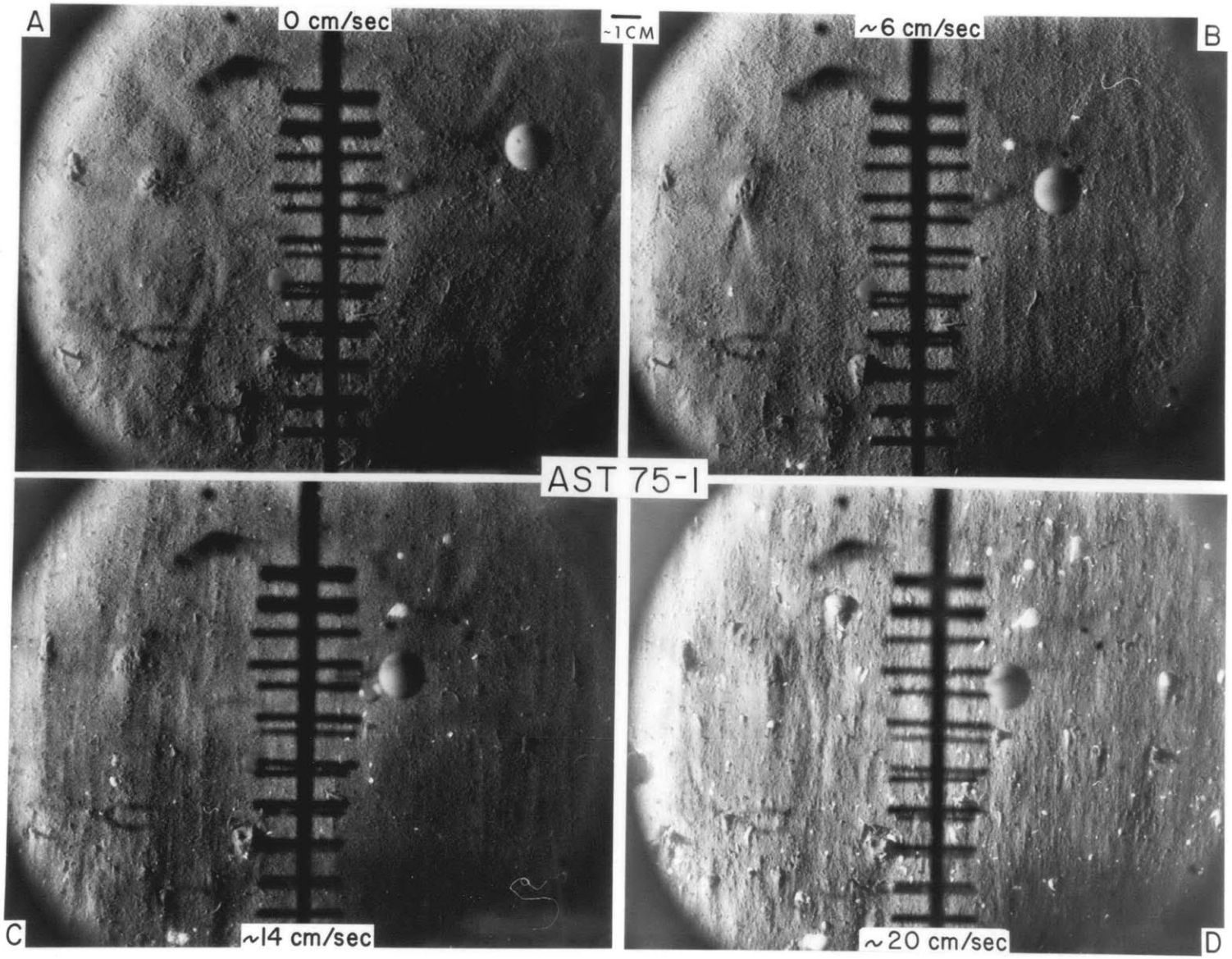
A
0 cm/sec
~1CM
~6 cm/sec
B
AST 75-1
C
~14 cm/sec
~20 cm/sec
D

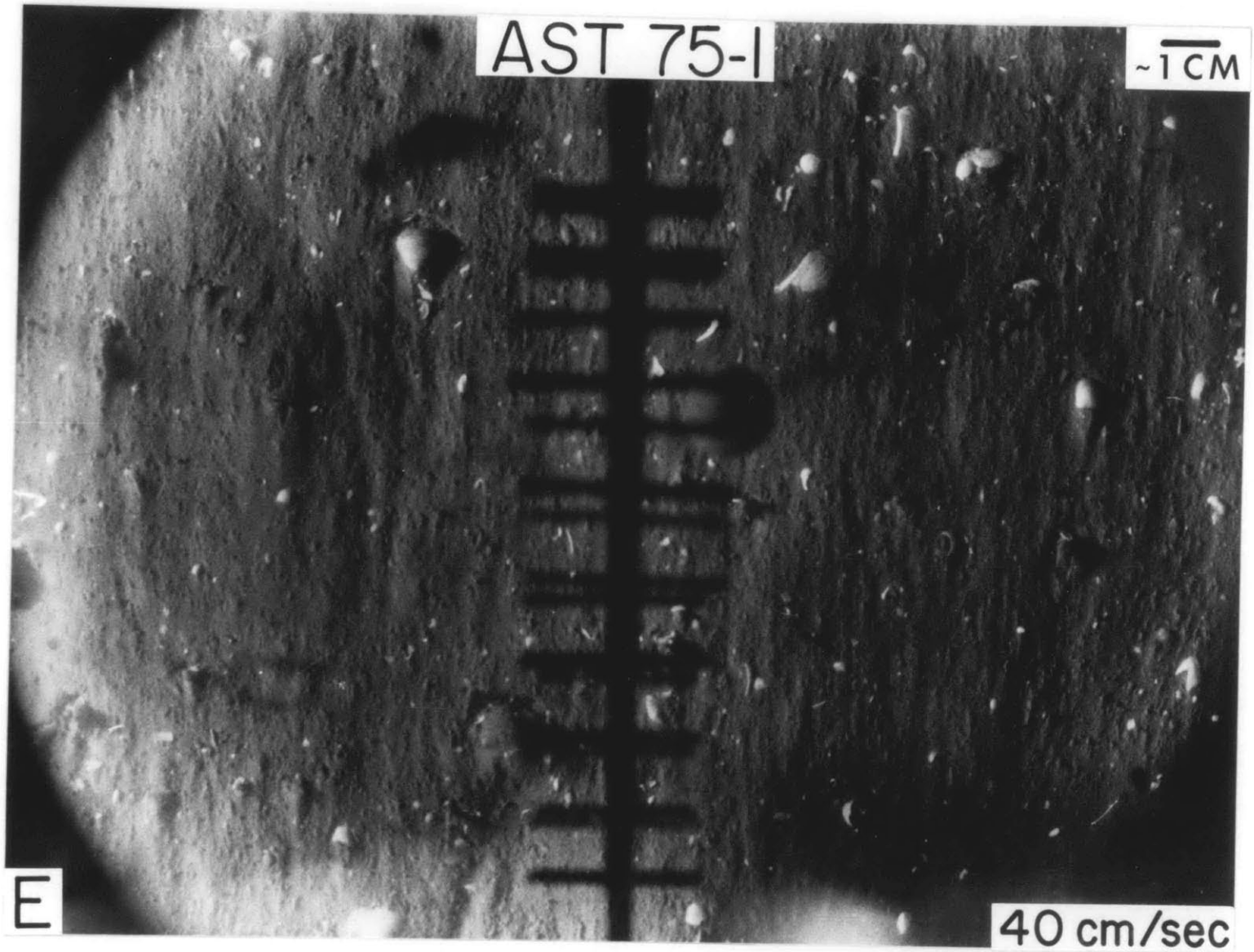
AST 75-1
~1 CM
E
40 cm/sec

Erosional Bedforms

Bedforms created during erosion consisted of small lee-drift deposits and longitudinal erosional furrows. No tendency toward formation of ripples, dunes, or other transverse wavelike features was observed during the experiments. Lee drifts formed behind shell fragments and small resistant mounds on the bed surface. Accumulation of sediments behind roughness elements can be interpreted in terms of flow separation processes around the roughness elements. Formation of lee drifts was investigated in the laboratory, and the results of the laboratory experiments are given in Chapter III.

Erosional Shear Stress and Bed Roughness

It was previously noted that bed shear stress is probably the best means of characterizing the flow forces required to initiate erosion in turbulent shear flows. This quantity was not measured directly but was estimated making use of Prandtl's power law for velocity distribution in a smooth walled conduit. Prandtl assumed that velocity distribution in a turbulent boundary layer of an enclosed flow system depends only on some power (in this case the seventh power) of the distance away from the wall. It was established

during a hydraulic model study of flow in the in situ flume (see Appendix B) that the velocity distribution in the channel is closely approximated by Prandtl's power law.

Prandtl used his seventh-power law to derive an expression for wall shear stress for flow in smooth-walled tubes having negligible pressure gradients and Reynolds numbers of less than 50,000. His expression for wall shear stress τ is usually given as (Prandtl and Tietjens, 1934, p. 75)

$$\tau = 0.0228\rho \left(\frac{u^7 \nu}{y} \right)^{1/4}$$

where ρ is fluid density, ν is kinematic fluid viscosity, and u is velocity at a distance of y from the wall.

It is common in hydraulics to make tube flow laws applicable to flows in conduits of other geometries by substituting hydraulic radius (defined as flow cross section divided by wetted perimeter) for pipe radius in the derivation. However, it was established during study of a hydraulic model of flow in the flume (Appendix B) that substitution of h/2, where h is channel height, for tube

radius in Prandtl's power law yielded calculated flow profiles closest to measured profiles. Substituting the above length scale in Prandtl's derivation (see Prandtl and Tietjens, 1934, p. 71, for details) does not alter the form of the final result, so the expression for shear stress given above was used to estimate boundary shear stress in the in situ flume with the implied boundary condition that $y < h/2$.

The expression for boundary shear stress also can be rewritten in a sedimentologically useful form as

$$u_* = (\tau/\rho)^{1/2} = 0.151 \left(\frac{u'\nu}{y}\right)^{1/8}$$

The quantity u_* is often referred to in discussions of sediment transport and will be used in this study as a measure of erosion resistance.

However, the Prandtl equation applies only to flows over smooth boundaries, so we must also determine under what conditions the sea floor is hydrodynamically smooth. A criterion used for classifying smooth and rough flows is whether roughness elements are large enough and so distributed on the flow boundary to protrude through and disrupt

the viscous sublayer. The viscous sublayer is a thin layer between the turbulent core of the boundary layer and the fixed boundary wherein flow is controlled mainly by viscous effects. The nominal thickness of the viscous sublayer y' is defined as (Daily and Harleman, 1966, p. 233)

$$y' = \frac{4\nu}{u_*} = \frac{4\nu}{U(c_f/2)^{1/2}}$$

where U is velocity outside the boundary layer and c_f is a local shear stress coefficient.

An approximation of sublayer thickness at the point in the flume where the camera is focused (about 3 m downstream from the entrance) can be made as follows. Assume that U is centerline velocity, ν = 0.11 stokes, and approximate the flume geometry as a straight rectangular conduit, to obtain y' = 0.39 cm for U = 2 cm/sec, and y' = 0.1 cm for U = 10 cm/sec. Thus, if the roughness elements on the sea floor average less than 0.1 cm in height, disruptions to the sublayer when U < 10 cm/sec will be minimal and flow will be hydrodynamically smooth. For U > 10 cm/sec flow may become transitional to fully rough, depending on the degree of disruption of the viscous sublayer.

A systematic study of sea-floor roughness was not made during the present experiments. However, an examination of the flume photographs and observations made while diving at the flume sites suggest that average bottom roughness ranges from 0.05 cm to 0.2 cm. In the initial stages of erosion, when flow velocity is low, the smooth-walled approximation for τ is considered sufficient for the purposes of this study. Transition from smooth to rough flow also may occur as the initially smooth bed surface is roughened by erosion.

Prandtl's relationship is used to approximate τ in the in situ flume by assuming that the velocity measured by the sphere current meter is representative of the velocity through the center of the sphere at a distance y from the flume top. The distance y is found from the simple relationship y^2 = (string length)^2 - (horizontal ball deflection)^2. Then, u at distance y from the wall is used in Prandtl's equation to estimate τ and u_*.

In an effort to standardize flow measurements and

sediment transport estimates, some workers in the field have found it sufficient to estimate τ, initiation of motion, and bed-load transport from u_{100}, the velocity measured one meter above the bed (e.g. see the predictive equations and graphs of Sternberg, 1972). Therefore, u_{100} was estimated by using the Prandtl-von Karman equation for velocity distribution in a smooth, turbulent boundary layer

$$\frac{u}{u_*} = 5.6 \log \frac{u_* y}{\nu} + 4.9$$

Here u is velocity at height y = 100 cm above the bed and u_* is the critical value of shear velocity at the initiation of erosion in the in situ flume. Values of u_c, u_*, and u_{100} for the in situ experiments are given in Table 4.

Tidal Shear Stress in Buzzards Bay

A brief survey of bottom current activity at Station K in Buzzards Bay was made to relate the results of flume studies to the dynamics of the natural erosional environment. Velocity profiles were taken hourly during a 12-hour period with a hand-lowered Savonius-rotor current meter which telemetered the speed and direction readings via cable

TABLE 4

Value of u_c measured by the in situ flume, and estimated values of u_*, τ, and u_{100}.

Experiment Number	u_c cm/sec	τ dynes/cm^2	u_* cm/sec	u_{100} cm/sec
AST 74-16	9.5	.24	.49	12.4
AST 74-17[a]	6.5	.12	.35	8.5
AST 74-17[b]	8.5	.20	.44	11.0
AST 74-18[a]	6.5	.12	.35	8.5
AST 74-18[b]	9.5	.24	.49	12.4
AST 74-19	7.5	.16	.39	9.6
AST 74-21	11.0	.31	.55	14.0
AST 74-23	6.0	.10	.32	7.9
AST 74-24	17.0	.71	.83	22.0
AST 75-1	6.0	.10	.32	7.9

a - erosion around biogenic tracks and trails

b - erosion of flat portions of the bed

to a deck read-out. The meter was positioned by first lowering it to the sea floor and then raising it to a selected height above the bed.

Seas were calm during most of the measurements, and the ship remained stable in the water. Consequently errors in measurement of current-meter height above bottom are estimated to be $\pm$ 15 cm, and errors in velocity due to lateral ship drift are thought to be negligible. Readings at each height above the bed were averaged over 30-45 second intervals. A complete set of readings during one lowering took from 10 to 15 minutes.

Velocities within 1.5 m of the bottom were generally less than 10 cm/sec during the measurement period (Figure 13), except for the lowering at 1150, when a near-bottom velocity of 10-12 cm/sec was measured. Comparable velocities at 60 cm above the sea floor were observed in a previous study by Rhoads (1973). Minimum velocities coincide with slack tides, and maximum velocities roughly coincide with peak flood and ebb tides. Cause of the local maxima between peak ebb and slack tide at 1430 is not apparent and is presumably related to some nontidal phenomenon.

The current-velocity profiles were used to determine the

Figure 13. tidal flow velocities at several heights above the sea floor at Station K, Buzzards Bay.

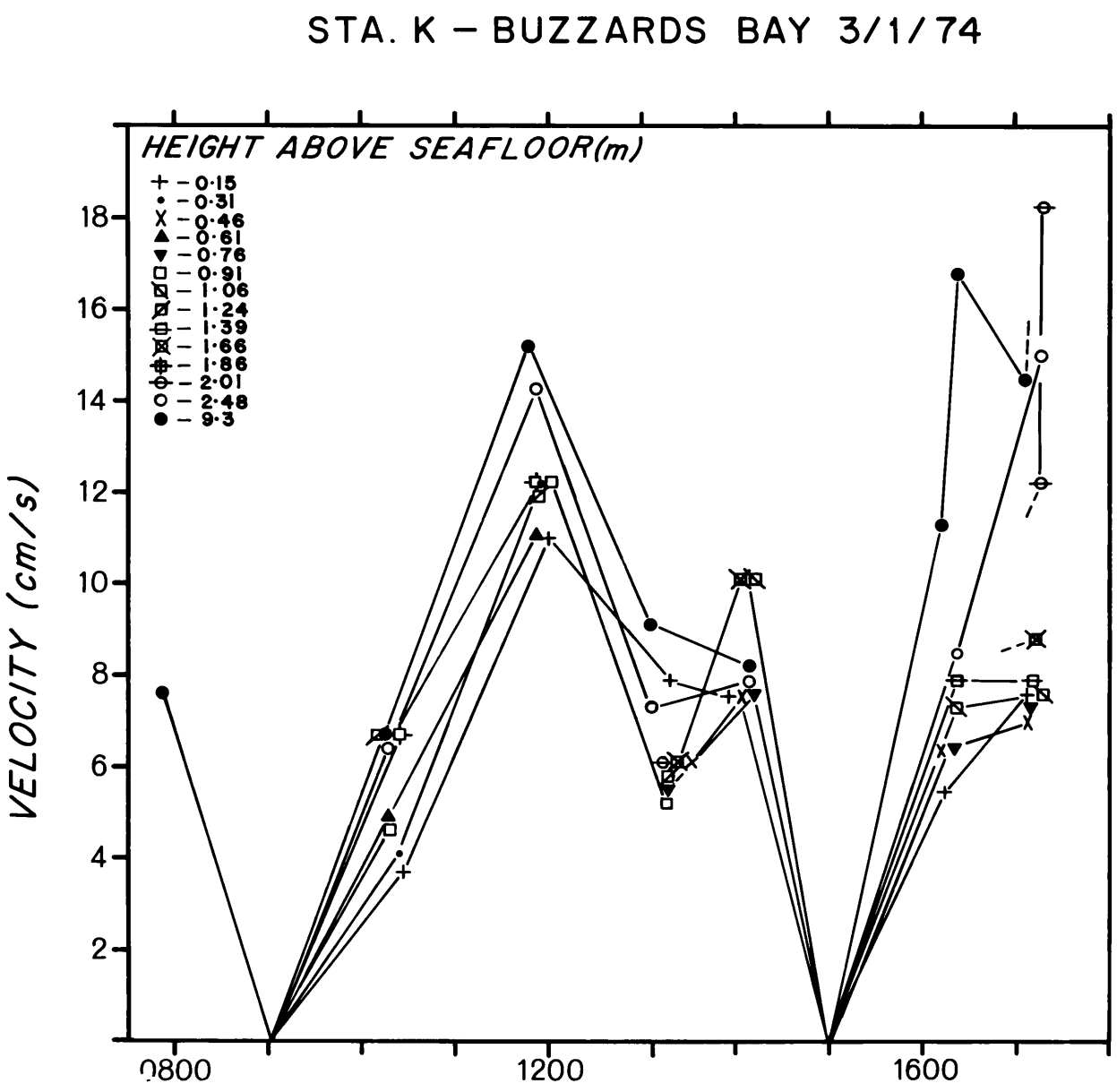
STA. K – BUZZARDS BAY 3/1/74
HEIGHT ABOVE SEAFLOOR(m)
+ – 0·15
• – 0·31
X – 0·46
▲ – 0·61
▼ – 0·76
□ – 0·91
⊠ – 1·06
⊠ – 1·24
⊟ – 1·39
⊠ – 1·66
⊞ – 1·86
⊖ – 2·01
○ – 2·48
● – 9·3
VELOCITY (cm/s)
18
16
14
12
10
8
6
4
2
0800
1200
1600

range of shear velocities being generated by the tidal currents for comparison with shear velocities determined during the flume experiments. The previously described Prandtl-von Karman equation for turbulent boundary layers over smooth walls was used to estimate shear velocity being generated in the boundary layer. (See also section on bed roughness in this chapter for discussion of the relative roughness of the sea floor in Buzzards Bay.) Linear regression analysis of u versus log y for each lowering indicated the presence of a well-developed boundary layer during three of the lowerings (where correlation coefficients > 0.75 at the 95% confidence interval; four or more points within the boundary layer), and these profiles were chosen for further analysis. Values of u_* so calculated are 0.5 cm/sec or less. No values of u_* have been previously published for in situ erosion of muddy sediments like those in Buzzards Bay, but for comparison critical values of u_* for erosion of fine to medium sands are about 1-2 cm/sec (Sternberg, 1971).

If they can be considered as representative, the range of tidal u_* values determined during this short study falls within the range of u_* values measured during the in situ flume experiments. Although no direct observations of sediment

erosion were made concurrent with the survey of bottom currents, the fact that the muddy bottom sediments in Buzzards Bay are constantly being resuspended and reworked has been well established (Young, 1971; Rhoads, 1973). Estimates of critical values of u_* and u_{100} made during the *in situ* flume experiments are therefore considered reasonable estimates of the values of u_* and u_{100} required to erode Buzzards Bay muds.

CHAPTER III

LABORATORY EROSION EXPERIMENTS

The laboratory experiments were designed to explore the basic flow mechanisms and sediment physical and biological parameters controlling erosion resistance. To accomplish this, modes of deposition, biogenic reworking, and organic content and composition were varied so that their individual effects could be studied. An exploratory experiment on the relationship between bottom roughness scale and lee-drift formation was also made.

All experiments were conducted using sediments collected at Station K in Buzzards Bay. These sediments have been described in Chapter II; their physical properties are summarized in Tables 2 and 3. Sediments were collected as needed, using a Van Veen 0.04 m^2 grab sampler.

METHODS

The special methods and equipment used are described below. The analytical techniques used to measure organic matter concentrations are also briefly described.

Laboratory Flume

The experiments were conducted in a recirculating flume 61 cm wide by 27 m long shown schematically in Figure 14.

The flow entering the channel passes through a straightener and is discharged at the downstream end into a large-volume tail-box from which the water is drawn for recirculation. Flat boards lowered tangent to the water surface were used to reduce surface waves. Mean flow velocity was measured with a calibrated orifice meter located in the upstream end of the return-flow pipe, and surface velocity in the channel was estimated by timing the passage of a small surface float over a 2 m course. It was assumed that the 11 m interval between the flume entrance and the experimental beds was sufficient to allow complete development of the boundary layer, and u_* was calculated from the mean velocity and surface velocity by the equations given in Southard et al (1971); u_{100} was estimated using the Prandtl-von Karman equation as described in Chapter II. Water surface and flume bottom were kept parallel by changing flume tilt with a jack-screw.

Sea water collected near Woods Hole was used in the flume, and tap water was occasionally added to offset evaporation. Spot checks showed that salinity varied between 25 °/oo and 33 °/oo.

Figure 14. Recirculating laboratory flume used for erosion experiments. The symbols represent the following parts of the flume. In the lower figure: (S) flow straightening section; (Q) surface wave quieter; (W) well area. Dashed lines over the well area indicate the position of the rectangular enclosure used for the flat bed experiments; (V) valve to regulate discharge through return-flow pipe; (P) pump in resevoir; (O) orifice meter. The upper figure shows details of how the movable plate was installed in the well opening. (T) indicates the turn-buckles used for raising and lowering the plate and (P) is the movable plate.

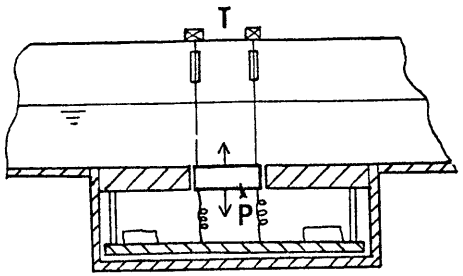

DETAIL OF WELL

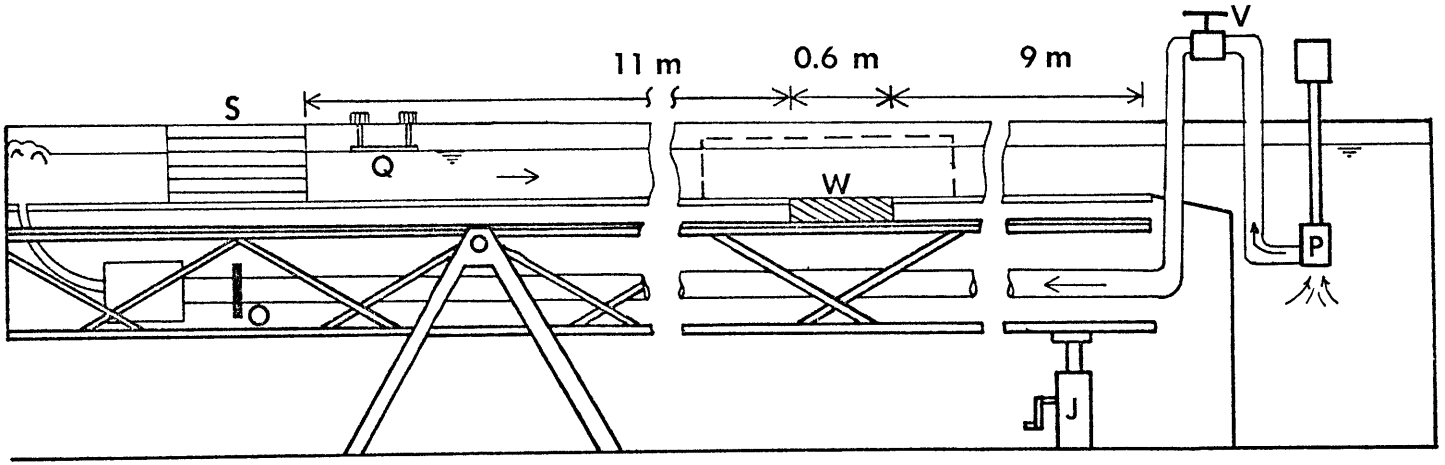

20 m RECIRCULATING FLUME

Preparation of Biogenically Reworked Beds

A well in the flume bottom (60 cm square by 10 cm deep) located about 11 m from the flume entrance (Figure 14) was used to prepare biogenically reworked beds for erosion. Beds were made by filling the well with freshly collected sediments and smoothing by hand to make the bed surface roughly coplanar with the flume bottom. The well was lined with a plastic box of the same size to facilitate removal of sediments.

Organisms in the mud seemed tolerant of the many shocks and changes of environment they underwent during redeposition, and evidence of biologic activity such as fecal mounds, trails, and burrow openings were generally apparent within hours after redeposition. It was found that complete reworking of the bed surfaces took from one to eight weeks.

The surface of the biogenically reworked beds had roughness elements up to 1 cm high. Abrupt differences in elevation between the sediments and the flume bottom were filled by hand with sediments to ease flow transition.

Phytoplankton growth, presumably algae, periodically clouded the flow during the longer biogenic reworking experiment,

forming small aggregates which moved as bedload down the flume channel to the sediment well. Little of the algal material was transported past the sediments in the well. Once on the bed, some of the cells were presumably ingested by the deposit feeders over a period of time, and the remainder were incorporated into the sediments by movements of the organisms. The presence of algae in the laboratory beds can be considered a condition similar to events on the sea floor of Buzzards Bay, since algae are a common constituent of the sediments in the Bay (Rhoads et al, 1974). Algae on the plastic flume bottom were removed by siphoning before each flat-bed and reworked-bed experiment.

Preparation of Flat Beds

To study the effect of particulate organic material concentrations on erosional resistance, flat beds were prepared from muds treated with 30% H_2O_2 for one week and then mixed in varying proportions with the $< 40\ \mu$ fraction of untreated muds. An additional sample was treated with Clorox in an attempt to completely remove organic material. The sediment mixtures were mixed with sea water, allowed to settle, and then decanted. This procedure was repeated three times to ensure removal of the oxidant. Total organic

carbon (carbonate-free) was analyzed on a LECO Carbon Determinator and is reported as percent carbon on a dry weight basis.

Microbial activity may also enhance organic binding of the sediments and hence increase erosional resistance in fine sediments. Therefore, adenosine triphosphate (ATP) concentrations were measured in the experimental beds. ATP is present in all living organisms, and, if measured on the fine size fraction of fresh sediments, is thought to be a reasonable approximation of microbial biomass.

Samples were analyzed for ATP as follows. ATP was extracted from three replicate samples by boiling them with 0.1 M $NaHCO_3$ in a closed vessel. A known volume of ATP standard was added to one replicate before boiling to evaluate extraction efficiency. Extracts were diluted ten-fold with Tris solution for stability and storage. The extract was split into three aliquots and ten ml of the extract injected into 0.1 ml of lucifern and luciferase in the light-tight measurement chamber of a DuPont Biometer. The bioluminescence created during the reaction of ATP and lucifern-luciferase is measured during the first three seconds of the reaction and the results given by the calibrated Biometer are in femtograms (10^{-15} gm) of ATP per gm

of extract, which is then recalculated as gm microbial carbon per gm dry sediment.

Previous results attained with this technique (Stanley Watson, unpublished data) show that the quantity of ATP standard injected during sediment preparation is accounted for by the analytical procedure, so that the analytical technique should provide meaningful estimates of microbial carbon and, by extrapolation, microbiomass. Other workers have used scintillation counters to measure light emission; comparative studies of the two instruments have given similar quantitative results (Stanley Watson, personal communication, 1975).

The flat beds were deposited from slowly flowing suspensions in a open-bottom enclosure 2 m long by 20 cm wide positioned over the well area of the flume. A false bottom was placed in the well area and its top made coplanar with the surrounding flume bottom (Figure 14). An (up-down) adjustable plate 15 cm square was centrally located in the false bottom. Suspensions were first thoroughly mixed in the enclosure by a small recirculating pump, then settled for 5-6 hrs in still water. Flow was restarted and the deposition continued from the slowly flowing suspension (mean velocity about 1-2 cm/sec) for 14 to 17 hrs. The enclosure was

then carefully removed and all sediments except for those on the adjustable plate were siphoned off the flume bottom. Finally, the plate was lowered until the bed surface coincided with the surrounding flume bottom. Small gaps around the movable plate were filled in during the beginning of the erosion experiment by deposition from the small amount of bed-load material. A smooth transition was thus created between the plastic flume bottom and flat sediment bed.

RESULTS

Biogenically Reworked Beds

Critical values of u_* (estimated by the resistance formula for open-channel flow given in Southard et al, 1971) for the erosion experiments on the biogenically reworked beds are given in Table 5; values of u_{100} calculated by the Prandtl-von Karman equation are also given. Values of u_* and u_{100} are also plotted on a graph below the body of the table. Erosion resistance (critical values of u_* and u_{100}) was found to decrease with time of reworking. It is interesting to note that only the values of u_* for the two-month bed fall within the range of critical u_* values for *in situ* erosion of the Buzzards Bay muds (see Table 4). This fact tends to confirm the importance of biogenic reworking

TABLE 5

Critical values of u_* and u_{100} for erosion of biologically reworked beds in a laboratory flume. Data are also plotted below the table.

Biologic Reworking Time (Days)	u_* (cm/sec)	u_{100} (cm/sec)
1	1.89	55
5	1.79	52
61	0.80	22

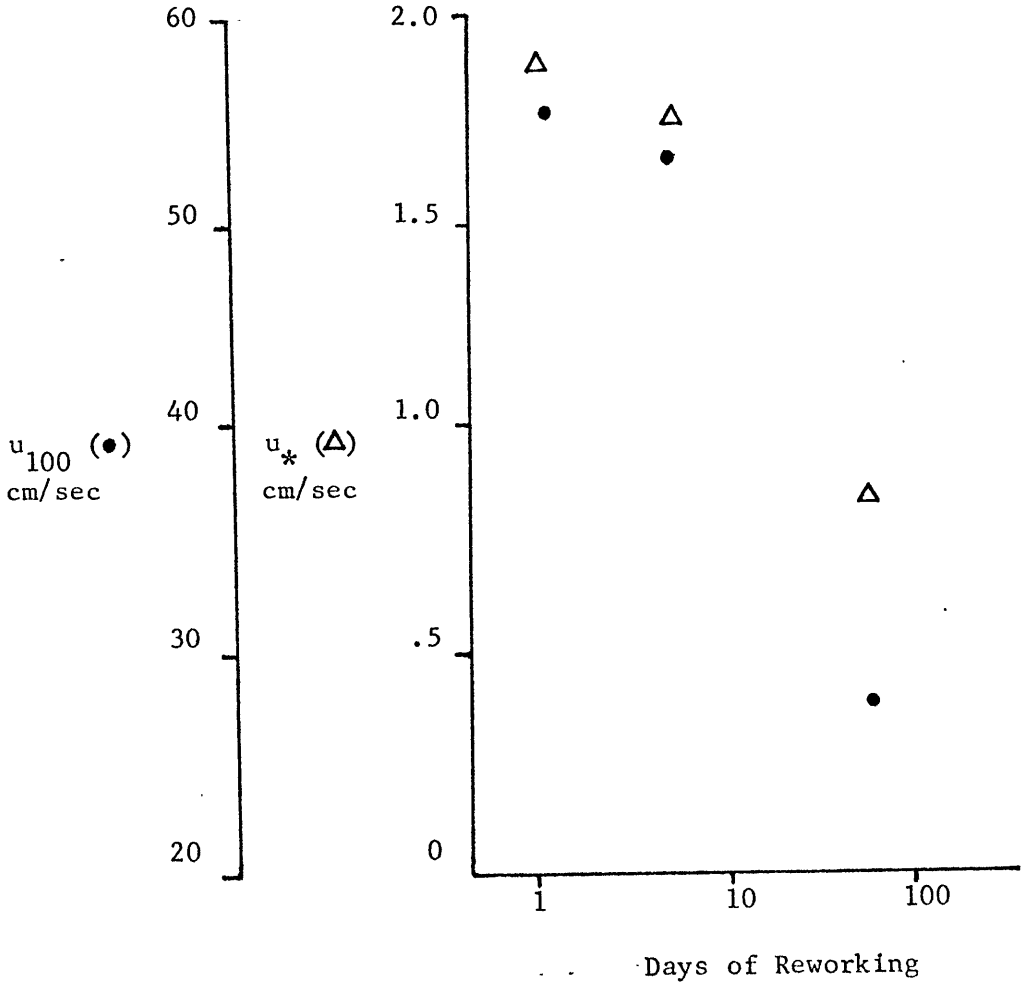

in erosion resistance of the fine sediments.

The uppermost layer of the two-month bed contained many aggregates of organic material and sediment. The strength of the pelletized material was small, and efforts to transfer a portion from the bed for closer inspection were not successful.

A burrowing snail seen in the center of the bed (Figure 15A) created a fresh trail during the experiment, and several other deeply-incised trails were also present, as were several fecal mounds. Bed-load transport was the principal mode of erosion observed, and it occurred as elongated streamers of sediment moving parallel to the flow. Sediments in the streamers rolled along the surface; at times individual streamers moved continuously from the point of erosion to the rear edge of the bed, but more often a streamer would come to rest after a short time and loose its identity.

As velocity increased, the biogenic trails were first filled with bed material and then smoothed as erosion continued. Longitudinal erosional furrows were created and lee drifts were formed behind the fecal mounds (Figure 15B).

By comparison with the two-month bed, surfaces of the one-day and five-day beds were hardly modified (Figures 16A,

Figure 15. Buzzards Bay muds which have been biogenically reworked for 61 days in a laboratory flume. Flow is from top to bottom (see arrow) and the bed is 60 cm from left to right.

A) Before erosion. Note the fresh trail being created by the benthic snail in the center of the bed and the fecal mounds in the right center of the bed.

B) After erosion (critical $u_* = 0.8$ cm/sec); longitudinal furrows are present and lee drifts have formed behind the erosion-resistant fecal mounds.


A

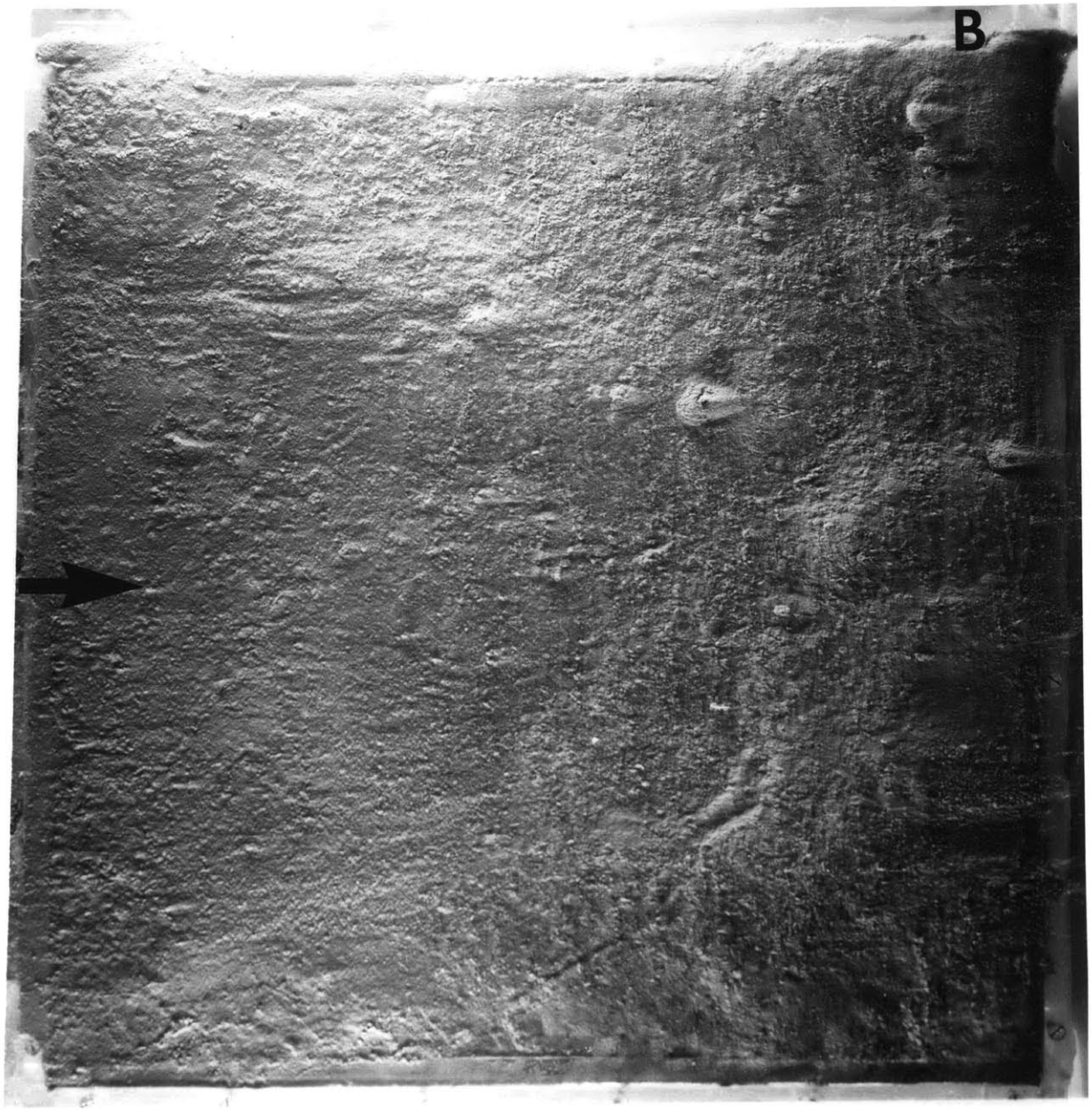
B

Figure 16. Buzzards Bay muds deposited in a laboratory flume and reworked for five days. Flow is from top to bottom (see arrow) and the bed is 60 cm across.

A) Bed surface at the beginning of the experiment. Some (worm ?) trails and several bivalves are present.

B) Critical $u_* = 1.79$ cm/sec; the jagged areas at the leading edge were eroded at velocities substantially less than $u_* = 1.79$ cm/sec. The longitudinal furrows are apparently related to flow disturbances at the leading edge. On the other hand, the small irregular patches eroded from the right center of the bed are probably representative of general erosion of the bed. Note that the layer being eroded gives the appearance of being uniformly thick over its entire extent whether associated with erosion from the leading edge or from erosion of the small patches on the rest of the bed.


A

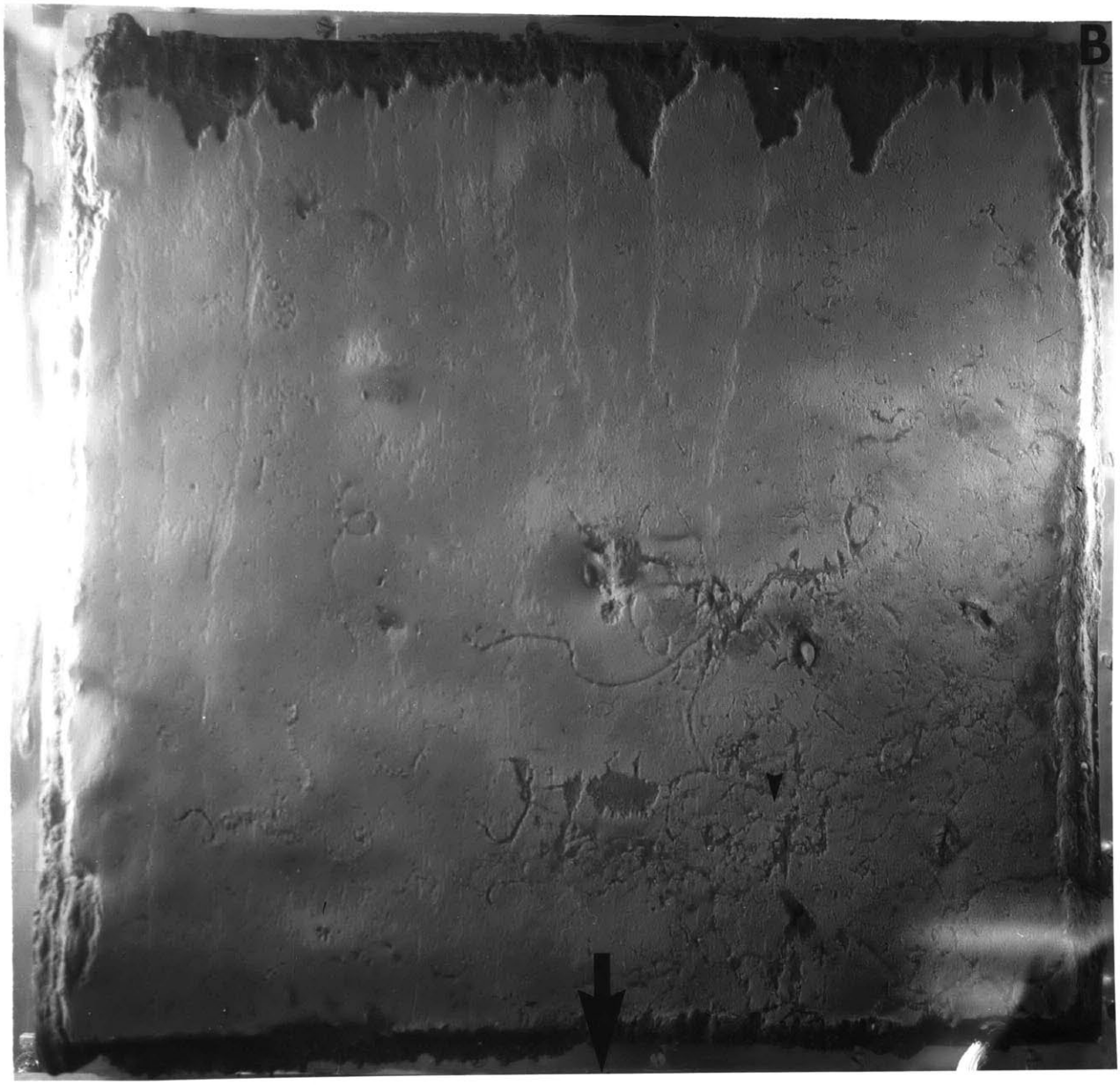
B

Figure 17. Buzzard Bay muds deposited in a laboratory flume and reworked for one day.

A) Beginning of the experiment. Note the open-bivalve shell protruding at the center of the bed. The leading edge of the bed has been smoothed by hand to produce a smoother flow transition.

B) Critical u_* = 1.89 cm/sec. Erosion has produced several small eroded patches on the left center and lower right portions of the bed.

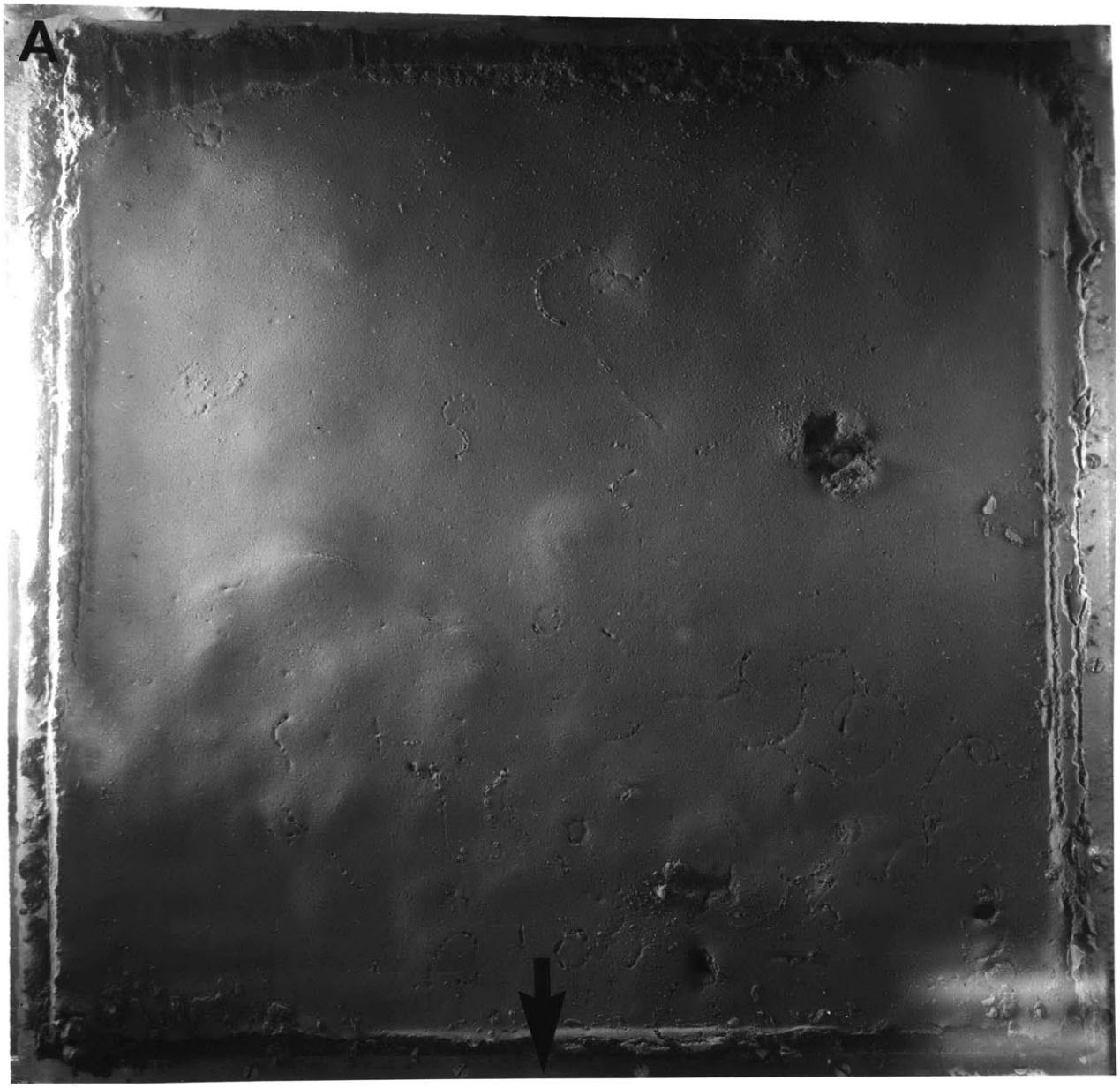
A

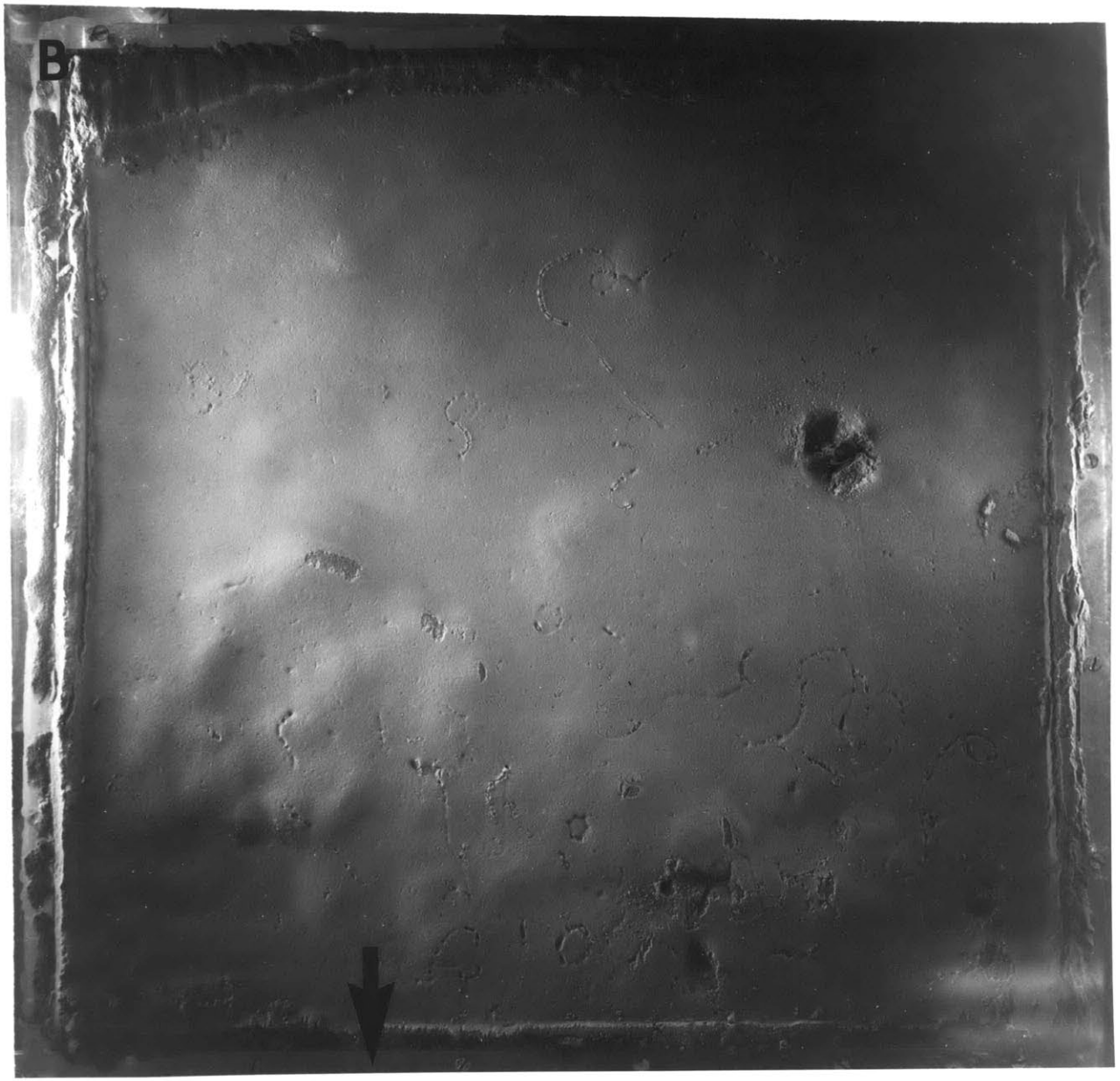
B

and 17A). Except for a few tracks, trails, and fecal mounds, the bed surfaces were smooth and did not appear pelletized. Several filter-feeding bivalves were present at the surface.

Erosion processes on these less thoroughly reworked beds were much different than those on the two-month beds. Erosion was initiated at localized areas as the removal of an almost uniformly thick surface layer (Figures 16B and 17B). Worm trails sometimes but bot always were the sites of the initiation of erosion. No tendency was observed for development of longitudinal furrows or lee drifts.

Flat Beds

The purpose of the flat-bed experiments was to establish whether erosion resistance was a smoothly and continuously increasing function of sediment organic content. As previously discussed, the mode of deposition was kept constant for each experiment so that the only independent variable was organic content. The flow and sediment properties pertaining to the flat-bed experiments are summarized in Table 6. In several flat-bed experiments, the unavoidable gap at the leading edge of the bed caused erosion at local weak areas along the leading edge. Erosion occurred as the stripping-away of a thin layer of the bed surface; the eroded

TABLE 6

Flow and sediment properties measured during laboratory erosion experiments on uniformly-deposited flat beds of varied organic concentration.

Run No.	u_s (cm/sec)	u_* (cm/sec)	u_{100} (cm/sec)	TOC (%)	ATP (mg-C/cm^2)
4	19.0	1.30	36.5	.82	n.d.
5	20.2	1.38	38.9	1.02	n.d.
9	24.9	1.64	46.9	1.28	1.31
6	23.5	1.54	43.8	1.62	.02
7	30.5	1.92	55.7	1.84	.431
2*	31.4	1.95	56.6	2.0	.14
3*	16.3	1.13	31.3	2.0	.13

* The same sediment mixture deposited in flowing (run 2) and still (run 3) water.

n.d. - not detected

area had a characteristic V-shape with the point directed downstream (see Figure 18). During the experiments small bed-load particles eventually filled the gap at the leading edge; in most cases this occurred before erosion of the undisturbed portions of the flat beds.

The initial gap at the leading edge of the bed may have influenced details of the boundary-layer structure, but, because the gap was small, these effects probably extended only a short distance downstream. A small difference in flow depth was created as the leading edge eroded, but again the scale of this irregularity was small and its influence probably extended only a short distance downstream. To avoid the possibility of being misled in choosing the critical erosion condition, attention was focused on parts of the bed far from the leading edge.

Erosional behavior of the flat beds was basically the same during all experiments and was similar to the behavior of the less thoroughly reworked experimental beds described in the previous section. Before general erosion began on the flat beds, the bed surface often became roughened with pits; tool marks caused by angular bed-load particles were also common. General erosion was characterized by removal of a uniform layer of surface material in the same manner as

Figure 18. Run number 7; an example of erosion at the leading edge of a flat bed containing 1.84% organic carbon. Flow is from top to bottom of the figure. Erosion seems to take place as the removal of thin layers of uniform consistency. Several layers at different depths below the surface of the bed can be seen in this photograph; see text for further discussion.

Figure 19. Run number 4; the eroded surface of a flat bed having 0.82% TOC. Flow is from top to bottom. Note that the irregular triangular patches in this figure are depressions in the bed. The sediments have a looser and more flocculent appearance than in beds with higher organic content; compare to Figure 18, run number 7.

previously described for erosion at the leading edge (see Figure 18). However, the eroded surface material had a much looser and more flocculent appearance in beds with low TOC (Figure 19) than in beds with high TOC (Figure 18).

Areas on the bed where general erosion was initiated were not always associated with the weakened zones around tool marks or pits. Spontaneous erosion from areas of the bed where the cause of weakness was not apparent was especially true for experiments 4 and 5 (Figure 19); sediments in those beds had low TOC (Table 6). Spontaneous erosion also occurred in beds with higher TOC, but it was just as common for erosion to be initiated at tool marks or small pits. Since the flat beds behaved in basically the same manner during erosion, the preceding figures can be considered representative of the processes observed on all beds during erosion.

When TOC concentrations are plotted against critical shear velocity (Figure 20A) it is clear that a correlation exists between concentration of organic matter and erosion resistance. On the other hand, relationship between ATP concentration and erosion resistance is not clear

Figure 20. Critical u_* for erosion of uniformly-deposited flat beds with varying concentration of organic matter. Solid symbols in both figures indicate values from run 3 when sediments were settled from a still suspension.

A) Total organic carbon versus u_*; total organic carbon content in percent of dry weight of sediment.

B) ATP concentration versus u_*; ATP concentration has been converted to mg carbon per gm dry weight of sediment.

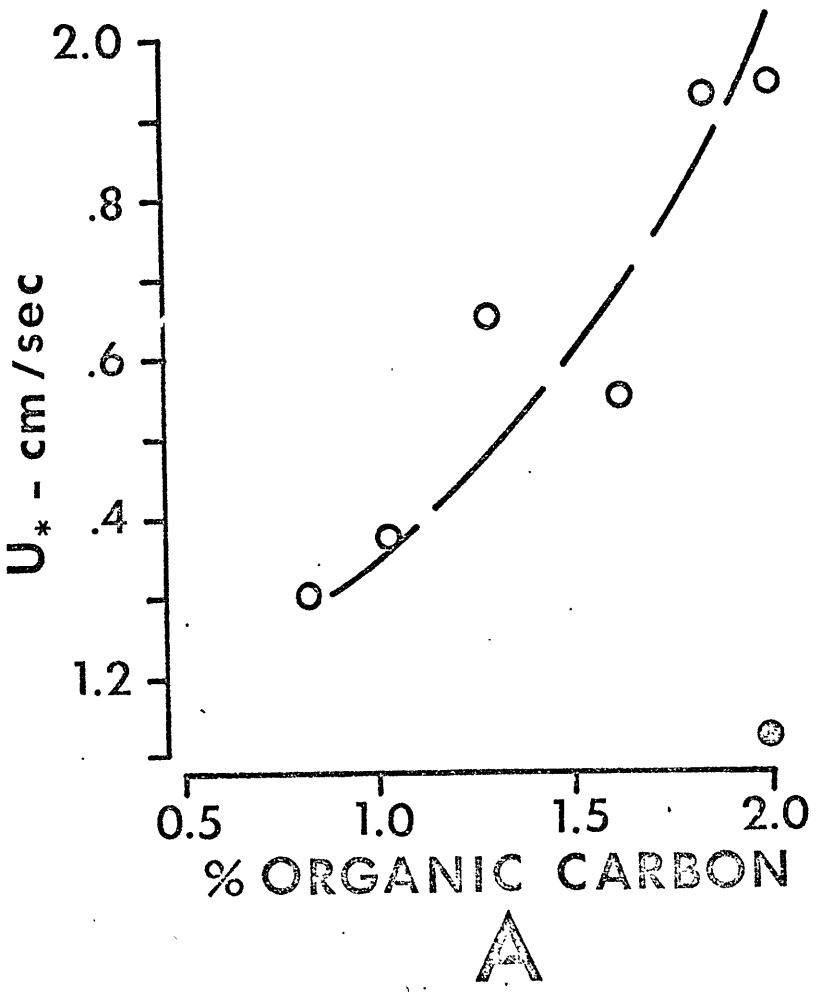

A

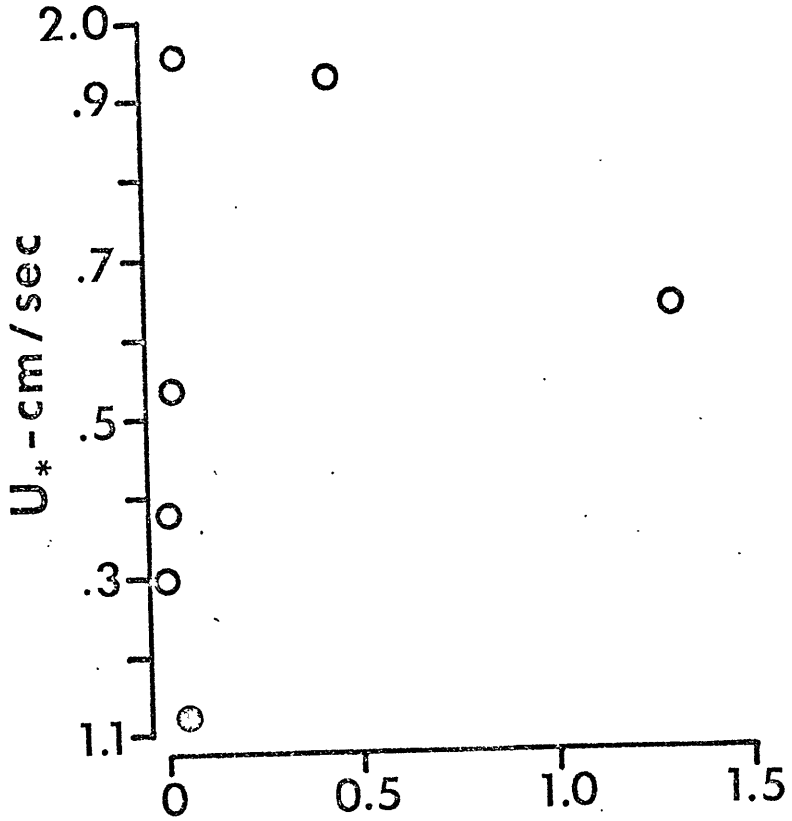

B

(Figure 20B). It is recalled that the original working hypothesis implied that the activity of microorganisms in the sediments might add to cohesion and hence to erosion resistance. It was assumed that ATP concentrations in the fine sediment fraction would be directly related to the biomass of the microorganisms. If these assumptions are correct then critical u_* values should increase as ATP concentration increases. This is not the case; possible explanations for this behavior are discussed in Chapter IV.

Lee-Drift Formation

Lee drifts were the most common bedforms observed during the in situ experiments and during the laboratory flume experiments on the reworked bed. Therefore, an exploratory experiment was designed to investigate how the growth of lee drifts is influenced by the size of the bed roughness elements which act as nuclei for their formation.

The bed for the experiment was prepared by first distributing conical mounds of clay in three uniformly sized groups in an 0.8 m long section of the flume bottom just upstream from the well area. A bed of Buzzards Bay mud was deposited overnight on the clay mounds by settling from a

slowly circulating dense suspension. The bed area was isolated between bulkheads erected across the channel. Deposition was uneven along the sides of the largest mounds but was even elsewhere. However, for the purposes of this exploratory study, the bed was considered to be satisfactory. The average relief of the three groups of mounds (measured with a point gauge) was 0.97 cm, 0.44 cm, and 0.20 cm (top to bottom of Figure 21). After the bulkheads were removed, flow velocity was quickly brought to just above the critical erosion velocity and the lee drifts were left to develop for about one hour before the photograph in Figure 21 was taken.

Flow separation and development of a low-velocity eddy in the lee of erosion-resistant mounds were the mechanisms referred to in Chapter II to explain accumulation of the lee drifts observed during the in situ experiments. Flow separation and related processes are considered below in a more complete analysis of the important fluid dynamical parameters involved in lee-drift formation.

Consider first a uniform flow past a submerged body. Flow separation takes place when the pressure gradient dp/dx at

Figure 21. Experimental formation of lee-drift deposits from a bed of clayey silt in a laboratory flume. Three separate groups of clay mounds are distributed across the bed from left to right. Each group has a characteristic height and occupies an area equivalent to about one-third the distance across the bed. Linear scars in the center and lower right were left by worms which have been previously eroded. See text for further explanation.

the surface of the body becomes greater than zero (i.e. flow at the surface is toward a region of higher pressure). If $dp/dx \gg 0$ the fluid near the boundary may have its velocity reversed. If reversal occurs, continuity requires the fluid to be deflected away from the wall, and flow separation is said to have taken place. At the point where the boundary layer separates from the body, a series of eddies are formed in the separation zone because of the vorticity developed between the separated flow and the reverse flow. The formation of a stable eddy in the lee of the submerged body then depends on the relative importance of inertial and viscous forces.

Consider next a submerged smooth body of size K and shape S in a flow of velocity u_o and kinematic viscosity ν. Daily and Harleman (1966) note that eddy formation on submerged bodies is related to the body Reynolds number $R_K = \frac{u_o K}{\nu}$. To apply this analysis to the present experiment, the shape of a roughness element is approximated by a short cylinder and u_o is defined as the value of velocity at a height above the bed equal to half the height of the roughness element. From this we obtain values of $R_k = 850$

for 0.097 cm mounds, R_k = 320 for the 0.044 cm mounds and R_k = 125 for the 0.20 cm mounds. Comparing these results to previous experiments on eddy formation behind vertical cylinders in steady unidirectional flow (Prandtl and Tietjens, 1934, Chapter 6), we find that stationary eddies are formed when $1 < R_k < 60$; for $R_k > 60$ the eddies formed in the separation zone are entrained in the wake of the body as coherent vortices.

Figure 21 shows that scour patches but no lee drifts formed behind the 0.97 cm high mound (R_k = 850), small drifts and some scour patches formed close behind the 0.44 cm mound (R_k = 320), and elongated drifts formed behind the 0.20 cm high mound (R_k = 125).

The paired scour patches behind the large and middle-sized mounds probably represent the points of reattachment for the separated boundary layer. The scoured moats in front of the large and medium sized mounds can probably be explained by acceleration of the flow above the critical erosion velocity as it is forced to bend around the larger mounds. The small mounds would also tend to accelerate the flow but, being closer to the bed, they are in a zone of lower velocity. Hence the accelerated flow would be less likely to exceed the critical erosion velocity.

Considering the approximations used, it is not surprising that the values of R_k for which lee drifts formed do not agree exactly with predicted values of R_k which would have formed stable eddies. Cones after all are not cylinders and the flow separation and eddy formation process is strongly dependent on geometry of the submerged body.

In summary, this brief study tends to confirm that a relationship exists between formation of lee drifts and size of roughness elements. This relationship may be expressed in the form of a body Reynolds number. Thus, lee drifts would tend to form in relatively fast flows behind small roughness elements and in slower flows behind larger elements. It also would seem likely that, for a roughness element of given size, there must be an upper limit to the particle size which will remain trapped behind it. Particles large compared to the roughness elements would protrude out of the low-velocity zone and would tend to be carried away.

CHAPTER IV

DISCUSSION OF THE EXPERIMENTS

One of the basic problems confronting marine sedimentologists is the uncertainty involved in extrapolating sediment transport theories and the results of laboratory experiments to sedimentary processes on the sea floor. This is especially true for processes involving fine-grained sediments; some of the complexities of this problem were discussed in Chapter I and Appendix A. In the study reported here an attempt has been made to bridge the gap between the laboratory and the real world with respect to understanding the erosional behavior of fine-grained marine sediments.

In the following two sections of this chapter, I will discuss and interpret the results of the in situ and field experiments. The final section of this chapter contains a summary of the most important conclusions.

IN SITU EROSION EXPERIMENTS

Seasonal and Spatial Variability

It might be argued that, because the bed area eroded by the in situ flume is small, it might not be representative

of the mud facies in Buzzards Bay. If u_c varied randomly and had no correlation with sedimentary or biogenic features in the mud facies, then some weight would have to be given to this argument. However, data from the in situ experiments (Table 4) suggest that for beds with similar biogenic and sedimentary features, the variance of u_c is relatively small. The observed variance of u_c is probably a good estimate of the natural variance expectable in Buzzards Bay, as discussed below.

The in situ experiments took place during Fall and mid-Winter (Table 1). Since activity of the benthic organisms depends, among other things, on season, we might also expect to find seasonal differences in erosion resistance of the sediment. The in situ data (Tables 1 and 4) suggest that small-scale spatial variability is more important than seasonal variability. For example, experiments AST 74-23 and AST 74-24 took place at Station K during the same day. The ship remained anchored between lowerings of the flume, and the anchor is not believed to have dragged along the bottom. Yet, the critical values of u_* for these two experiments are the highest and lowest u_* values of all the experiments. Large variations in erosion resistance

over small distances are apparently possible in the mud facies of Buzzards Bay. A similar comparison of u_* for experiment AST 74-19, which took place during the Fall, and u_* for experiment AST 75-1, which took place during mid-Winter, shows that the sediments eroded at similar critical u_* during these experiments. Pending further experiments encompassing other seasons and different areas of the mud facies, it appears that seasonal variations in erosion resistance may not be as important as small-scale spatial variations in erosion resistance.

Erosion Resistance as a Function of Biogenic Reworking

One of the most important observations made during the in situ experiments was how infaunal organisms affect erosional resistance of fine marine sediments. In all experiments where the dominant bed surface features were clearly biogenic (Figures 5, 6, and 7), critical values of u_* were low (0.39 cm/sec or less), while when biogenic effects were less apparent (Figures 8, 11), values of u_* were higher, reaching 0.83 cm/sec during experiment AST 74-24. Flat portions of the bed eroded at slightly higher u_* than the tracks and trails made by the organisms (Table 4).

Several different aspects of infaunal activity are probably responsible for the relatively low values of u_*. Deposit feeders induce high water content in the Buzzards Bay muds by fecal and pseudofecal pelletization of the sediments, and by physical mixing and reworking during burrowing activities. As a first approximation, fine sediments with high water content are known to erode more easily than beds of fine sediment with low water content (Postma, 1967; Rhoads, 1970)

Movements of the benthic snails and bivalves, besides contributing to the high water content of the surface sediments, also result in relatively deep surface furrows (Figures 5, 6, 7, 16, and 17). The small levees along the furrows protrude into a region of higher velocity in the flow, and should therefore have a higher potential for erosion. Smoothing of surface furrow and trails are in fact some of the first observable evidence for erosion in the field and laboratory experiments.

Polychaete worms which burrow near the sediment-water interface produce several different effects on the properties of the sediments; these effects are probably species-dependent. Some species tunnel through the sediment by

ingesting and periodically excreting detritus. If organisms tunnel horizontally near the sediment-water interface, the tops of their tunnels can push up and physically disrupt the sediment surface. This behavior was observed in the laboratory experiments described in Chapter III (Figure 15). It can be hypothesized that when sediments lose physical support and attachment and are broken up, they should be more easily eroded.

Other worm species are tube builders. Tube walls consist of thin layers of sediment agglutinated or "glued" together by organic secretions. The presence of groups or patches of these tubes has been shown to significantly increase the bulk shear strength of the sediments (Rowe, 1974). Burrowing anemones found in the mud facies also bind the surrounding sediments with organic secretions and increase sediment shear strength (Rhoads et al, 1974; Rowe, 1974). Both types of tube-builders tend to create patches of sediment having higher resistance to erosion.

Erosion of Bottom Sediments by Tidal Currents

Estimates of u_* made in this study from current velocities at Station K (Chapter II) were based on the assumption of steady uniform flow and the development of a logarithmic

boundary layer profile. The velocity data (Figure 13) indicate that a logarithmic boundary layer was present during only three of the nine lowerings (see discussion in Chapter II). This may be explained by referring to the dynamics of flow in a shallow marine embayment. In such embayments, tidal excursions produce periods of generally steady flow during flood and ebb of the tide. But, wind waves are superimposed on this steady flow situation, and development of the near-bottom tidal boundary layer is intermittently disrupted by the rapid development and disappearance of wave boundary layers. The velocity measurements at Station K (Figure 13), and the sparcity of logarithmic bottom-velocity profiles during the period of measurement, seem to support the above analysis. It should therefore be recognized that the range of u_* values estimated at Station K are minimum estimates which assume steady flow.

Sedimentary environments in Buzzards Bay are in many ways typical of shallow marine areas of mud deposition throughout the world ocean. If so, then estimates of critical u_* obtained during the in situ experiments may be representative of erosional resistance of bioturbated shallow-water muds in general. Other factors will tend of course to either

increase or decrease erosion resistance. These factors include variations in sedimentation rates, mineralogical and organic composition, water chemistry, and flow dynamics.

Conceptual Model for Erosion of Fine-Grained Sediments

The next matter to consider is the feeling held by some workers that instantaneous shear stress rather then mean shear stress is the fluid dynamical property which controls erosion. Consider first a turbulent boundary layer flowing over an erodible boundary. Several recent studies (Kline et al; 1967; Corino and Brodkey, 1969; Grass, 1971; Eckelmann, 1974) have shown that flow in a turbulent boundary layer near rough and smooth boundaries is characterized by ejection of low-momentum fluid parcels away from the boundary and inrush of high-momentum fluid parcels toward the boundary. This phenomenon has been termed bursting; the three-dimensional picture is one of eddies bursting from the bed, being entrained in the flow near the bed, and stretching in a downstream sense (Kim et al, 1971). It has further been suggested (Grass, 1971) that this process of momentum exchange is primarily responsible for turbulence production near the boundary.

What does this imply with respect to erosion processes

in the in situ flume? The impression gained from the bursting phenomenon described above is that energetic parcels of water are intermittently impinging directly onto the bed. The inrushing fluid parcels can impart instantaneous values of τ which are as much as thirty times the mean value of τ (Eckelmann, 1974).

But how do these highly energetic fluid parcels actually erode the sediments? Only a partial answer to this question can be given. Partheniades (1961) and Mitchell (1964) among others, have hypothesized that a network of inter-particle bonds exists in a bed of cohesive sediments which can only be described in a statistical sense (see Appendix A). That is, if the network of bonds between the particles is constantly changing due to small-scale thermodynamic processes (Mitchell, 1964), then the probability that every potential bond site on a given particle will be filled is a function of time and thermal structure in and around the individual particles. The number of bonds that a particle shares with its neighbors will largely determine its resistance to erosion. Unfortunately, neither the bonding probability function nor the temporal and spatial distribution of instantaneous shear stress have been adequately described

for most flow and sediment situations, so it seems that, for the present, we are limited to use of mean values to describe erosion processes.

Details of flow within the in situ flume channel must also be considered. Leutheusser (1963), for example, has shown that τ in a wide rectangular duct does not become uniformly distributed until the duct Reynolds number (based on centerline velocity and half-channel height) exceeds about 10^5. Reynolds numbers in the in situ flume were below 10^5, but Leutheusser's data also infer that at lower Reynolds numbers local values of shear stress along the central one-third of the duct top and bottom are no more than 10% greater than the mean value of the shear stress for the entire duct. Since measurement of axial velocity with the sphere current meter may vary ± 10% of the actual velocity, small errors in estimating τ fall well within the "noise" range of the velocity signal. Prandtl's power-law method used in this study to calculate τ from axial velocity measurements has τ varying as $u^{7/4}$, so, if u(actual) = u(measured) ± 0.1u(measured), then τ(actual) = τ (calculated) ± 0.15 τ(calculated).

LABORATORY EROSION EXPERIMENTS

Previous erosion studies in the laboratory have concentrated on establishing the relationships among erosional resistance, water content, compaction time, and depositional environment. In the study presented here, these results have been extended to include the effects of sampling disturbance, biogenic reworking, and organic content.

It has been shown, for example, that the resistance of fine-grained sediment to erosion can be thought of as a balance between biological and sedimentological effects. For muds in shallow marine environments where wave and current activity is low and in which faunal activity is high, the effects of biogenic reworking can dominate the sedimentological effects produced by cohesion and organic "glueing". When wave and current activity is greater, such as during storms, the biologically reworked surface layer can be eroded, exposing layers of more compact sediment that have higher erosion resistance.

The bottom sampling device used to obtain sediments for laboratory experiments, and the techniques used to deposit the beds, caused complete destruction of the original sediment surface layer. This is probably equivalent to the vigorous erosion of the bottom of Buzzards Bay by strong tidal or wave-

induced currents followed by formation of a new flocculent bed surface by deposition from a dense suspension. Thus, the results of the experiments on the partially (one and five day) reworked laboratory beds can be thought of as a possible model for certain transient sedimentary environments in Buzzards Bay. The relatively high values of u_* required to erode beds which had compacted for one to five days with little concurrent biogenic reworking probably reflects the thixotropic properties of the clays in the sediments. As biogenic reworking becomes more complete, thixotropic properties, which are short range interparticle properties, become subordinated to the disruptive effects of pelletization and bioturbation.

Laboratory Models of Biogenic Reworking

If the distribution and abundance of organisms in the three biogenically reworked beds used in the laboratory experiments is similar to *in situ* distribution and abundances, then the net rate of reworking of these beds should also be similar, and the degree of reworking in the laboratory should be mainly a function of time. However, a recent study of benthic invertebrates in Buzzards Bay muds (Nichols-Driscoll et al, in preparation) indicates that

organisms may not be homogeneously distributed. Since a census of organisms in the reworked beds was not made, other ways of estimating the representativeness of the fauna must be found.

The sediment volumes obtained by the bottom sampler used in this study (0.04 m^2 Van Veen grab sampler) and by Nichols-Driscol et al (0.04 m^2 box cores) are about equal; only the method of obtaining the samples differed. Divers obtained the latter sample from grid locations preselected from a table of random numbers, while the sediments used for laboratory erosion experiments in this study were obtained by lowering the grab sampler from a slowly drifting ship in the vicinity of Station K. Since sampling points were purposely randomized in the former study and were operationally randomized by the drifting of the ship during the present study, I infer that the real distribution and number of organisms per unit area of sea floor is well represented by either method of sampling.

Changes in species distribution may occur during the year at Station K (Nichols-Driscoll et al, in preparation), but the net biogenic effect on sediment properties remains about

the same. This is because the cold-tolerant species have life-habits which are similar to their warm-tolerant counterparts (Jean Nichols-Driscol, personal communication). Abundance of total fauna apparently increases during late Fall but remains fairly constant during other parts of the year (Jean Nichols-Driscol, personal communication).

Since the mode of initial deposition and organic and mineralic composition of the experimental beds was the same in all cases, it seems reasonable to conclude that any differences in erosion resistance among the three beds was primarily due to the degree of reworking.

Erosion Resistance and Concentration of Organic Matter

The laboratory experiments on flat beds suggest that erosion resistance may be a function of organic matter concentration in the absence of reworking by large organisms (Figure 20A). Mode of erosion, discussed in a following section, also seems to depend on concentration of organic matter. A simple explanation for the non-linear relationship between microbial biomass (ATP) concentration in the sediments and erosional resistance (Figure 20B) is that contamination during sampling gave

false values of ATP. This does not seem likely because of the size of the samples (1 to 5 grams). Concentrations of microorganisms in large samples of organic-rich sediments would probably be orders of magnitude larger than any contamination in the clean plastic sample bags or laboratory glassware. Another possibility is that microorganisms which add to sediment cohesion are not a constant fraction of the microbial population. This is an interesting possibility, but there are no data to test it. Still another possibility is that the particulate (non-living) fraction of the organic material imparts the major biogenic effect on cohesion in the absence of meio- and macrobenthonic organisms. If this is true, then microbial concentration need not be directly related to erosion resistance. Finally, duration of the experiments must be considered. Under ideal conditions, populations of some microorganisms (e.g. bacteria) are known to double as rapidly as every 20 minutes while others (algae and other phytoplankton) double their population every 8 to 24 hours. Time between measurement of the critical erosion condition and sampling of the sediment ranged from two to four hours dur-

ing the experiments. Thus, both number and kinds of microorganisms living in the bed could change in a nonuniform way between the time erosion was initiated and the ATP in the bed sample was extracted.

Mode of Erosion

During the laboratory experiments it was also observed that the mode of erosion of both the flat laboratory beds and the essentially unreworked (one and five day) beds was characterized by the removal of thin uniform layers of sediments. This may be interpreted in terms of the methods used for bed preparation. Flat beds were prepared by deposition from a dense flowing suspension onto a basal layer deposited from a still suspension. Biogenically reworked beds were formed initially by stirring the upper several cm of a remolded bottom sample and settling in a very slowly flowing dense suspension. Flocculation effects and differential settling may have produced beds in which two microfabrics were present, one representing the basal layer and another representing the surface layer. The basal layer formed during deposition from still water would consist of larger and faster-settling flocs composed of silt and some clay-sized particles. The deeper layers would be

deformed by the overburden and start to compact. As deposition started from flowing water, the compacting basal layers would be covered by layers of smaller flocs and grains. It is easy to imagine that, under the conditions outlined above, the surface layers deposited from flowing water would be more flocculent and loosely bound than the basal layer. Further experiments are needed, however, at suspension concentrations similar to the low concentrations in natural bottom waters to determine if the two-layer sediment structure is formed during deposition.

Lee Drifts

Erosional bedforms common in both modern and ancient fine-grained sediments generally fall into the category of: scour pits; flute marks; and tool marks; a review of these bedforms is given by Allen (1971). However, little attention has been given to the formation of depositional bedforms such as lee-drift deposits, and whether fine-grained sediments can form larger wavelike bedforms such as ripples or dunes is a matter still open to question (Heezen and Hollister, 1971, p. 349, Figures 9.44 and 9.46).

In the experiment described in Chapter III, boundary layer separation was related to the formation of lee drifts

through a critical body Reynolds number. Theoretical and experimental results indicate that lee drifts should form when the body Reynolds number R_K falls below a critical value. Theory indicates that critical body Reynolds number should also be a function of shape, but this effect was not investigated during the present experiments. As velocity increases, there is a decrease in the size of the body behind which lee drifts can form; the opposite is also true.

Temperature (viscosity) of the water may also influence the formation of lee drifts, since $R_K \propto 1/\nu$. Viscosity varies by nearly a factor of two between surface and deep ocean waters, and by a similar amount during summer and winter seasons in shallow water. Thus, lee drifts of fine-grained sediments can form in any steady unidirectional flow of the proper temperature in which there is a sufficient supply of sediment and a body of proper size and shape protruding from the bed.

COMPARISON WITH PREVIOUS WORK

The results of several previous studies can be compared with the results of the present study. Partheniades (1962) and Krone (1962) studied the erosional and depositional behavior of an estuarine sediment similar in lithology and

organic concentration (but including no living organisms except possibly microorganisms) to the Buzzards Bay sediments. Critical τ for their sediment (0.7 dynes/cm^2) falls within the range of critical τ values obtained during the in situ flume experiments. In the present study, biological reworking of the sediments often produced critical τ values lower then 0.7 dynes/cm^2, while, when bioturbational effects were minor or absent, critical τ values were much closer to the values reported by the above investigators.

So far as the mode of erosion is concerned, erosion by removal of small aggregates from the bed surface, as proposed by Partheniades (1962), is probably a valid concept for uncompacted beds of relatively high water content. Krone (1962) has estimated that typical floc aggregates deposited at the bed surface are crushed after burial of one or two cm, thus increasing interparticle bonding and cohesion. Such sediments would be more difficult to erode. Partheniades (1962) showed that, at erosion velocities above the critical velocity, rates of erosion tended to sharply decrease with time as deeper layers of the bed were exposed.

Lonsdale and Southard (1974) used a laboratory flume to erode beds of deep-sea red clay which had a range of bulk

water contents similar to those of the in situ Buzzards Bay sediments. Critical erosion velocities in their experiments were two to three times higher than the erosion velocities observed during in situ flume experiments in the present study. But, as these investigators have noted, it was not possible to successfully simulate in the laboratory the effects of deep-sea organisms on the upper few cm of the bed. Estimates of critical erosion velocities as a function of water content made by Lonsdale and Southard, may therefore be higher than would be measured on the deep sea floor.

More compacted fine-grained sediments with low water contents require higher erosion velocities (Postma, 1962; 1967; Lonsdale and Southard, 1974). A different sort of erosion mechanism is proposed for these beds: mass erosion or the removal of macroscopic pieces of the bed surface. This mode of erosion may be more directly related to the bulk shear strength of the sediments than is the erosion of small aggregates piece-by-piece from the bed. Further study on the microfabric of fine sediments is necessary before more definite conclusions can be drawn about the erosion mechanisms.

SUMMARY AND CONCLUSIONS

1. Observations made with the in situ flume suggest that erosion resistance of sea floor sediments is related to the extent and mode of biogenic reworking; even slightly compacted sediments are eroded at u_* values nearly twice that of biogenically reworked sediments. This also points out the importance of thixotropic strength increases over relatively short time periods.

2. Seasonal variations in erosion resistance of Buzzards Bay muds are probably no greater than variations in erosion resistance caused by subtle lateral inhomogeneities in sediment physical and biological properties.

3. Sampling disturbances alter the network of cohesive bonds and biogenic structures which determine the erosion resistance of fine-grained marine sediments. Therefore, the erosional behavior of azoic or resedimented fine-grained sediments in the laboratory cannot be compared to the erosion of undisturbed sediments in nature.

4. In the absence of biogenic reworking, concentration of organic matter seems to control erosion resistance; the larger the concentration of organic

matter, the greater the resistance to erosion. At the same time, compaction and thixotropic effects work to increase erosion resistance with time, regardless of organic content.

5. Behavior of fine-grained sediments during erosion by steady unidirectional currents is characterized by the formation of lee drifts behind bed roughness elements. Lee drifts form only when the body Reynolds number, determined by the size and shape of the roughness elements and viscosity and velocity of the water, is below a critical value. Further experiments are necessary to verify these results.

6. This study has only " scratched the surface" toward understanding behavior of fine-grained sediments during erosion on the sea floor. It has, however, shown that with the proper research tools, it is possible to obtain reliable quantitative estimates of erosion of undisturbed sediments on the sea floor.

References

Allen, J.R.L., 1971, Transverse erosional marks of mud and rock: their physical basis and geological significance, Sed. Geol., 5, 167-385.

Bennett, R.H., G.H. Keller, and R.F. Busby, 1970, Mass property variability in three closely spaced deep-sea cores, Jour. Sed. Petr., 40, 1038-1043.

Bingham, E.C., 1922, Fluidity and Plasticity, McGraw Hill, New York, 386 p.

Bowles, F.A., 1968, Microstructure of sediments. Investigations with thin sections, Science, 159, 1236-1237.

Collins, K. and A. McGown, 1974, The form and function of microfabric features in a variety of natural soils, Geotechnique, 24, 233-254.

Corino, E.R. and R.S. Brodkey, 1969, A visual investigation of the wall region in turbulent flow, Jour. Fluid Mech., 37, 1-30.

Daily, J.W. and D.R.F. Harleman, 1966, Fluid Dynamics, Addison-Wesley, Reading, Mass., 454 p.

Eckelmann, H., 1974, The structure of the viscous sublayer and the adjacent wall region in a turbulent channel flow, Jour. Fluid Mech., 65, 439-459.

Edzwald, J.K., J.B. Upchurch and C.K. O'Melia, 1974, Coagulation in estuaries, Envir. Sci. Tech., 8, 58-63.

Einsele, G., R. Overbeck, H.U. Schwarz and G. Unsold, 1974, Mass physical properties, sliding and erodibility of experimentally deposited and differently consolidated clayey muds, Sed., 21, 339-372.

Einstein, H., 1941, The viscosity of highly concentrated underflows and its influence on mixing, Trans. A.G.U., 22, 597-603.

Einstein, H. and R.B. Krone, 1961, Experiments to determine modes of cohesive sediment transport in salt water, Jour. Geophys. Res., 67, 1451-1464.

Goldschmidt, V.M., 1926, Undersokelser over lersedimenter, Nordisk jordbrugsforskning, no. 4-7, 434-445.

Grass, A.J., 1971, Structural features of turbulent flow over smooth and rough boundaries, Jour. Fluid Mech., 50, 233-255.

Hahn, H.H. and W. Stumm, 1970, The role of coagulation in natural waters, Amer. Jour. Sci., 268, 354-368.

Heezen, B.C. and C.D. Hollister, 1964, Deep sea current evidence from abyssal sediments, Mar. Geol., 1, 141-174.

Heezen, B.C. and C.D. Hollister, 1971, The Face of the Deep, Oxford, 659 p.

Hjulstrom, F., 1939, Transportation of detritus by moving water in P.D. Trask, ed., Recent Marine Sediments, A.A.P.G., 3-31.

Holt, M., 1961, Dimensional analysis in V.L. Streeter, ed., Handbook of Fluid Dynamics, McGraw Hill, New York, Chapter 15.

Hough, J.L., 1940, Sediments of Buzzards Bay, Massachusetts, Jour. Sed. Petr., 10, 19-32.

Inman, D.L., 1963, in F.P. Shepard, ed., Submarine Geology, Harper and Row, Chapter V.

Keller, G.H. and R.H. Bennett, 1970, Variations in the mass physical properties of selected submarine sediments, Mar. Geol., 9, 215-223.

Kline, S.J., W.C. Reynolds, F.A. Schraub, and P.W. Runstadler, 1967, The structure of turbulent boundary layers, Jour. Fluid Mech., 30, 741-773.

Kim, H.T., S.J. Kline, and W.C. Reynolds, 1971, The production of turbulence near a smooth wall in a turbulent boundary layer, Jour. Fluid Mech., 50, 133-160.

Kranck, K., 1973, The nature and deposition of suspended marine sediment, Report D-BI-R-73-12, Bedford Inst. Oceanogr.

Krone, R.B., 1962, Flume studies of the transport of sediment in estuarial shoaling processes, Final Report Hydr. Eng. and San. Eng. Res. Lab., Univ. Calif., Berkeley, June, 1962.

Krone, R.B., 1963, A study of rheologic properties of estuarial sediments, S.E.R.L. Report 63-8, Univ. Calif., Berkeley, Calif., 91 p.

Kuenen, Ph. H., 1965, Experiments in connection with turbidity currents and clay suspensions in W.F. Whittard and R. Bradshaw, eds. Submarine Geology and Geophysics, Butterworth's, London, 47-71.

Langhaar, H.L., 1951, Dimensional analysis and theory of models, Wiley, New York.

Leutheusser, H.J., 1963, Turbulent flow in rectangular ducts, Proc. A.S.C.E., HY3, 89, 1-19.

Lonsdale, P. and J.B. Southard, 1974, Experimental erosion of North Pacific red clay, Mar. Geol., 17, M51-M60.

MacIlvaine, J.C., 1973, Sedimentary processes on the continental slope off New England, Tech. Rpt. W.H.O.I., 73-58, unpublished manuscript.

Meade, R.H., 1964, Removal of water and rearrangement of particles during the compaction of clayey sediments, review, U.S.G.S. Prof. Paper, 497-B, B1-B23.

Migniot, C., 1968, Etude des propriete physiques de differents sediments tres fins et leur comportements sous des actions hydrodynamiques, La Houille Blance, 7, 591-620.

Mitchell, J.K., 1964, Shearing resistance of soils as a rate process, Proc. A.S.C.E., SM1, 90, 29-61.

Moore, J.R., 1963, Bottom sediment studies, Buzzards Bay, Massachusetts, Jour. Sed. Petr., 33, 511-558.

Neumann, A.C., C.D. Gebelein and T.P. Scoffin, 1970, The composition, structure and erodibility of subtidal mats, Abaco, Bahama, Jour. Sed. Petr., 40, 274-297.

Nichols-Driscoll, J., C.H. Clifford, G.T. Rowe, and R.A. Young, 1975, In situ experiments on the burial of marine invertebrates, in preparation.

Partheniades, E., 1962, A study of erosion and deposition of cohesive soils in salt water, Ph.D. Thesis, Dept. C.E., Univ. Calif., Berkeley, Calif., 182 p.

Pierce, T.J., R.T. Jarman, and C.M. de Turville, 1970, An experimental study of silt scouring, Proc. Inst. Civ. Engineering (England), 38 231-243.

Postma, H., 1962, Sediment in Demerara Coastal Investigation, Hyd. Lab., Delft, The Netherlands, 105-164.

Postma, H., 1967, Sediment transport and sedimentation in the estuarine environment in G.H. Lauff, ed., Estuaries, AAAS Publication 83, Wash., D.C., 158-179.

Prandtl, L. and O.G. Tietjens, 1934, Applied Hydro- and Aero-mechanics, Dover, New York, 311 p.

Pusch, R., 1970, Clay microstructure, Document D8:1970, Nat. Swedish Inst. for Building Res., Stockholm, 76 p.

Rhoads, D.K., 1970, Mass properties, stability and ecology of marine muds related to burrowing activity in T.P. Crimes and J.C. Harper, eds., Trace Fossils, Geol. Jour. Spec. Issue 3, 391-406.

Rhoads, D.C., 1973, The influence of deposit-feeding benthos on water turbidity and nutrient recycling, Amer. Jour. Sci., 273, 1-22.

Rhoads, D.C. and D.K. Young, 1970, The influence of deposit-feeding organisms on sediment stability and community trophic structure, Jour. Mar. Res., 28, 150-178.

Rhoads, D.C., K. Tenore and M. Brown, 1974, The role of resuspended bottom muds in the food chain of shallow embayments, Proc: 2nd Int. Estuarine Symp., Myrtle Beach, South Carolina (in press).

Rowe, G.T., 1974, The effects of the benthic fauna on the physical properties of deep-sea sediments in A.L. Inderbitzen, ed., Deep Sea Sediments, Plenum, New York, 381-399.

Rowe, G.T., G. Keller, H. Edgerton, N. Staresinic, and J. MacIlvaine, 1974, Time-lapse photography of the biological reworking of sediment in Hudson submarine canyon, Jour. Sed. Petr., 44, 549-552.

Sanders, H.L., 1958, Benthic studies in Buzzards Bay, I. Animal-sediment relationships, Limn. Oceanogr., 3, 245-258.

Sanders, H.L., 1960, Benthic studies in Buzzards Bay, III. The structure of the soft-bottom community, Limn. Oceanogr., 5, 138-153.

Scoffin, T.P., 1968, An underwater flume, Jour. Sed. Petr., 38, 244-247.

Shields, I.A., 1936, Application of similarity principles and turbulence research to bed-load movement, translated from "Anwendung der Aehnlichkeitsmechanick und der Turbulenzforschung auf die Geschiebebewegung," by W.P. Ott and J.C. van Uchelen, Publ. 167, Hyd. Laboratory, Cal. Inst. Tech., Pasadena.

Smerdon, E.T. and R.P. Beasley, 1961, Critical tractive forces in cohesive soils, Agricultural Eng., 42, 26-29.

Southard, J.D., R.A. Young, and C.D. Hollister, 1971, Experimental erosion of calcareous ooze, Jour. Geophys. Res., 76, 5903-5909.

Sternberg, R.W., 1969, Camera and dye-pulser system to measure bottom boundary layer flow in the deep sea, Deep-Sea Res., 16, 549-554.

Sternberg, R.W., 1971, Friction factors in tidal channels with differing bed roughness, Mar. Geol., 6, 243-260.

Sternberg, R.W., 1972, Predicting initial motion and bed load transport of sediment particles in the shallow marine environment in D.J.P. Swift, D.B. Duane, and O.H. Pilkey, eds., Shelf Sediment Transport: Process and Pattern, Dowden, Hutchinson and Ross, Stroudsburg, Pa. , 61-82.

Sundborg, A.F., 1956, The river Klarelven, a study on fluvial processes, Geogr. Ann. Arg., 37, 125-316.

Terwindt, J.H.J., H.N.C. Breuser, and J.N. Svasek, 1968, Experimental investigation of the erosion-sensitivity of a sand-clay lamination, Sedimentology, 11, 105-114.

Terzaghi, K., 1925, Erdbaumechanik auf Bodenphysikalischer Grundlage, Deuticke, Vienna.

Van Olphen, H., 1963, An Introduction to Clay Colloid Chemistry, Wiley, New York, 301 p.

Whitehouse, U.G., L.M. Jeffrey, and J.D. Debbrecht, 1958, Differential settling tendencies of clay minerals in saline waters, Proc. Seventh Nat. Conf. Clays and Clay Minerals, Pergamon, 1-79.

Young, D.K., 1971, Effects of infauna on the sediment and seston of a subtidal environment, Vie et Milieu, Supp. 22, 557-571.

APPENDIX A

SEDIMENT PROPERTIES RELATING TO EROSIONAL RESISTANCE OF FINE-GRAINED SEDIMENTS

INTRODUCTION

The physical properties and processes which probably relate most directly to erosional resistance of fine marine sediments include cohesion, flocculation, consolidation and thixotropy, bed microfabric, mineralogic and organic composition and concentration, grain size distribution of flocs and primary particles, and water temperature and chemistry. Functional relationships among these properties are not always predictable, but Figure A-1 shows how each of the properties may depend on the others.

Empirical relationships among sediment bulk physical properties have been used to derive equations predicting the resistance of fine-grained sediments to erosion in fresh water (see Smerdon and Beasley, 1961). However, wide variations in the values of bulk physical properties have been observed for both closely and widely spaced marine sediment samples taken in erosional and depositional environments (Bennett et al, 1970; Keller and Bennett, 1970), so there is some doubt that the approach used by Smerdon and Beasley would be useful in marine erosion problems. In any case, there is some evidence, discussed below, that

Figure A-1. Chart illustrating the relationships among the physical and biological properties influencing erosional resistance of fine sediment deposits.

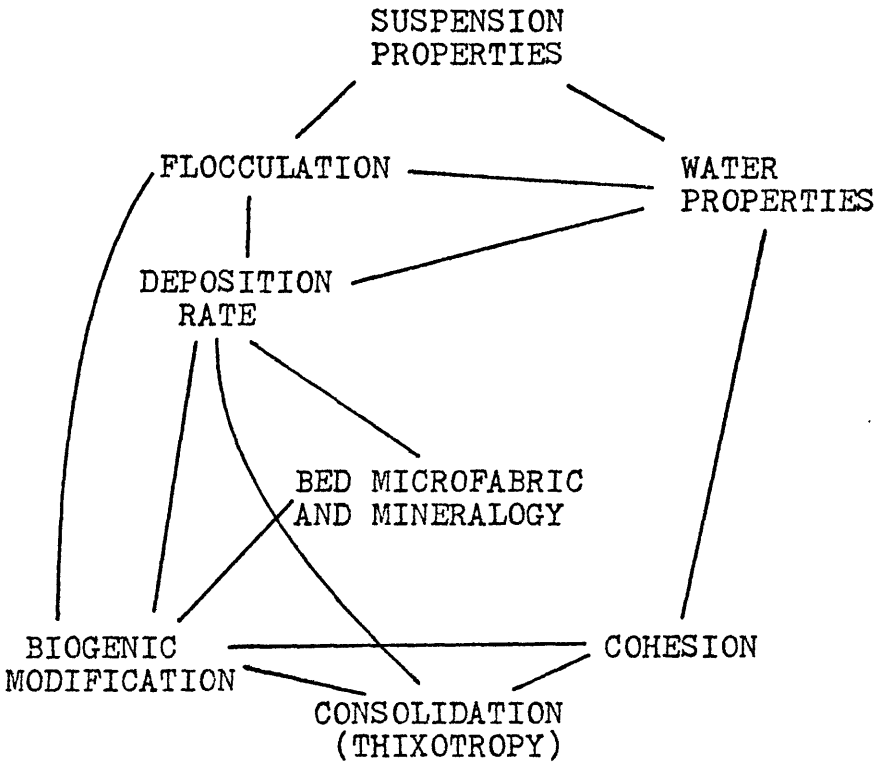

= EROSION RESISTANCE

bulk physical properties do not represent the physical properties of the sediments at the sediment-water interface where erosion is initiated.

COHESION

If erosion resistance of fine-grained sediments depended only on particle size and weight, then weak currents would easily erode them. Since most fine-grained marine sediments are not easily eroded, other forces such as cohesive forces must represent a major component of their erosional resistance.

Cohesion arises mainly from attractive forces between clay particles, organic binding, and incipient cementation of unconsolidated sediments. The relative contributions of these three factors varies according to sedimentary environment, but, for low carbonate, recent sediments, incipient cementation is probably the least significant factor, whereas interparticle attraction and possibly organic binding are the most significant.

Clay particles are thought to have negative surface charges on their faces and net positive charges on their edges because of isomorphous substitutions in their crystal lattice (Van Olphen, 1963). Individual particles of the

common clays (montmorillonite, kaolinite, illite, chlorite) are flat and have low edge-to-face ratios. Thus, the faces of the clay particles exercise strong control on particle behavior.

In fresh water the surface charges on the particle faces attract a diffuse cloud of cations and anions. This is called the electrical double layer because the anions are more concentrated in the inner region of the double layer and cations are more concentrated in the outer region. Clay particles tend to repel each other in fresh water because of the similar charges in the outer parts of the double layer.

As electrolyte concentration increases the electrical double layer is compressed. When the electrolyte concentration is sufficiently high (a salinity of 2 to 4‰ in the case of sea water) the clay particles can approach closely enough to each other so that the short-range attractive forces (London-van der Waal's forces) associated with atoms in the crystal lattice of the particles can become effective (Van Olphan, 1963, Figure 12). Formation of these bonds and bond networks is called salt flocculation and the aggregates so formed are called flocs. Since clay particles are usually flat and flake-like with high face/edge ratios,

salt water is more effective in promoting flocculation than is fresh water.

A traditional way of defining cohesion (C) is by Coulomb's equation, $\tau = C + \sigma' \tan \phi$ where τ is sediment shear strength at failure, σ' is effective stress, and ϕ is a measure of that part of total shearing resistance dependent only on inter-particle friction. When shear strength is measured by a shear vane or similar device under undrained, saturated conditions, $\sigma' \to 0$ and $\tau \to C$.

Cohesion of the first few floc layers at the sediment-water interface is thought to be lower than cohesion in deeper bed layers because lower layers have greater numbers of interfloc bonds (Krone, 1961; Partheniades, 1961). Unfortunately, shear vane measurements cannot characterize cohesion at the sediment-sea water interface where erosion is initiated. This is probably because shear vane measurements give the total shear strength of the layer intercepted by the vane blade, a layer normally 0.5 cm or more in thickness. Since floc diameters rarely exceed 10-20 μ, individual flocs or small aggregations of flocs probably represent only a small fraction of the total sample thickness in vane shear tests.

The magnitude of cohesive forces between small floc

units would probably provide a meaningful estimate of the erosion resistance of flocculated sediments. Based on Bingham's (1922) study of viscosity of suspensions, Einstein (1941) proposed that the (Bingham) yield stress of a suspension of fine-grained, cohesive sediment being forced through a capillary viscometer was proportional to the bond strength (or cohesion) between the shearing flocs in the capillary tube. Subsequent studies (Krone, 1962; Migniot, 1968) have suggested that the fluid shear stress necessary to initiate erosion of sediments in situ can be related to the Bingham yield stress. Based on a laboratory flume study of 15 estuarine sediments, Migniot (1968) has defined an erosion criterion for cohesive sediments as $u_* = 0.5\tau_y^{1/2}$, Migniot found that this relationship holds only when τ_y exceeds 10 dynes/cm^2. Since τ_y values measured in other studies are significantly less than the critical value given by Migniot (e.g. less than 8 dynes/cm^2 for seven of 8 sediments measured by Krone (1962); less than 3 dynes/cm^2 for Buzzards Bay muds measured during this study on a capillary viscometer similar to Krone's), Migniot's erosion criterion seems limited in usefulness.

FLOCCULATION

The physical properties of near-surface sediments are often highly dependent on deposition rate and floc size (see Figure A-1), which depend on flocculation in the water column. In still waters interparticle or interfloc collisions cause flocculation through Brownian movements or because flocs of different settling rate collide; in flowing water, velocity gradients (internal shear rate) and turbulence promote flocculation. Some workers (Krone, 1962; Hahn and Stumm, 1970) believe flocculation of dispersed fine-grained suspension occurs mainly through scavenging of the slowly-falling smaller flocs by the faster-falling larger ones.

Turbulence generated at the bed or as internal shear in the flow well above the bed has been shown to influence flocculation rates. Krone (1962) suggested that since the shear rate near the bed is always higher than the internal shear rate, aggregations of flocs formed in equilibrium with the lower internal shear rates would probably be broken down to some degree as they approached the region of higher shear rates near the bed. This mechanism could result in non-deposition of the broken flocs if, as Krone suggests,

the settling velocities of the floc fragments are lower than that of the unbroken floc aggregates.

Consideration of net differences in attractive force between different clay mineral species has led some workers to speculate that mineralogy should be significant in flocculation processes (Hahn and Stumm, 1970). A recent study of flocculation kinetics in extremely dilute suspensions of pure clay and fine estuarine sediments suggests that this may be true (Edzwald et al, 1974). However, Kranck (1973), who studied suspensions in coastal ocean waters, has speculated that mineralogy has a secondary effect, and that floc size distributions in sea water are primarily determined by an equilibrium between sediment supply (concentration) and hydrodynamic conditions (internal shear rates).

Water chemistry, salinity in particular, also influences flocculation. Whitehouse et al (1958) and Edzwald et al (1974) have demonstrated empirically that increases in salinity beyond 2 to 4 °/oo have virtually no effect on flocculation and settling velocity in monomineralic suspensions of various pure clays and clay mixtures. The most obvious changes in flocculation kinetics and settling velocities occur in estuaries where fresh and salt water mix. Once

flocculated, sediments are transported into the open ocean where the salinity is well above 6 °/oo; small seasonal or longer termed salinity variations should have little effect on flocculation or on cohesion. Within an estuary salinity varies as the salt wedge moves up and down the floor of the estuary. This may have effects on the state of flocculation of sediments exposed to changes salinity.

Seasonal temperature variations in shallow marine waters influence ion activity and physical properties of water which will in turn affect cohesion and flocculation. Temperature variations and their effect on settling rates have been demonstrated in the laboratory by Whitehouse et al (1960); higher temperatures produced faster flocculation and settling rates.

Organic binding of particulate suspended matter and pelletization by pelagic organisms may also be an important factor in the formation of flocs. Exploratory experiments using pure organic compounds in sea water (Whitehouse et al, 1960) have shown that the flocculation and settling behavior of some montmorillonites and kaolinites are changed in the presence of dissolved organic material (Figure A-2).

Because flocs settle slowly, microbial activity

Figure A-2. Changes in settling behavior of monomineralic clay mineral suspensions caused by addition of pure organic compounds. Three or more species of each clay mineral group were treated with a number of organic compounds from the organic compound groups roughly defined as humic acids, proteins, and carbohydrates. The given curves are averages of the maximum settling velocity changes compared to settling velocities of untreated suspensions (data from Whitehouse et al, 1958).

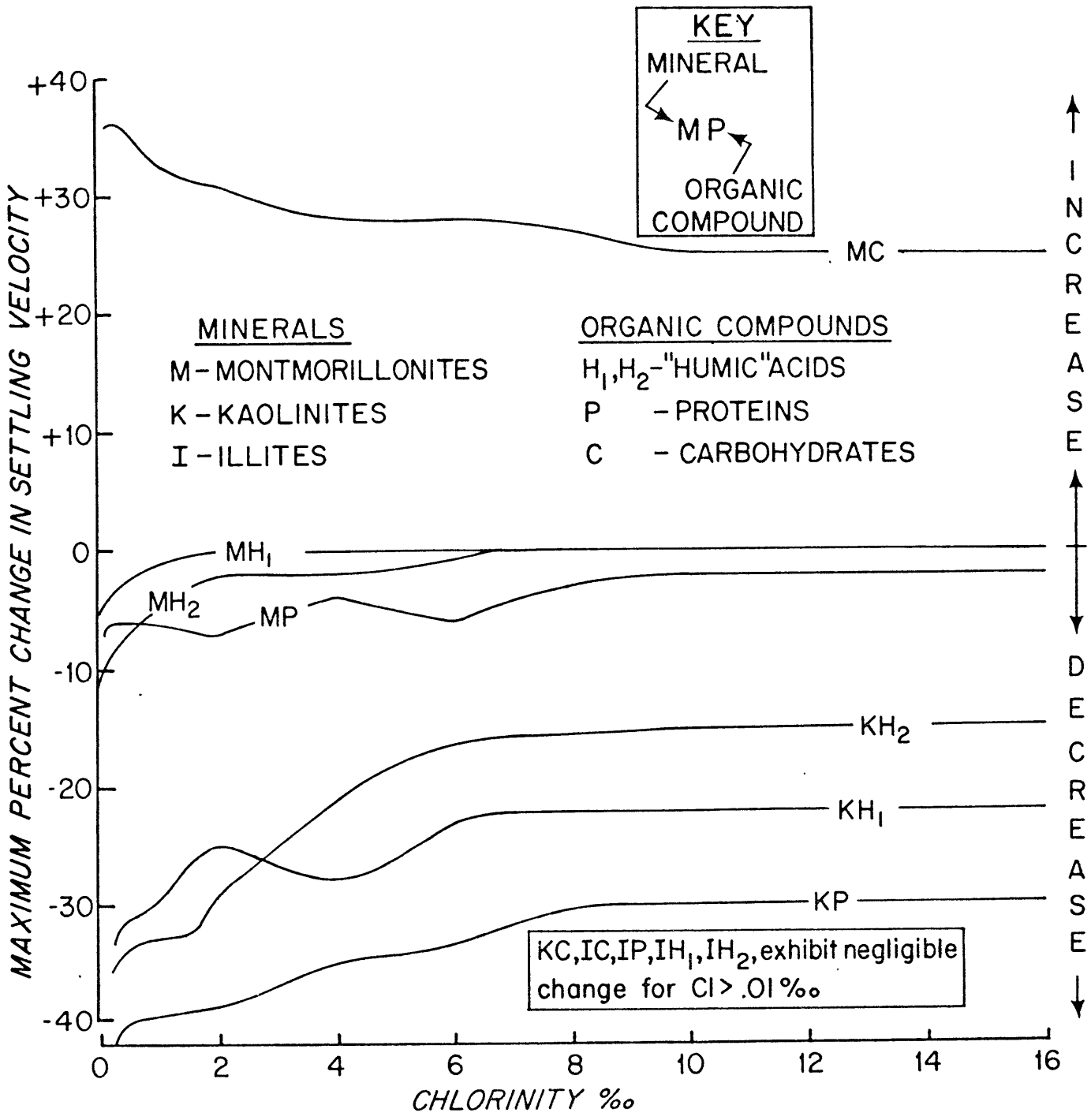

EFFECT OF ORGANIC MATERIALS ON SETTLING VELOCITIES OF CLAY MINERALS IN ARTIFICIAL SEA WATER OF VARYING SALINITY

within flocs may cause alteration of floc strength or structure before deposition. It is speculated here that microbial activity also may affect erosional resistance of the sediments. Laboratory experiments were conducted to test this hypothesis and are reported in the text in Chapter III.

CONSOLIDATION AND THIXOTROPY

The resistance of a sediment to deformation by an applied shear stress is termed its shear strength and is a measure of its state of consolidation. If the applied stress versus strain relationship of a sediment changes with time, or is dependent on the rate of deformation, the material is said to be thixotropic. Uncompacted muddy sediments exhibit thixotropic properties. That is, at high rates of deformation (such as under the influence of strong bottom currents) watery mud deposits may behave more like liquids than solids (see Einstein and Krone, 1961). Thixotropic strength changes can also occur spontaneously as the number of bonds between individual particles and flocs shift to more closely approach thermodynamic equilibrium (Mitchell, 1964).

In nearshore and some continental shelf environments,

waves, currents, and organisms frequently interrupt consolidation, while the time scale for disturbances of deep sea sediments may be on the order of ones to tens of years. Thus, as a first approximation, one would expect freshly deposited muds to be eroded more easily than older deposits of otherwise similar sediments. Deep-sea deposits should have the greatest erosional resistance if only consolidation time is considered.

Consolidation as it relates to erosion resistance has not been systematically studied in marine sediments, but a possible indication of the influence of consolidation was noted during two recent laboratory erosion experiments. During these experiments the critical erosion velocity of a deep-sea carbonate ooze and a deep-dea red clay approached a quasi-equilibrium value over a period of several tens of hours after initial deposition (Southard et al, 1971; Lonsdale and Southard, 1974).

MICROFABRIC

It has not been possible to clearly observe the three-dimensional fabric of sediment flocs either before or after deposition. Many descriptions of possible sediment microfabrics have been suggested including microfabrics resembling

honeycombs (Terzaghi, 1925), cardhouses (Goldschmidt, 1926), and various other edge-face and edge-edge structures between individual particles (Van Olphen, 1963). However, it has been possible to observe the two-dimensional fabric of marine muds from natural and laboratory deposits under the scanning electron microscope (Bowles, 1968; Pusch, 1970; Collins and McGown, 1974).

Briefly, two types of floc aggregation have been observed: elementary particle arrangements; and particle assemblages (Collins and McGown, 1974). Elementary particle arrangements include face-face and edge-face arrangements between individual clay and silt particles or between small packets of similarly arranged silt and clay particles. Both face-face and edge-face elementary particle arrangements have been reported as common in marine sediments.

The second type, particle assemblages, are defined as units of particle organization having defineable boundaries which are composed of one or more types of elementary particle arrangements.

A dominant set of elementary arrangements or assemblages was usually present in natural sediments, but several of the common elementary arrangements and assemblages present in

natural sediment were not observed in laboratory preparations of monomineralic clays. This suggests basic differences in the microfabric of laboratory and natural sediments, but the possible consequences of the differences in fabric related to erodibility of the sediments were not explored.

Studies of the physical properties of naturally and laboratory-compacted muddy sediments (Meade, 1964; Bowles, 1968) infer that interfloc pore spaces decrease with increasing burial depth, but that great overburden pressures are required before individual flocs are deformed. This also suggests that the uncompacted surface layers of a marine mud are a network of flocs rather than a network of individual particles. If the floc units aggregate in some characteristic way as they are deposited on the bed, the bond strength between the basic floc assemblages should largely determine the erodibility of the sediments. This hypothesis is difficult to test because of the practical difficulty in obtaining undisturbed samples of the sediment-sea water interface. The usefulness of the Bingham yield stress as an estimate of interfloc bond strength was discussed in a previous section.

SUMMARY

The resistance of fine-grained marine sediments to

erosion is dependent on many physical, biological, and chemical properties of the sediments and surrounding waters. The complex and interdependent nature of the most important properties was discussed and it was shown that it is difficult or impossible to measure several of these important properties. For example, it is not possible at present to measure cohesion of the first few floc layers at the sediment-water interface. Neither has the composition and concentration of detrital and living organic material in the sediments and its effect on erosional resistance been adequately studied. Many basic studies of the relationships between the basic sediment properties defined here and erosion resistance can be accomplished in the laboratory. However, such studies will have limited usefulness until we can measure or estimate the same properties in undisturbed sediments undergoing erosion in their natural environments.

APPENDIX B

DESIGN OF THE IN SITU FLUME

DESIGN OF THE IN SITU FLUME

The in situ flume is a research tool designed to study interaction between flow and sediment during in situ erosion of undisturbed beds of marine sediments. The concept of an in situ flume is not new. A small, hand-operated in situ flume previously has been used (Neumann et al, 1970; Scoffin, 1968) in shallow tidal channels to study erosion velocities of algal mats. The flume described herein, however, is an autonomous instrument, capable of automatically performing erosion experiments at abyssal depths. Its potential use in the deep sea will be limited only by the difficulties inherent in lowering and recovering any unattached oceanographic instrument at sea.

DESCRIPTION OF FLUME SYSTEMS

A schematic drawing of the flume is shown in Figure B-1. Certain minor structural details and electrical conductors are omitted for clarity. Systems decribed in the following paragraphs are labeled in Figure B-1.

Flume Channel

The channel is 4.27 m long and 0.61 m wide. Acrylic

Figure B-1. Schematic side view of the in situ flume. The bottom contact switch located at the upstream end is not shown, and the strobe light on the opposite side of the flume is hidden by the camera and aluminum U-beam over the camera.

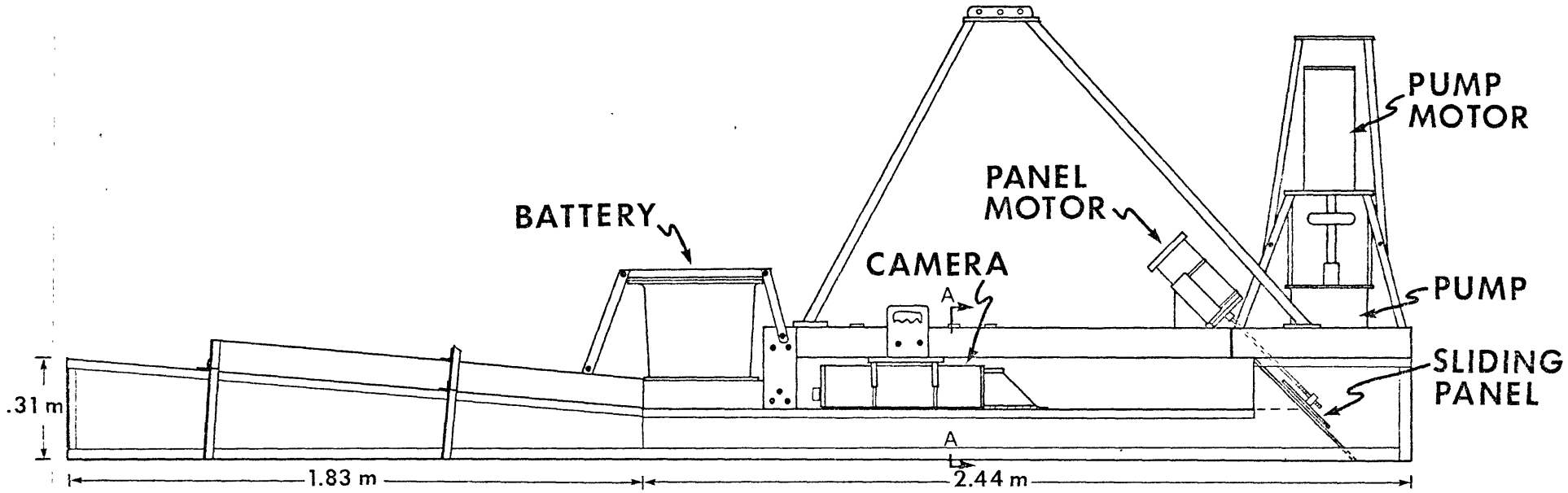

IN SITU FLUME

plastic is used to form the walls and top, and corner joints are held together by aluminum angles. The entrance section, which forms the upstream half of the channel, is 1.83 m long. The walls of this section slope from a height of 0.31 m at the upstream opening to 0.15 m where this section joins the straight observation section. The cross-section of the observation section is 0.15 m x 0.61 m. A 2" x 4" aluminum U-beam located axially along the channel serves as the central strength member to which all other components are fastened. A tubular aluminum tripod which serves as the lifting point is bolted to the U-beam.

A shorter entrance section with better hydrodynamic design would have allowed a longer space for development of the flume boundary layer. But, it would also have allowed initiation of erosion along a much greater part of the bed surface with the possibility of obscuring photographs of the bed surface. The design compromise finally settled on appears to be effective and the results of a model study, described later, indicate that the boundary layer is nearly fully developed at the point of observation.

Control of Channel Discharge

A panel-valve to control discharge is located in the chamber beneath the pump. A plastic panel with a 45^{o} slope forms the upstream wall of the pump chamber. It has two trapezoidal openings, one in its upper half the other in its lower half. The upper opening allows water to enter the pump directly from the outside of the flume. The lower opening is between the inside of the channel and the pump chamber. A sliding plastic plate of the same size as the fixed-plate openings moves along the top of the fixed plate. By sliding this plate off of the channel opening and onto the outside opening, the channel discharge is slowly increased while the total discharge of the pump is almost unchanged. This arrangement produces the smoothest possible increase of flow speed in the channel, given the difficult conditions of the sea floor experiments.

Pump

A vertical propeller pump was used on the flume because it was able to smoothly pump large water volumes of corrosive sea water. No direct measurement of pump discharge was made, but, assuming frictional losses in the flume equivalent to about a five-foot gravity head, the manufacturer's data

suggest an approximate maximum discharge of about 700 gal/min (26.6 l/min) at 1200 RPM.

Pump Motor

No reasonably priced submersible DC motor to drive the pump was available, so this component had to be developed. A 0.96 HP, 12 VDC, shunt-wound, aircraft motor was chosen initially for this purpose. The motor armature and commutator was encapsulated and impregnated with epoxy to reduce hydraulic drag losses while running in oil. Threads (20/inch) were cut 0.010" deep into the commutators and brush tension was increased to prevent hydroplaning and electrical arcing at high armature speeds. Under load this motor drew 40 amps at 12 VDC and developed 1150 RPM.

In spite of these modifications, carbon deposits apparently formed on the commutator after about 50 hours causing the field coils to burn out. A 0.75 HP permanent magnet, series wound motor modified in a similar way was then installed which proved more efficient then the previous motor in terms of power drain (25 amps at 12 VDC and 1150 RPM). Speed of the DC motors described above is not easily regulated, so control of flow velocity was achieved by the panel-valve,

previously described.

An oil-filled, pressure-compensated motor housing was machined from aluminum pipe. Aluminum end caps were sealed using compressional O-rings. Electrical cables were passed through the end caps. The oil used to fill the motor housing (low viscosity hydraulic fluid) was slightly more compressible than sea water. Pressure compensation was accomplished by attaching an oil-filled neoprene flexible bladder to the housing. A low-pressure relief valve also was installed on the upper end cap to allow for excessive thermal oil expansion and escape of any electrically-generated gas bubbles. Exchange of oil and water at the rotating motor shaft was prevented by a flexible neoprene oil seal fitted into the bottom end cap. The oil seal proved to be effective even at the moderately high motor shaft speed of about 1150 RPM.

Panel-Valve Motor

The movable panel-valve plate is slowly slid up a 45^{o} ramp by a rotating threaded rod which screws though a threaded block fixed to the moving plate. The motor needed to turn the threaded rod requires high torque, very low speed (2 RPM), and a low power drain. Finding the

proper motor for the panel-valve proved to be one of the most difficult tasks in constructing the flume.

After trying and rejecting several small DC motors a 2.1 RPM, 120 volt AC gear motor was installed temporarily to operate the panel-valve. This necessitated a direct AC power hook-up from the ship to the flume. This motor proved reliable as an interim step while development of a suitable DC motor took place.

The DC motor finally used was a precision bifilar stepping motor having 400 oz-in of torque. The motor has only one moving part (an armature), and no brushes; it can generate very high torques at slow RPM and has low power drain (2 amps/coil). It is mounted in an oil-filled PVC tube, and the shaft is sealed with a neoprene oil seal. Since little thermal expansion and no gas bubbles were expected, pressure compensation was achieved by covering the upper tube end with a flexible neoprene diaphragm. A solid-state motor-control circuit, controls the motor stepping speed. It consists of a simple R-C oscillator which sequentially triggers four power transistors to energize the four motor coils. Part of the solid-state circuit consists of a pulse-counting device to turn off

the motor after it has completely opened the panel-valve.

Power

A pair of 6 volt lead-acid storage batteries connected in series supply 12 volt DC power to the pump-motor and panel-valve motor. It was found that the voltage supplied by these batteries began to drop between 45 to 60 min after the motors were turned on; the pumping rate then begins to decrease.

In order to isolate the batteries from sea water, they are enclosed in an oil-filled fibreglass box. A low-pressure relief valve in the removable box top allows gas to escape during battery charging and discharging and during flume ascent. An oil-filled flexible neoprene bladder acts as an oil resevoir for pressure compensation.

Camera and Strobe

Initially, a single-frame Super 8 movie camera was used to record data, but, resolution and focusing of the close-up photographs proved troublesome with this system. Consequently, when an E.G. and G. 35 mm deep-sea camera and 100 W-sec strobe became available, they were adapted for flume photography by refocusing the lens and setting the timing motor for a repetition rate of about 6 sec between

frames. The camera-strobe unit is powered by its own 6 VDC Yardney Silvercell battery.

In the present configuration the timing motor must be turned on at the surface before sealing the strobe pressure case. No pictures are taken, however, until after the flume reaches the sea floor, when a relay is energized which connects the camera to the strobe. For deep water use, it will be a comparatively simple task to modify the camera system so that the power is turned on by the same bottom-contact switch which starts the pump motor and panel-valve motor.

Camera and Strobe Mounting

The camera is mounted horizontally under the 2" x 4" U-beam passing over the observation section on a cradle which also provides a convenient means of mounting and removal. A 45° mirror in front of the camera lens-port is used to photograph a section of the sea floor about 1.1 m downstream from the beginning of the observation section. The mirror is part of a semi-enclosed chamber which encompasses the water volume between the camera lens-port and the flume top. The chamber helps to keep suspended matter from settling onto the flume top and obscuring the

photographs.

The strobe housing is mounted parallel to the camera on brackets extending from the 2" x 4" U-beam to the flume wall. In this position, light can be reflected from a mirror along side the flume through the wall to the sea floor beneath the camera mirror. By covering the flume top under the strobe light, only low-angle light illuminates the sea floor. This configuration helps to bring out small-scale relief of the relatively smooth sediment surface.

Bottom-Contact Switch and Relays

A mercury tilt switch in a small pressure case is used to turn on the pump systems and camera. The switch is suspended by a short cable from an arm extending horizontally from the flume top at the upstream end of the flume. Tilting of the switch upon bottom contact is ensured by the presence of a curved foot-plate on the bottom of the switch housing.

Closing of the bottom contact switch activates two relays, one to start the pump motor and another to start the panel-motor and connect the strobe to the camera. These relays are enclosed in an oil-filled box mounted near the pump (not shown in Figure 1).

DEPLOYMENT

For the first experiments it was necessary to supply surface-generated AC power to the flume, so the lowerings were done with the ship at anchor. After the flume was slowly lowered to the sea floor on the winch wire, drift of the ship necessitated periodic slacking and taking-up of the electrical cable and winch wires. Observations made by SCUBA divers during the lowerings verified that there was minimal disturbance to the sediment during emplacement and no vibration or dragging as a consequence of direct connection to the winch wire (see Chapter II for more detailed discussion of emplacement tests).

After installation of the DC motor to operate the panel-valve, it became possible to completely free the flume from the ship after lowering. In water depths to 300 m, a nylon rope was used to raise and lower the flume to the sea floor. After bottom contact, the excess rope was tied to a small surface float and cast off, thus completely freeing the flume from the ship.

The limited deck space and boom scope on the ship limited the sea conditions under which the flume could be deployed to relatively calm days with seas less than

1 to 2 feet. Considering the brittleness of the plastic used for its construction, the flume proved surprisingly able to absorb moderately severe shocks and bumps during deployment. With minor strengthening modifications, the flume should be capable of withstanding the more rigorous environments encountered during deep-sea deployment.

FLOW SPEED IN THE CHANNEL

To reduce mechanical and electrical complexity, a simple sphere-on-a-string meter mounted in the field-of-view of the camera was used to measure flow speed. The 1.1 cm diameter nylon sphere was ballasted with small metal inserts to make it negatively buoyant. The horizontal deflections of the sphere produced by the unidirectional flow in the channel (as measured on photographs taken during the experiments) are referred to a calibration curve produced by three laboratory flume runs (Figure B2).

Flows slower than about 5 cm/sec produced random fluctuations and barely discernible ball deflections. Flows between 5 cm/sec and 8 cm/sec produced deflections of 0.5 cm or less, which were difficult, but not impossible, to measure. From about 8 cm/sec to about 45 cm/sec the plot of deflection versus velocity is relatively well

Figure B-2. Calibration curve for sphere current meter. Each of the three different symbols represents a separate calibration run in a 6 m long enclosed flume having a 17 cm width. Flow depths were between 13-15 cm.

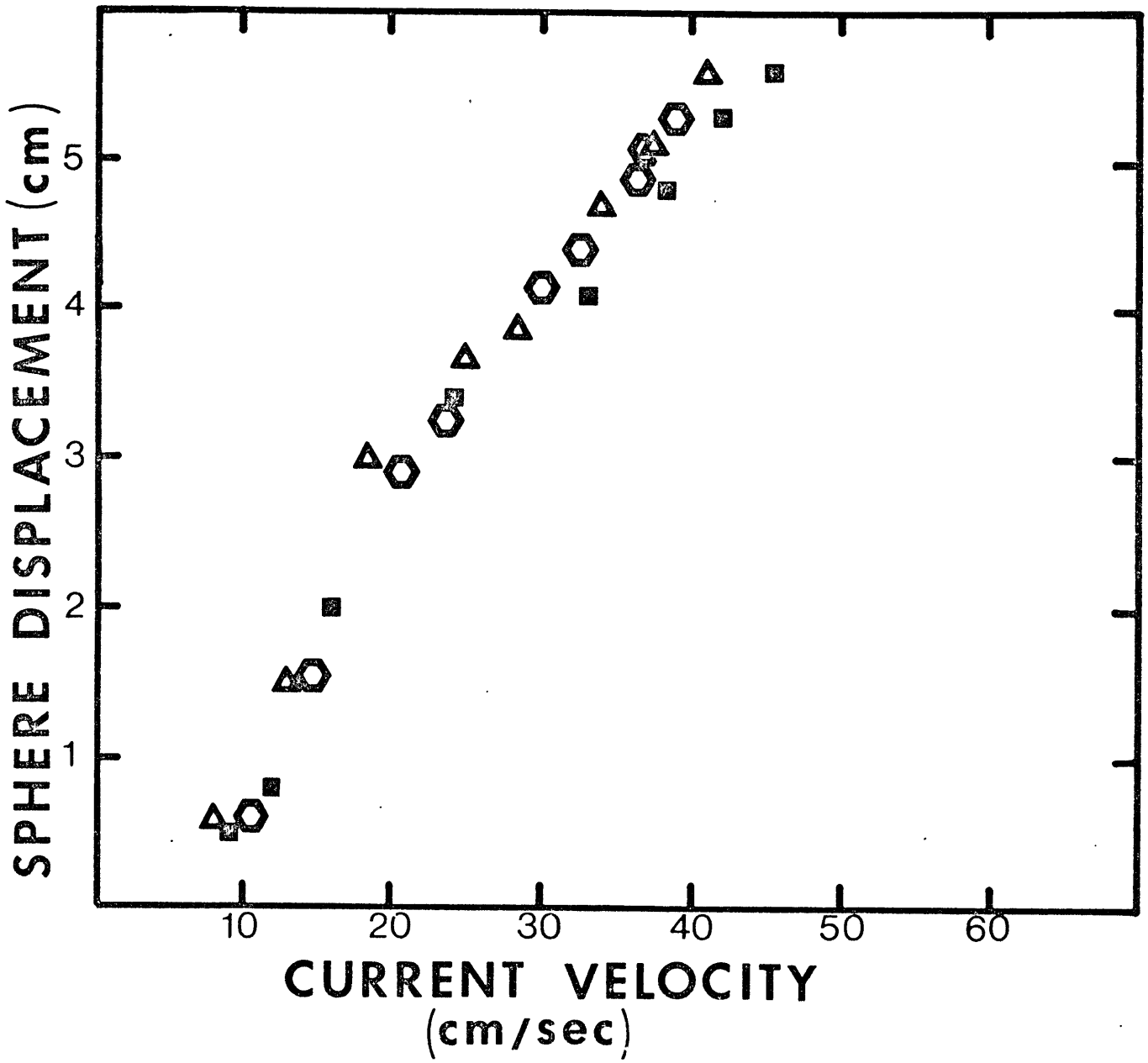
SPHERE DISPLACEMENT (cm)
1
2
3
4
5
10
20
30
40
50
60
CURRENT VELOCITY
(cm/sec)

defined. Above 45 cm/sec ball deflection rapidly decreases with increasing velocity, so that this represents the upper limit of flow measurements.

ANALYSIS OF FLOW IN THE FLUME CHANNEL - MODEL STUDIES

A half-scale model was used to investigate boundary-layer development downstream of the junction between the sloping entrance section and rectangular observation section of the flume. The analytical framework for extrapolating the flow dynamics of a model to the flow dynamics in a geometrically identical prototype is encompassed in the principles of dynamic similitude as summarized by Langhaar (1951) and Holt (1961), among others.

Basically, dynamic similarity of two geometrically similar, enclosed, flow systems occurs when the Reynolds' numbers of the two systems have the same value. This can be written as

$$\text{Reynolds number} = \left(\frac{ul}{\nu}\right)_{\text{model}} = \left(\frac{ul}{\nu}\right)_{\text{prototype}}$$

where u and l are a characteristic velocity and length of the flow systems, and ν is kinematic fluid viscosity.

For the case of the *in situ* flume and its model, the length-scale ratio was fixed at one-half giving $l_M = 0.5\ l_P$,

and the viscosity ratio was fixed at $\nu_M = 0.83\,\nu_P$. Thus, if the mean velocity $\bar{u}$ is chosen as the characteristic velocity in both systems, Reynolds' number similarity implies $\bar{u}_P = 0.6\,\bar{u}_M$. This analysis can be extended to measurements of local velocity at all geometrically similar points in the model and prototype flumes and allows detailed analysis and comparison of velocity profiles which will be discussed in the following paragraphs.

The model flume was made of plywood painted with marine epoxy paint and sanded smooth. Velocity distributions were measured with a 0.3 mm diameter Prandtl tube (combination total and static pressure tube). Circular openings were made in the top of the model at three locations and the openings fitted with removable plastic plugs made flush with the top. One of the plugs was drilled through to accomodate the shaft of the Prandtl tube.

Pressure differences sensed by the Prandtl tube were measured on a fluid manometer and converted to velocity by the well known relationship $u = (2gh\,\gamma_M/\gamma_w)^{\frac{1}{2}}$, where g is gravitational acceleration, h is the height difference of the two manometer columns, γ_w the specific gravity of the flume water, and γ_M the specific gravity of the manometer fluid (carbon

tetrachloride) minus specific gravity of the flume water. Differences in the fluid levels of the two vertical manometer columns could be estimated to about 0.2 cm.

Model tests were conducted in a recirculating laboratory flume filled to completely submerge the model. The model was oriented parallel to the channel walls, weighted with bricks, and had its lower edges sealed with clay to prevent fluid exchange.

Results

The results of the two series of measurements made at relatively high and low velocities indicate that the boundary layer is almost completely developed by the time it reaches the location in the model (probe station 2) equivalent to the location in the prototype where the sphere velocity meter is hung. Figure B-3 illustrates boundary layer development for the high velocity run. A tendency for the slope of the velocity profile to be steeper in the upper part of the channel than in the lower part was noted in each series of measurements.

Asymmetry in the velocity profiles may be produced by differences in frictional resistance at the top and bottom walls or by transition between converging and

Figure B-3. Velocity profiles in the model flume showing boundary layer development downstream of the transition between convergent and parallel flow. The upper part of the figure shows velocity profiles at the three measuring stations. The lower part of the figure is a comparison between measured velocity profiles (dots) and a calculated velocity profile based on Prandtl's seventh-power law (triangles).

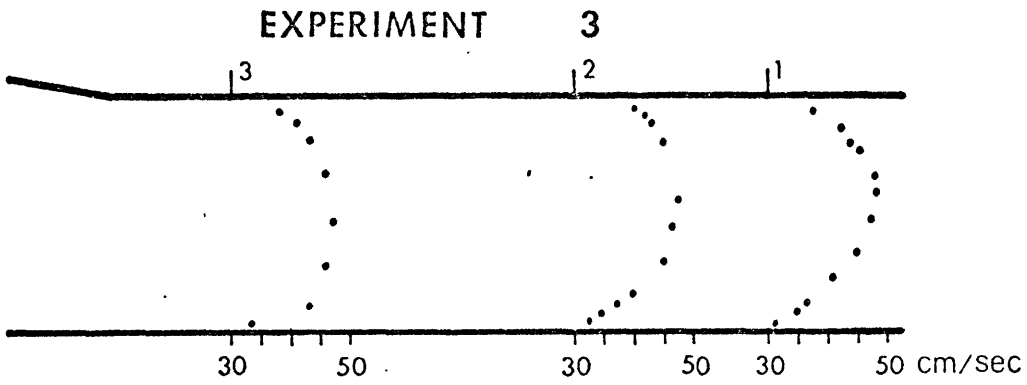

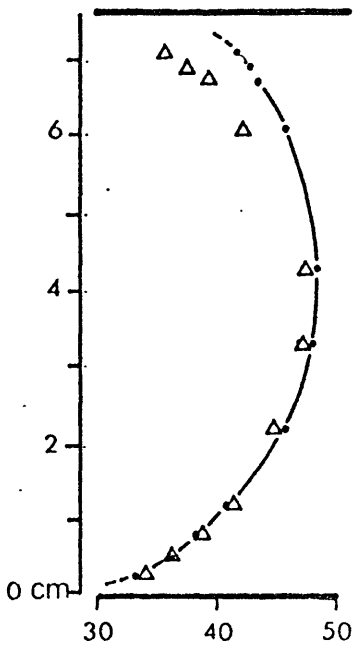

EXPER. 3

$U_{max} = 48.9$

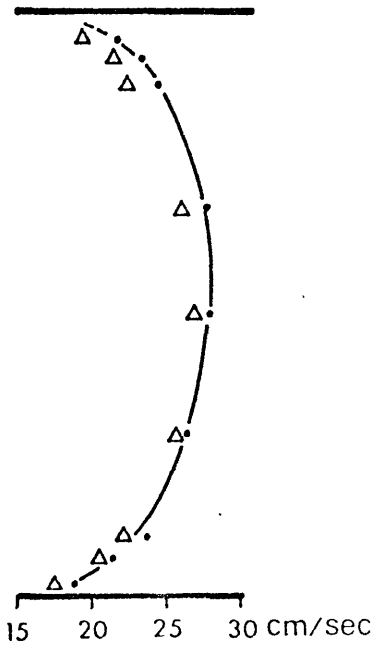

EXPER. 4

$U_{max} = 28.7$ CM/SEC

parallel flow portions of the flume. In the model flume, where top and bottom walls are smooth, it is more reasonable to assume that the velocity profile asymmetry is the result of transition from convergent to parallel flow. Greater bottom roughness in the prototype flume will cause some accentuation of the flow asymmetry. However, since sea-floor roughness is small and flow is considered hydraulically smooth to transitional in roughness (see Chapter II), it is not expected that flow asymmetry in the prototype will greatly exceed that observed during the model study and thus need not be considered further in the analysis.

The in situ flume was designed to produce estimates of bed shear stress during erosion using photographs of the sediments and the sphere current meter. It is therefore of great practical importance to determine how closely the velocity distribution in the flumes (model and prototype) conforms to ideal flow through a straight rectangular duct.

An empirically well verified flow law for velocity distribution in the region between the core of the flow and the wall layer is Prandtl's power law. This flow law states that velocity depends only on a power of the distance

from the wall. Stated explicitly for a rectangular duct, $u = u_{max} (y/d)^{1/7}$, where u_{max} is maximum velocity and d is some measure of flow depth. In this study the value d = 0.5 times channel height was found to yield calculated velocity profiles agreeing most closely with the measured profiles.

Since the velocity profiles are slightly asymmetrical and the sphere current meter in the prototype flume measures velocity at only a single point, an important question is to what extent the flow asymmetry affects estimates of wall shear stress. To investigate this question a comparison was made between predicted and measured velocity profiles (Figure B-4). It is readily seen that differences greater than about 5% between observed and predicted velocities occur at distances from the wall of less than about 2 cm in the model, corresponding to about 4 cm in the prototype. Since the sphere current meter comes no closer to the wall than about 4.4 cm when the velocity in the full size flume is about 50 cm/sec, it can be expected that the velocity measured by the sphere current meter will differ by no more than 5% from the predicted velocity. Since velocity can be determined only to within about $\pm$ 10% by the sphere (see previous section on sphere calibration), the error in

Figure B 4. Percent difference between measured and calculated velocity profiles in the model flume. Percent difference is defined as (measured velocity minus calculated velocity) divided by the calculated velocity.

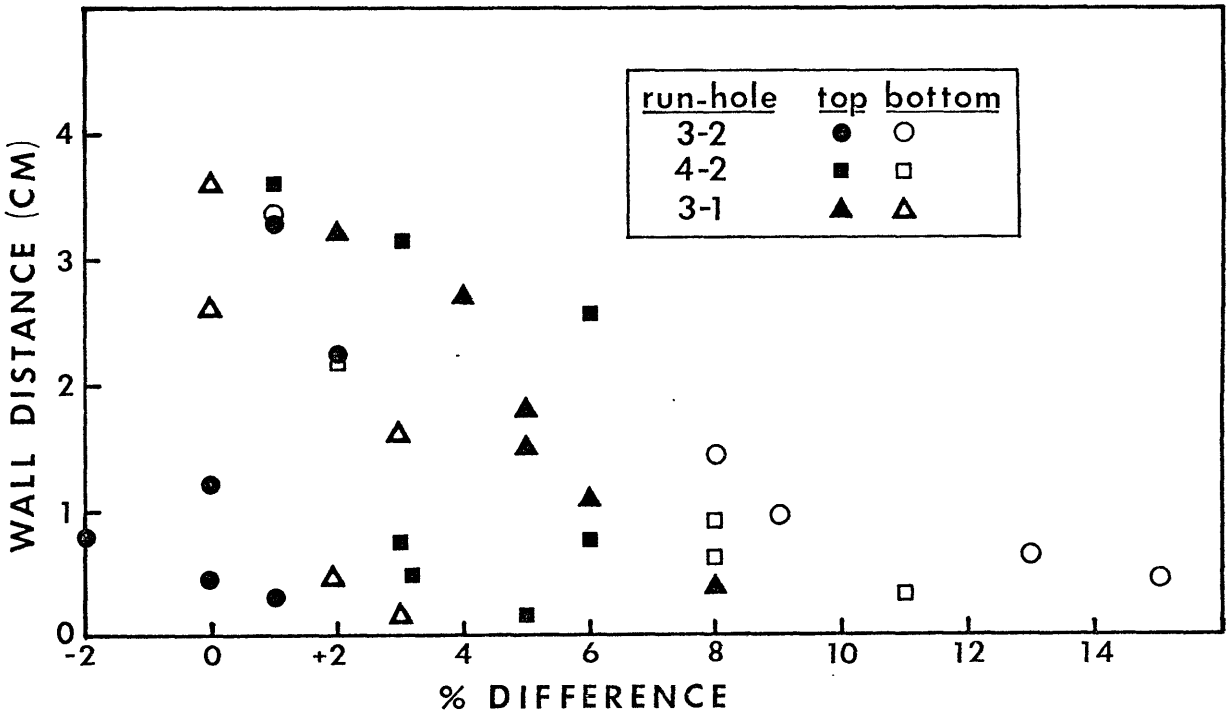
run-hole
top
bottom
3-2
4-2
3-1
WALL DISTANCE (CM)
0
1
2
3
4
-2
0
+2
4
6
8
10
12
14
% DIFFERENCE

calculating bed shear stress using the uncorrected sphere velocity should be negligible.